

**Assessment of morphological and molecular genetic variation of freshwater mussel species
belonging to the genera *Fusconaia*, *Pleurobema*, and *Pleuronaia* in the upper Tennessee
River basin**

Daniel E. Schilling

Thesis submitted to the faculty of the Virginia Polytechnic Institute and State University in
partial fulfillment of the requirements for the degree of

Master of Science

in

Fisheries and Wildlife

Jess W. Jones, Chair

Eric M. Hallerman

James H. Roberts

Eric P. Smith

June 2nd, 2015

Blacksburg, VA

Keywords: Freshwater Mussels, *Fusconaia*, *Pleurobema*, *Pleuronaia*, Phylogenetic Assessment,

Morphological Variation

All Material © 2015 by Daniel E. Schilling

**Assessment of morphological and molecular genetic variation of freshwater mussel species
belonging to the genera *Fusconaia*, *Pleurobema*, and *Pleuronaia* in the upper Tennessee**

River basin

by

Daniel E. Schilling

ABSTRACT

Select freshwater mussels in the genera *Fusconaia*, *Pleurobema*, and *Pleuronaia* were collected primarily in the upper Tennessee River basin from 2012 to 2014 for phylogenetic and morphological assessments. Freshwater mussels in these genera are similar in appearance, hence the need for phylogenetic verification and morphological assessment. Phylogenetic analyses of the mitochondrial gene *NDI* and the nuclear gene *ITS1* revealed three unrecognized, phylogenetically distinct species. These species were separated from their closest congener by 2.85%, 3.17%, and 6.32% based on pairwise genetic distances of *NDI*. Gaps created from aligning *ITS1* sequences were coded as fifth characters, which phylogenetically separated most closely related species. Analyses of *NDI* agreed with previous literature on the phylogenetic distinctiveness of *Pleuronaia* species, with the exception of the DNA sequences of *P. gibberum*, which grouped outside this genus based on the analyses conducted in this study.

Morphological variation was recorded for eight of the species to include quantitative and qualitative characters as well as geometric morphometric analyses of the data. Three decision trees were created from quantitative and qualitative characters using classification and regression tree analyses. The best-performing tree used quantitative and qualitative characters describing shell-only scenarios and obtained 80.6% correct classification on terminal nodes. Canonical variates analysis on geometric morphometric shell data revealed large morphological overlap

between species. Goodall's F-tests between pairs of species revealed significant differences ($\alpha=0.05$) between all but one species pairs; however, examination of landmarks on shells concluded large overlap of these landmarks between species pairs. Lack of morphologically distinct characters to readily identify these phylogenetically distinct species indicates large morphological overlap among these species. Biologists need to be cognizant that morphologically cryptic species may exist in stream systems often explored.

Three dichotomous keys were created from classification trees to identify select individuals in the genera *Fusconaia*, *Pleurobema*, and *Pleuronaia*; two of these keys, one for shells and one for live mussels were tested by participants with varying mussel identification skills to represent novices and experts. Both keys used continuous (quantitative) and categorical variables to guide participants to identifications. Novices, who had no prior mussel identification experience, correctly identified mussels with a 50% accuracy using the shell key and with a 51% accuracy using the live key. Experts, who had at least three years of experience identifying mussels, correctly identified mussels with a 58% accuracy using the shell key and with a 68% accuracy using the live key; however, one expert noted that they did not use the live key to correctly identify one mussel. Morphological overlap of variables between mussels likely resulted in failure to consistently identify mussels correctly.

Important management decisions and project implementations require accurate assessment of species' localities and populations. Incorrect species identification could hinder species' recovery efforts or prevent projects that otherwise could have continued if a species was correctly identified. If a mussel collection is thought to be a new record or could affect a project, I recommend that molecular genetic identifications be used to verify the species identity.

ACKNOWLEDGEMENTS

The Virginia Department of Game and Inland Fisheries provided primary funding, and Virginia Polytechnic Institute and State University provided additional monetary assistance and facilities for this project. I would like to thank Drs. Jess Jones and Eric Hallerman for advising me through my Master of Science degree. I also thank graduate advising committee members, Drs. James Roberts and Eric Smith for guiding this project. I would like to thank Michael Pinder for recognizing the need for this project and supporting funding. This project would not have been possible without the assistance of fellow graduate students and professional colleagues. I thank Andrew Phipps for his countless hours assisting field collections and laboratory work. I also thank my fellow graduate students, Tim Lane, Hua Dan, Matthew Johnson, and Jen Rogers, for their assistance in the field. Many professional colleagues assisted during field collections and advanced my understanding of freshwater mussel ecology and molecular genetics; thus, I thank Brian Watson, Brett Ostby, Megan Bradley, Shane Hanlon, Brian Evans, Braven Beaty, Steve Ahlstedt, Bob Butler, Steve Fraley, Don Hubbs, Jason Wisniewski, Nathan Johnson, Jim Williams, Chuck Howard, and Jon Mollish. I am indebted to Hugh Faust for volunteering his time to assist in fieldwork, as well as providing valuable knowledge on freshwater mussels and aquatic systems. I also thank my fellow graduate students in the Department of Fish and Wildlife Conservation for providing relaxing environments to discuss various scientific aspects that advanced my learning. Finally, I would like to thank my parents, Edward and Elizabeth, for encouraging me to learn about natural ecosystems; their love and encouragement helped me in completing this project.

TABLE OF CONTENTS

Chapter 1. Molecular phylogenetics of select mussel species in the genera *Fusconaia*, *Pleurobema*, and *Pleuromma* using mitochondrial *ND1* and nuclear *ITS1* DNA sequences

.....	1
Abstract	2
Introduction	3
Methods	7
Mussel Collections.....	7
DNA Extraction	8
Polymerase Chain Reaction	8
Data Analyses	10
Results	12
Mussel Collections.....	12
<i>ND1</i>	14
Phylogenetic and Pairwise Analyses of <i>ND1</i>	17
<i>ITS1</i>	19
Discussion	22
Development of Molecular Markers.....	22
Phylogenetic and Pairwise Analyses of <i>ND1</i>	23
<i>ITS1</i>	25

Molecular Genetic Marker Comparison	27
Management Implications.....	28
Literature Cited.....	30
Appendix A: Haplotype Collections.....	62

Chapter 2. Identification of morphological characters for use in taxonomic delineation of selected mussel species in the genera *Fusconaia*, *Pleurobema*, and *Pleuonaia* in the upper

Tennessee River basin of Tennessee and Virginia67

Abstract68

Introduction70

Methods72

 Species Collections72

 Morphology.....72

 Classification and Regression Tree Analysis of Morphological Data74

 Geometric Morphometrics76

Results77

 Morphological Assessment and Species Descriptions.....77

 Assessment of Glochidia Dimensions among Species83

 Classification and Regression Tree Analysis of Morphological Data83

 Geometric Morphometrics85

Discussion85

 Classification and Regression Tree Analysis of Morphological Data85

 Geometric Morphometrics88

 Cryptic Species Discovered89

 Morphological Similarities91

Management Implications.....	92
Literature Cited.....	95

Chapter 3. Development and testing of morphology-based dichotomous keys for selected freshwater mussels in the genera *Fusconaia*, *Pleurobema*, and *Pleuronaia* in the upper Tennessee River basin of Tennessee and Virginia133

Abstract134

Introduction136

Methods137

 Creating the Dichotomous Keys137

 Testing the Dichotomous Keys138

 Effectiveness of the Dichotomous Keys140

Results141

 Testing the Effectiveness of Dichotomous Keys141

Discussion143

 Creating the Dichotomous Keys143

 Testing the Dichotomous Keys144

 Effectiveness of the Dichotomous Keys145

 Management Implications146

Literature Cited149

List of Tables

Chapter 1. Molecular phylogenetics of select mussel species in the genera *Fusconaia*, *Pleurobema*, and *Pleuronaia* using mitochondrial *NDI* and nuclear *ITS1* DNA sequences:

Table 1.	Site numbers and locality information for sites sampled for freshwater mussels primarily in the Tennessee River basin from 2012 through 2014. NA = information not available.....	38
Table 2.	Sample sizes for freshwater mussels collected at sites from 2012-2014, with species identifications confirmed by analysis of the mitochondrial gene region <i>NDI</i>	39
Table 3.	Variable nucleotide sites for haplotypes at the mitochondrial gene <i>NDI</i> , where species abbreviations are: Fcor = <i>Fusconaia cor</i> ; Fcun = <i>F. cuneolus</i> ; Fmas = <i>F. masoni</i> ; Fsub = <i>F. subrotunda</i> ; Pbar = <i>Pleuronaia barnesiana</i> ; PcfB = <i>P. sp. cf. barnesiana</i> ; Pdol = <i>P. dolabelloides</i> ; PcfD = <i>P. sp. cf. dolabelloides</i> ; Pgib = <i>P. gibberum</i> ; Povi = <i>Pleurobema oviforme</i> ; PcfO = <i>P. sp. cf. oviforme</i> ; Srub = <i>Sintoxia rubrum</i> . Identical nucleotide sites to the first sequence are indicated by "." and missing data is indicated by "-".....	41
Table 4.	Pairwise nucleotide distances between species' haplotypes at the mitochondrial gene <i>NDI</i> . Pairwise differences were calculated using the general time reversible model with rates gamma (GTR+G) in PAUP. Bold numbers indicate intraspecific variation. Species abbreviations are defined in Table 3.....	49

Table 5.	<p>Variable nucleotide sites for haplotypes at the nuclear gene region <i>ITS1</i> using the alignment algorithm from Clustal W. A blank at a nucleotide site indicates identical nucleotide as first sequence.</p> <p>Haplotype numbers do not correspond with those for mitochondrial DNA data. Species abbreviations are defined in Table 3.</p> <p>Insertions or gaps are indicated by "-"; identical nucleotide positions to the first sequence are blank.....</p>	50
Table 6.	<p>Variable nucleotide sites for haplotypes at the nuclear gene region <i>ITS1</i> using the alignment algorithm from webPRANK. A blank at a nucleotide site indicates identical nucleotide as first sequence.</p> <p>Haplotype numbers do not correspond with those for mitochondrial DNA data. Species abbreviations are defined in Table 3.</p> <p>Insertions or gaps are indicated by "-"; identical nucleotide positions to the first sequence are blank.....</p>	51
Table 7.	<p>Pairwise nucleotide distances between species' haplotypes at the nuclear gene <i>ITS1</i> using the alignment algorithm from Clustal W. Pairwise distances were calculated using uncorrected <i>p</i>-distances in PAUP. Species abbreviations are defined in Table 3. Bold numbers indicate intraspecific variation; <i>N</i>=1 indicates that only one haplotype was recovered for the species, thus intraspecific variation cannot be computed.....</p>	52
Table 8.	<p>Pairwise nucleotide differences between species' haplotypes at the nuclear gene <i>ITS1</i> using the alignment algorithm from</p>	

webPRANK. Pairwise distances were calculated using uncorrected *p*-distances in PAUP. Species abbreviations are defined in Table 3. Bold numbers indicate intraspecific variation; *N*=1 indicates that only one haplotype was recovered for the species, thus intraspecific variation cannot be computed.....53

Appendix A: Haplotype collections

Table A. 1. Site numbers and counts of haplotypes analyzed for the mitochondrial gene region *ND1*. Species abbreviations are defined in Table 3.....62

Table A. 2. Site numbers and counts of haplotypes analyzed for the nuclear gene region *ITS1*. Species abbreviations are defined in Table 3.....66

Chapter 2. Identification of morphological characters for use in taxonomic delineation of selected mussel species in the genera *Fusconaia*, *Pleurobema*, and *Pleuonaia* in the upper Tennessee River basin of Tennessee and Virginia:

Table 1. Locality information for sites sampled for freshwater mussels in the Tennessee River basin from 2012 through 2014. Data from live mussels collected at these sites were used to conduct the morphological analyses in this study.....99

Table 2. Sample sizes for live individuals identified to species using mitochondrial DNA (mtDNA), and for observations of morphological traits for specimens sampled in Upper Tennessee

	River basin from 2012-2014. Sample sizes of non-genetically identified shells from the FMCC collection also are included.....	100
Table 3.	Sample sizes of foot-color observations on live mussels of each species collected in the Upper Tennessee River basin from 2012-2014.....	101
Table 4.	Categorical variables for shell traits and respective sample sizes per species.....	102
Table 5.	Number of charged gills and their color for gravid mussels sampled in the Upper Tennessee River basin from 2012-2014. *No specimens were observed gravid during study; thus, number of charged gills is based on observations reported in literature.....	104
Table 6.	Mean height, length, and hinge length of glochidia for species observed gravid. No individuals of <i>Fusconaia cuneolus</i> were observed gravid during this study.....	105
Table 7.	Tukey's comparisons for glochidia measurements of species observed gravid. <i>P</i> -values are listed in the order of height, length, and hinge length.....	106
Table 8.	Species predictions (<i>N</i> =384) using classification and regression tree analysis of traditional shell measurements and foot color data. Actual species identifications are reported in the rows and predictions made by the Classification and Regression Tree Analysis (CART) are reported in the columns.....	107

Table 9.	Species predictions ($N=160$) using classification and regression tree analysis of quantitative, foot color, and categorical variables from sacrificed live individuals. These data include non-genetically identified individuals from the FMCC shell collection. Actual species identifications are reported in the rows and predictions made by the Classification and Regression Tree Analysis (CART) are reported in the columns.....	108
Table 10.	Species predictions ($N=160$) using classification and regression tree analysis of shell-only quantitative and categorical variables from sacrificed individuals. These data include non-genetically identified individuals from the FMCC shell collection. Actual species identifications are reported in the rows and predictions made by the Classification and Regression Tree Analysis (CART) are reported in the columns.....	109
Table 11.	Species predictions using canonical variates analysis (CVA) of geometric morphometric data.....	110
Table 12.	Goodall's F -test for morphological differences using geometric morphometric data. All pairwise comparisons between species are significantly different ($p<0.05$), except between <i>Pleurobema oviforme</i> and <i>Pleuonaia</i> sp. cf. <i>barnesiana</i> .	111

Chapter 3. Development and testing of morphology-based dichotomous keys for selected freshwater mussels in the genera *Fusconaia*, *Pleurobema*, and *Pleuronaia* in the upper Tennessee River basin of Tennessee and Virginia:

Table 1.	Key to the shells of non-live individuals of select freshwater mussel species in the genera <i>Fusconaia</i> , <i>Pleurobema</i> , and <i>Pleuronaia</i> in the upper Tennessee River basin of Tennessee and Virginia using categorical and continuous variables. See Figure 1 for explanations of shell characters and the species accounts for illustrations of morphological traits (Figures 2-9).....	151
Table 2.	Key to the live individuals of select freshwater mussel species in the genera <i>Fusconaia</i> , <i>Pleurobema</i> , and <i>Pleuronaia</i> in the upper Tennessee River basin of Tennessee and Virginia using categorical and continuous variables. See shell diagram page for explanations of shell characters and species accounts for illustrations of morphological traits (Figures 2-9).....	153
Table 3.	Key to gravid individuals of select freshwater mussel species in the genera <i>Fusconaia</i> , <i>Pleurobema</i> , and <i>Pleuronaia</i> in the upper Tennessee River basin of Tennessee and Virginia using categorical variables. See Figure 1 for explanations of shell characters and species accounts for illustrations of morphological traits (Figures 2-9).....	155
Table 4.	List of terms used in the keys to identify shells and soft-anatomy of study species in the genera <i>Fusconaia</i> , <i>Pleurobema</i> , and	

	<i>Pleuronaia</i> in the upper Tennessee River basin of Tennessee and Virginia; terms modified from Parmalee and Bogan (1998) and Williams et al. (2008).....	156
Table 5.	Participant accuracy in correctly identifying select mussel species in the genera <i>Fusconaia</i> , <i>Pleurobema</i> , and <i>Pleuronaia</i> using the dichotomous keys based on quantitative and categorical variables.....	157
Table 6.	Species identifications ($N=72$) assigned by novices ($N=9$) using dichotomous key of shell-only quantitative and categorical variables. These data include non-genetically identified individuals from the FMCC shell collection. Actual species identifications are in the rows and participant's identifications are in the columns.....	158
Table 7.	Species identifications ($N=88$) assigned by experts ($N=11$) using dichotomous key of shell-only quantitative and categorical variables. These data include non-genetically identified individuals from the FMCC shell collection. Actual species identifications are in the rows and participant's identifications are in the columns.....	159
Table 8.	Species identifications ($N=48$) assigned by novices ($N=6$) using dichotomous key quantitative and categorical variables representing live mussels. These data include non-genetically identified individuals from the FMCC shell collection. Actual	

species identifications are in the rows and participant's
identifications are in the columns.....160

Table 9. Species identification ($N=88$) assigned by experts ($N=11$) using
dichotomous key of quantitative and categorical variables
representing live mussels. These data include non-genetically
identified individuals from the FMCC shell collection. Actual
species identifications are in the rows and participant's
identifications are in the columns.....161

List of Figures

Chapter 1. Molecular phylogenetics of select mussel species in the genera *Fusconaia*, *Pleurobema*, and *Pleuronaia* using mitochondrial *ND1* and nuclear *ITS1* DNA sequences:

- Figure 1. Sampling localities and site numbers for freshwater mussels collected primarily in the Tennessee River basin from 2012 through 2014. Craig Creek collection localities are not shown 55
- Figure 2. Phylogenetic relationships showing Bayesian consensus tree for freshwater mussels inferred from the mitochondrial gene region *ND1*. Numbers on branches are posterior probabilities of tree topology. The analysis was run for 10 million generations with split frequencies of 0.0065, with the most likely tree possessing a -ln likelihood of -6286.032 and the mean -ln likelihood of -6367.785 57
- Figure 3. Phylogenetic relationships showing the Bayesian consensus tree for freshwater mussels inferred from the nuclear gene *ITS1* using the alignment algorithm from Clustal W. Numbers on branches are posterior probabilities of tree topology. The analysis was run for 2 million generations with split frequencies of 0.0067, with the most likely tree possessing a -ln likelihood of -1514.34 and the mean -ln likelihood of -1566.02 59
- Figure 4. Phylogenetic relationships showing the Bayesian consensus tree for freshwater mussels inferred from the nuclear gene *ITS1* using the alignment algorithm from webPRANK. Numbers on branches

are posterior probabilities of tree topology. The analysis was run for 2 million generations with split frequencies of 0.0065, with the most likely tree possessing a -ln likelihood of -1487.89 and the mean -ln likelihood of -1539.72.....61

Chapter 2. Identification of morphological characters for use in taxonomic delineation of selected mussel species in the genera *Fusconaia*, *Pleurobema*, and *Pleuonaia* in the upper Tennessee River basin of Tennessee and Virginia:

Figure 1. External (top) and internal (bottom left) shell characters investigated in this study, including anatomical regions (bottom right) of the shell.....112

Figure 2. Sampling localities and site numbers for freshwater mussels collected primarily in the Tennessee River basin from 2012 through 2014.....114

Figure 3. Light-box used to hold specimens while photographs were taken; lid not shown.....115

Figure 4. Geometric morphometric measurements of freshwater mussel shells. Calipers held specimens parallel to the camera lens in order to standardize all photographs. A radial overlay was superimposed on the photograph, aligning the terminating segments of the hinge ligament to serve as a baseline (red dots). Nine semi-sliding landmarks (yellow dots) were digitized where the radial overlay intersected the shell margin.....116

Figure 5.	<p>Individuals of <i>Fusconaia cor</i> depicting size classes and variation in periostracum color and ray patterns: (A) 23 mm from North Fork Holston River, km 142.7; (B) 35 mm from Clinch River, km 435.8; (C) 49 mm from Clinch River, km 435.8; (D) 53 mm from Clinch River, km 435.8; (E) 61 mm from Clinch River, km 437.9; (F) 79 mm from Powell River, km 214.0.....</p>	117
Figure 6.	<p>Individuals of <i>Fusconaia cuneolus</i> depicting size classes and variation in periostracum color and ray patterns: (A) 27 mm from Clinch River, km 309.8; (B) 32 mm from Clinch River, km 309.8; (C) 41 mm from Clinch River, km 309.8; (D) 51 mm from Clinch River, km 309.8; (E) 65 mm from Clinch River, km 401.7; (F) 75 mm from Clinch River, km 401.7.....</p>	118
Figure 7.	<p>Individuals of <i>Fusconaia subrotunda</i> depicting size classes and variation in periostracum color and ray patterns: (A) 37 mm from Clinch River, km 305.4; (B) 42 mm from Clinch River, km 305.4; (C) 53 mm from Clinch River, km 435.8; (D) 75 mm from Clinch River, km 435.8; (E) 84 mm from Clinch River, km 435.8; (F) 97 mm from Clinch River, km 378.3.....</p>	119
Figure 8.	<p>Individuals of <i>Pleurobema oviforme</i> depicting size classes and variation in periostracum color and ray patterns: (A) 27 mm from North Fork Holston River, km 175.2; (B) 38 mm from Copper Creek, km 24.1; (C) 52 mm from Beech Creek, km 10.8; (D) 71 mm from Indian Creek (Clinch Drainage), km 0.8; (E) 80 mm</p>	

from Beech Creek, km 25.6; (F) 93 mm from North Fork Holston River, km 191.7.....120

Figure 9. Individuals of *Pleurobema* sp. cf. *oviforme* depicting size classes and variation in periostracum color and ray patterns: (A) 37 mm from Little River, km 47.6; (B) 44 mm from Little River, km 47.6; (C) 65 mm from Little River, km 47.6; (D) 79 mm from Little River, km 33.2; (E) 89 mm from Little River, km 47.6; (F) 104 mm from Little River, km 47.6.....121

Figure 10. Individuals of *Pleuonaia barnesiana* depicting size classes and variation in periostracum color and ray patterns: (A) 29 mm from Copper Creek, km 4.2; (B) 45 mm from Beech Creek, km 10.8; (C) 60 mm from Possum Creek, km 12.2; (D) 63 mm from Copper Creek, km 21.7; (E) 72 mm from Powell River, km 210.5; (F) 80 mm Copper Creek, km 87.2.....122

Figure 11. Individuals of *Pleuonaia* sp. cf. *barnesiana* depicting size classes and variation in periostracum color and ray patterns: (A) 28 mm from Clinch River, km 441.9; (B) 35 mm from Clinch River, km 435.8; (C) 47 mm from Copper Creek, km 24.1; (D) 55 mm from Indian Creek (Powell Drainage), km 0.3; (E) 60 mm from Clinch River, km 435.8; (F) 71 mm from Clinch River, km 435.8.....123

Figure 12. Individuals of *Pleuonaia dolabelloides* depicting size classes and variation in periostracum color and ray patterns: (A) 25 mm from Clinch River, km 435.8; (B) 43 mm from Clinch River, km 441.9;

	(C) 49 mm from Middle Fork Holston River, km 15.4; (D) 58 mm from Clinch River, km 441.9; (E) 69 mm from Powell River, km 210.5; (F) 83 mm from Middle Fork Holston River, km 16.3	124
Figure 13.	Conglutinates and glochidia of: <i>Fusconaia cor</i> (A, B) from Clinch River (rkm 435.8); <i>Fusconaia subrotunda</i> (C, D) from Clinch River (rkm 441.9); <i>Pleurobema oviforme</i> (E, F) from North Fork Holston River (rkm 175.2); and <i>Pleurobema</i> sp. cf. <i>oviforme</i> from Little River (rkm 47.6).....	125
Figure 14.	Conglutinates and glochidia of: <i>Pleuonaia barnesiana</i> (A, B) from Copper Creek (rkm 21.7) and Possum Creek (rkm 12.2), respectively; <i>Pleuonaia</i> sp. cf. <i>barnesiana</i> (C, D) from Clinch River (rkm 441.9) and Copper Creek (rkm 21.7), respectively; and <i>Pleuonaia dolabelloides</i> from Middle Fork Holston River (rkm 16.3).....	126
Figure 15.	Decision tree from classification and regression tree analysis using traditional morphometric and foot color data. Overall accuracy on terminal nodes was 61.98%.....	128
Figure 16.	Decision tree from classification and regression tree analysis using quantitative, foot color, and categorical variables from individuals sacrificed to represent live individuals. These data include non-genetically identified individuals from the FMCC shell collection. Overall accuracy on terminal nodes was 77.50%.....	129

Figure 17.	Decision tree from classification and regression tree analysis using quantitative and categorical variables from individuals sacrificed to represent shell-only individuals. These data include non-genetically identified individuals from the FMCC shell collection. Overall accuracy on terminal nodes was 80.63%	130
Figure 18.	Canonical variates analysis (CVA) plot using geometric morphometric data depicting canonical variates one and two as X- and Y- axes, respectively. Larger symbols indicate species means	131
Figure 19.	Mean outline of shells for each species using coordinates from geometric morphometrics data; outlines were created by displaying mean coordinates for each species, then lines were manually drawn.....	132

Chapter 3. Development and testing of morphology-based dichotomous keys for selected freshwater mussels in the genera *Fusconaia*, *Pleurobema*, and *Pleuroaia* in the upper Tennessee River basin of Tennessee and Virginia:

Figure 1.	External (top) and internal (bottom left) shell characters investigated in this study, including anatomical regions (bottom right) of the shell	162
Figure 2.	Typical external and internal traits of <i>Fusconaia cor</i>	163
Figure 3.	Typical external and internal traits of <i>Fusconaia cuneolus</i>	164
Figure 4.	Typical external and internal traits of <i>Fusconaia subrotunda</i>	165
Figure 5.	Typical external and internal traits of <i>Pleurobema oviforme</i>	166
Figure 6.	Typical external and internal traits of <i>Pleurobema</i> sp. cf. <i>oviforme</i>	167

Figure 7.	Typical external and internal traits of <i>Pleuonaia barnesiana</i>	168
Figure 8.	Typical external and internal traits of <i>Pleuonaia</i> sp. cf. <i>barnesiana</i>	169
Figure 9.	Typical external and internal traits of <i>Pleuonaia dolabelloides</i>	170

CHAPTER 1

Molecular phylogenetics of select mussel species in the genera *Fusconaia*, *Pleurobema*, and *Pleuonaia* using mitochondrial *ND1* and nuclear *ITS1* DNA sequences

ABSTRACT

Freshwater mussels in the genera *Fusconaia*, *Pleurobema*, and *Pleuroaia* appear similar in their external shell morphology, which has made classification of species within these genera difficult and has led to many taxonomic revisions. I collected large samples ($N=476$) of select mussel species in these genera from 2012 through 2014, primarily in the upper Tennessee River basin of Tennessee and Virginia. I analyzed mitochondrial *NDI* and nuclear *ITS1* DNA sequences in order to determine phylogenetic relationships among taxa. Nine species were phylogenetically verified as distinct at *NDI*, three of which are potentially unrecognized or cryptic species, each separated at this gene region by 2.85%, 3.17%, and 6.32% from their respective closest congener for each species. I analyzed the nuclear *ITS1* gene region's nucleotide-site insertion/deletion (indel) patterns as single mutational events rather than as fifth character states or missing data. Most species were phylogenetically distinct at the *ITS1* region when incorporating indels into analyses, but some estimated interspecific pairwise distances were lower than corresponding intraspecific estimates. Due to the limited known geographical distribution of these three cryptic species, each may require protection under the U.S. Endangered Species Act. While this study collected large sample sizes for each species, many streams in the basin remain unsampled and could potentially contain populations of these species or additional cryptic species.

KEYWORDS: Cryptic Species, Phylogenetic Assessment, Mitochondrial DNA, Nuclear DNA, *NDI*, *ITS1*, *Fusconaia*, *Pleurobema*, *Pleuroaia*

INTRODUCTION

Freshwater mussels are considered the most imperiled taxonomic group in North America (Williams et al. 1993; Neves et al. 1997). Of the 297 recognized species in the families Unionidae and Margaritiferidae in North America, 213 – or approximately 70% – are considered endangered, threatened or of special concern (Williams et al. 1993). Extinction rates for freshwater taxa are five times greater than those for terrestrial fauna and similar to rates estimated for tropical rainforest communities (Ricciardi and Rasmussen 1999). Freshwater mussel habitat has been lost, fragmented, and degraded due to anthropogenic effects from dam construction, sedimentation, and water pollution (Williams et al. 1993; Watters 1996; Hughes and Parmalee 1999; Haag 2012). The sedentary nature of adult unionid mussels and their general reliance on fish hosts to disperse their glochidia makes recolonization of isolated stream reaches difficult, especially those blocked by dams. Translocation and propagation efforts for mussels are underway to restore mussels to rivers with suitable water and habitat quality (Jones and Neves 2002; Haag and Williams 2014). Protection and restoration of habitat is important for freshwater mussels, not only to address their imperiled status, but also because they serve valuable roles in stream ecosystems (Spooner and Vaughn 2006; Vaughn et al. 2008).

Since the late 1600s, taxonomic classification of freshwater mussels has been based primarily upon shell morphology (Williams et al. 2008). Approaches to classification have changed as authors have incorporated additional characters, including soft anatomy, larval morphology, and life-history traits. With the recent advent of molecular genetic techniques, mussel taxonomy has undergone further reorganization at the species, genus and family levels (Graf and Cummings 2007).

Isaac Lea (1836), one of the earliest malacologists, devised a classification system to group species into genera based solely on shell morphology. Charles Simpson (1900) revised Lea's work and rearranged the classification of many species and genera based upon larval morphology. Simpson's taxonomy then was revised by Arnold Ortmann (1912), who relied on soft anatomy and shell characteristics. More revisions were made during the 20th and 21st centuries as authors utilized more characters, such as number and position of marsupial gills and variation at molecular markers (Ortmann 1912; Heard and Guckert 1970; Williams et al. 2008). For example, molecular markers have been used to distinguish various mussel genera and species, leading to a number of recent taxonomic revisions (Gangloff et al. 2006; Jones et al. 2006; Zanatta and Murphy 2006; Jones and Neves 2010; Campbell and Lydeard 2012a,b).

Ideally, studies delineating taxa should analyze taxonomic relationships using data from a variety of character sets, including morphology, molecular markers and life-history traits (Jones et al. 2006). This comprehensive approach encompasses a fuller range of the phenotypic and molecular genetic variation needed to reliably distinguish populations, species, and groups at higher taxonomic levels. Introgressive hybridization, cryptic species, phenotypic plasticity, and variable life-history strategies can mask characters within and among species. For example, a phenomenon that can mask species divergence is introgression of deoxyribonucleic acid (DNA) from one species into another species (Ballard and Whitlock 2004). In such cases, examining a single gene region may not reveal the phylogeny of the species, but rather the phylogeny of the DNA region. If the selected gene region had been introgressed from another species, the lack of observed variation between distinct species would indicate only one species, whereas other genetic regions and morphological traits potentially could indicate introgression and differentiate the respective species. Another phenomenon masking species divergence is the occurrence of

genetically diverged species that appear morphologically similar, i.e., cryptic species (Bickford et al. 2007). In contrast, morphologically distinct populations may not represent unique species, but rather appear different because expressed phenotypic traits are being influenced by contrasting environmental conditions (Scheiner 1993); therefore, it is important to incorporate genetic markers into phylogenetic analyses to reduce over-classification of phenotypically plastic species. Further, life-history strategies often reflect a species' success in expressing foraging, defense, and reproductive behaviors, and can cause genetic isolation of populations by geographic or behavioral barriers that may not be observable through morphological traits alone (Miyatake and Shimizu 1999). For example, Bart et al. (2010) showed that morphologically distinct *Ictiobus* Buffalofishes exhibited interspecific introgression to such an extent that they did not form distinct phylogenetic clades based upon both mitochondrial (mtDNA) and nuclear DNA, illustrating how reliance on only molecular markers would have resulted in failure to recognize morphologically distinct species. Additionally, Christian et al. (2008) found cryptic mussel species that appeared morphologically similar, but were genetically distinguishable based upon mtDNA, illustrating that reliance on only morphological characters would not have recognized distinct species. Langerhans et al. (2004) discovered phenotypic plasticity in Mosquitofish *Gambusia affinis* morphology driven by the presence or absence of predators in both wild and captive-bred populations. Vences et al. (2002) demonstrated that diversification in *Boophis* frogs was due to behavioral isolation caused by differences in breeding habitat; pond-breeders exhibited lower diversification than brook-breeders due to lack of consistently available breeding habitats, which led to higher numbers of effective migrants and hence greater mixing of genes between populations. Therefore, when studying differences among taxa, it is important to

study multiple character sets; over-reliance on one data type can lead to misclassification of taxa (Jones et al. 2006).

The Tennessee and Cumberland River basins, major tributaries of the Ohio River, collectively hold the highest diversity of freshwater mussel species in North America (Haag 2012). Several mussel species of interest in this study, *Fusconaia cor*, *Fusconaia cuneolus*, and *Pleuroaia barnesiana*, are endemic to the Tennessee River basin, with *Pleuroaia gibberum* endemic to the Cumberland River basin, whereas *Pleurobema oviforme* and *Pleuroaia dolabelloides* are endemic to the Tennessee and Cumberland River basins, and *Fusconaia subrotunda* occurs broadly throughout the Ohio River basin (Parmalee and Bogan 1998; Watters et al. 2009). The United States Fish and Wildlife Service (USFWS) listed *F. cor* and *F. cuneolus* as endangered in 1975 (USFWS 1975), *P. gibberum* as endangered in 1991 (USFWS 1991), *P. dolabelloides* as endangered in 2013 (USFWS 2013) and *P. oviforme* as a federal species of concern. Traditionally, *P. barnesiana*, *P. dolabelloides* and *P. gibberum* were classified in the genera *Fusconaia*, *Lexingtonia*, and *Pleurobema*, respectively, but were taxonomically revised by Campbell et al. (2005) based on results of a phylogenetic assessment using mtDNA sequences; these three species grouped together within a clade separate from species in the genera *Fusconaia* and *Pleurobema* (Campbell et al. 2005). From existing taxonomic nomenclature and type specimens, Williams et al. (2008) designated *P. barnesiana* as the type species for the revitalized genus *Pleuroaia*, which includes *P. barnesiana*, *P. dolabelloides* and *P. gibberum*. Ortmann (1918) considered *P. barnesiana* as "distinguished from the other [*Fusconaia*] species by very shallow beak cavities."

Against this background, the purpose of this study was to conduct a phylogenetic assessment of mussels in the genera *Fusconaia*, *Pleurobema*, and *Pleuroaia* in the upper

Tennessee River basin (UTRB). While previous studies typically have relied on small sample sizes to infer phylogenetic relationships within and among freshwater mussel species, this study surveyed more collection sites and utilized larger sample sizes per site and species in order to detect genetic variation and potential cryptic biodiversity among taxa. This study is based on the assumption that assessment of DNA variation will provide a foundation for understanding phenotypic variation among these conchologically similar taxa. The specific objectives of this study were to: (1) conduct phylogenetic assessments of select morphologically defined mussel species in the genera *Fusconaia*, *Pleurobema* and *Pleuroaia* in the UTRB and assess species identity using the phylogenetic species concept, and (2) provide genetically identified individuals of each species for use in morphological assessment (Chapter 2) and for use in development and testing of a morphology based identification key for this group of mussels (Chapter 3).

METHODS

Mussel Collections. – Freshwater mussels were collected from 2012 through 2014 in the UTRB primarily in three areas, the upper Clinch, Holston and Powell river watersheds, and also in select tributaries of the Tennessee River downstream of that region (Figure 1). Mussels also were collected from the Collins River, TN in the upper Cumberland River basin and from Craig Creek, VA in the upper James River basin. Sites were selected based on the results of previous sampling efforts to represent each species' geographical distribution in the UTRB. Freshwater mussels representing the respective genera and species were hand-collected via snorkel search or using view scopes and transported to the Virginia Tech Freshwater Mollusk Conservation Center, Blacksburg, Virginia, in a 75-liter cooler with a portable aerator. Upon arrival, mussels were acclimated to water held in a temperature-controlled, 1000-liter recirculating aquaculture

system (RAS) by placing aliquots of water from the RAS into the cooler containing the mussels, thereby allowing slow adjustment to water chemistry and temperature. After acclimation, mussels were placed into the RAS in separate plastic containers labeled with collection information until tissue samples, measurements and photographs were taken of each individual.

DNA Extraction. – Mussels were removed from the RAS and gently opened to a maximum width of 6-8 mm to non-lethally obtain a tissue sample using an Isohelix (Harrietsham, UK) SK-2 buccal swab (Moyer and Díaz-Ferguson 2012). The foot was swabbed vigorously with four to six strokes to obtain tissue for DNA extraction (Henley et al. 2006), and then the mussel was returned to the RAS. The tissue sample was transported to the Integrated Life Sciences Building at Virginia Tech, where it was chemically stabilized and DNA extraction was performed using the Isohelix (Harrietsham, UK) DDK Isolation Kit according to the manufacturer's instructions.

Polymerase Chain Reaction. – The first subunit of the NADH dehydrogenase (*NDI*) region of mtDNA and the nuclear ribosomal Internal Transcribed Spacer region (*ITS1*) were amplified by polymerase chain reaction (PCR). Sequences from several species for each respective genus were amplified using primers and conditions reported by Serb et al. (2003) for *NDI* and King et al. (1999) for *ITS1*. Primers for *NDI* were modified and used in a multiplex to include one forward primer for all genera and two reverse primers, one to amplify species in the genera *Fusconaia* and *Pleuonaia*, and the other to amplify species in the genera *Pleurobema* and *Sintoxia* (Campbell and Lydeard 2012a) as detailed below. Primer sequences used to amplify *NDI* sequences for *Fusconaia* and *Pleuonaia* species were: forward: 5'–

GAAAAGTGCATCAGATTAAAGCTCT -3'; and reverse: 5'-
CCTGCTTGGAAGGCAAGTGTACT -3'. The forward *NDI* primer for *Pleurobema* and
Sintoxia species was the same, but the reverse primer was: 5'-
AGATTTTCAGGCTATTGCTATTAG -3'. Primers for *ITS1* were modified to exclude a poly-
adenine region thought to influence primer annealing, and were: forward: 5'-
GGTGAACCTGCGGAAGGATCATTACC -3'; and reverse: 5'-
TGCGTTCTTCATCGACCCACGAGCCG -3'. The *NDI* and *ITS1* PCR reaction mixtures
consisted of 1 μ L of unquantified genomic DNA, 2.2X PCR buffer, 3.96 mM MgCl₂, 0.36 mM
each dNTP, 0.36 μ M each primer, 0.36 mg/mL BSA, 0.5U GoTaq DNA polymerase and ddH₂O
added to a total volume of 22 μ L. Touchdown PCR protocols were used instead of traditional
PCR protocols in order to increase the amplification success rate; the primers and protocols used
in previous studies led to inconsistent amplification of the target molecular markers. The
thermal cycling profile consisted of an initial 95 °C for 3 min; followed by a touchdown PCR
protocol that consisted of 10 cycles of denaturation at 95 °C for 30 sec, annealing at 62 °C for 45
sec and extension at 72 °C for 60 sec, with the annealing temperature decreased by 0.5 °C per
cycle; followed by 25 cycles of denaturation at 95 °C for 30 sec, annealing at 56 °C for 45 sec
and extension at 72 °C for 60 sec, with the annealing temperature decreased by 0.3 °C per cycle
and extension time increased by 5 sec per cycle; with a final extension step at 72 °C for 2 min;
and a final hold at 4 °C.

After PCR reactions, DNA concentration was quantified using a Hoefer DyNA Quant
200 fluorometer (Hoefer Pharmacia Biotech, San Francisco, CA), diluted to 10 ng/mL, and sent
to the Virginia Bioinformatics Institute, where samples were prepared using an Applied
Biosystems (Thermo Fisher Scientific, Massachusetts, USA) Big Dye Terminator 3.1 Cycle

Sequencing Kit and then sequenced on an Applied Biosystems 3730 DNA Analyzer with Pop-7 polymer (Thermo Fisher Scientific, Massachusetts, USA).

Data Analyses. – Forward and reverse *NDI* and *ITS1* DNA sequences were assembled and edited using the program Geneious version 7.1.5 (Biomatters, San Francisco, California). Mitochondrial *NDI* and nuclear *ITS1* sequences were aligned using the default settings in the program Clustal W (Thompson et al. 1994) imbedded in MEGA version 5.05 (Tamura et al. 2011). Because *ITS1* is a nuclear gene in ribosomal DNA (rDNA), it has biparental inheritance where offspring can inherit *ITS1* gene regions with differing sequence lengths or nucleotides. Also, the *ITS1* gene region is located within rDNA and is highly used by cells of organisms; thus, multiple tandem copies of the *ITS1* gene region occur. Since some individuals in my study contained multiple distinct *ITS1* sequences of different lengths within an individual and proved difficult to resolve unambiguously, DNA sequences from these individuals were excluded from the analyses (Campbell et al. 2008). Data from heterozygous individuals with nuclear *ITS1* sequences containing single nucleotide polymorphisms that were not insertions or deletions were coded and reported using standard International Union of Biochemistry codes. DNA sequences were queried using the Basic Local Assignment Search Tool, also known as BLAST (Altschul et al. 1990), against the National Center for Biotechnology Institute database to verify gene identity and species-level assignment. However, because aligned *ITS1* sequences have insertions/deletions (indels) that can affect alignment accuracy, they also were aligned a separate time using default settings in webPRANK (Löytynoja and Goldman 2010) to characterize topological differences of phylogenetic tree results using different alignment algorithms (Nagy et al. 2012). For each *ITS1* alignment, indels were coded using binary characters to represent gaps

as either present, absent, or unknown (Simmons and Ochoterena 2000; Nagy et al. 2012) using the program FastGap (Borchsenius 2009).

Haplotype diversity was analyzed using DnaSP 5 (Librado and Rozas 2009); variable and phylogenetically informative sites for each haplotype were identified. The program jModelTest (Darriba et al. 2012) was used to determine the best nucleotide substitution model for *NDI* and *ITS1* sequences separately; the number of substitution schemes analyzed in jModelTest was reduced from the default of eleven schemes to three schemes in order to reflect the substitution models available for coding in the program MrBayes v3.2.1 (Huelsenbeck and Ronquist 2001). To test the validity of combining data, *NDI* and *ITS1* sequences were combined and analyzed in PAUP (Swofford 2002) for incongruent length differences in tree topologies using the homogeneity partition test (Dowton and Austin 2002); the homogeneity partition test determines if random selections of combined gene regions differs significantly in topological arrangement from each gene tree analyzed separately; congruence of sequences is generally recognized at $p > 0.05$ (Dowton and Austin 2002). Results from the homogeneity partition test were significant ($p = 0.01$), indicating incongruence between nuclear and mitochondrial trees, and thus DNA sequences were not combined for subsequent phylogenetic analyses.

Phylogenetic trees were constructed using Bayesian inference in MrBayes using two runs each with three cold chains and one hot chain and allowed to run until split frequencies, or the difference in standard deviations between the two runs, consistently stayed below 0.01; hot chains are randomly chosen at each generation in an attempt to swap frequencies while cold chains remain unchanged during each generation. Results from jModelTest indicated that the General Time Reversible model with invariable sites and a gamma-shaped distribution (GTR+I+G) was the best nucleotide substitution model for *NDI*. Phylogenetic analysis of *NDI*

was run in MrBayes for 10 million Markov chain Monte Carlo generations, with a burn-in of 2.5 million generations, tree search temperature set at 0.05, and sampling every 1000 generations, resulting in split frequencies of 0.0065. Results from jModelTest indicated that the Jukes-Cantor model was the best nucleotide substitution model for *ITS1*. Aligned sequences with coded gaps from Clustal W and webPRANK for all individuals were run in MrBayes for 2 million generations, with a burn-in of 0.5 million generations, default tree search temperature of 0.10, and sampling every 100 generations, resulting in split frequencies of 0.0067 and 0.0065 for each sequence alignment, respectively. The program FigTree v1.4.0 (Rambaut 2007) was used to view and modify phylogenetic trees created by MrBayes. Phylogenetically based species were identified by observing statistically well supported monophyletic clades within phylogenetic trees. Pairwise genetic distances between putative phylogenetic species were estimated in PAUP. Arbogast et al. (2002) recommended incorporating the best-fitting nucleotide substitution model when assessing divergence between species; hence pairwise genetic distances for *ND1* were analyzed using the substitution model GTR+G instead of GTR+I+G because the program could not accept invariable sites for the analysis; thus, the next highest Bayesian information criterion (BIC) model was implemented. Because nucleotide substitution models in PAUP cannot incorporate binary characters, mean uncorrected *p*-distances between species were estimated for *ITS1*.

RESULTS

Mussel Collections. – A total of 476 freshwater mussels were collected from 53 sites (Table 1) in 23 streams in the UTRB for phylogenetic assessment of nucleotide variation at the mitochondrial gene *ND1* and nuclear gene region *ITS1* (Table 2). At most collection sites, a

maximum of 20 individuals were retained for morphological analyses (see Chapter 2); additional collections were made at some sites in order to obtain gravid individuals for future analyses or because the species was not abundant at other sites. Since mussel densities or time spent collecting were not recorded during the study, any particular collection should be viewed as indicating the presence of a species rather than its absence. In this regard, several notable collections or lack thereof were made during this project. For example, in North Fork Holston River, Jones and Neves (2007) found *F. cor* and *P. dolabelloides* abundant at the Possum Hollow Road site in 1999–2000; but during this project in 2012, few mussels were collected there, including only two individuals of *F. cor*, results similar to those of Ostby et al. (2010). One of these individuals was a young *F. cor* measuring 23 mm, indicating that the species is still reproducing in this section of river even after a significant population decline (Ostby et al. 2010). Earlier surveys indicated that *P. dolabelloides* likely still occurs in this stream reach, but it was not collected at this site during my study. Similar to the results of Johnson (2011), *P. oviforme* was not found during this study in the Powell River or in one of its main tributaries, Indian Creek.

Pleuronaia sp. cf. *barnesiana* was collected primarily in upper Clinch River or its tributaries in Virginia. In addition, one individual was collected from each of the Powell and South Fork Chickamauga drainages. However, it is likely that this species occurred in many small tributaries of the UTRB, but since it occurred sympatrically with *P. barnesiana* and *P. oviforme* it has been misidentified due to its similarity in shell morphology to these other two species; thus, accurate collection records for *P. sp. cf. barnesiana* do not exist.

ND1. – I amplified approximately 900 base-pairs (bp) of DNA sequence for individuals in the genera *Fusconaia* and *Pleuroaia* and approximately 825 bp for individuals in the genera *Pleurobema* and *Sintoxia*. Within and among these species and genera, 151 haplotypes were observed among 476 individuals, with 330 polymorphic nucleotide sites (Table 3), with many of the haplotypes observed for each species shared among sampling sites (Table S1).

Forty-six individuals of *F. cor* were sampled from the Powell ($N = 3$), Clinch ($N = 41$), and North Fork Holston ($N = 2$) drainages (Table 2). Seven haplotypes were observed among individuals from these three drainages, two in the Powell, all seven in the Clinch, and one in the North Fork Holston (Table S1). Haplotypes observed in the Powell and North Fork Holston drainages were shared with those from the Clinch drainage, with the latter containing five unique haplotypes. Using the substitution model GTR+G, intraspecific distances among all haplotypes ranged from 0.0011–0.0091 and averaged 0.0042.

Twenty-eight individuals of *F. cuneolus* were sampled from the Clinch ($N = 27$) and Little River, Blount County, TN ($N = 1$) drainages (Table 2). Thirteen haplotypes were observed among individuals from these two drainages, all 13 in the Clinch and just one in the Little (Table S1), with the haplotype from the Little drainage shared with individuals from the Clinch drainage. Intraspecific distances among all haplotypes ranged from 0.0011–0.0103 and averaged 0.0055.

Forty-four individuals of *F. subrotunda* were sampled from the Powell ($N = 9$), Clinch ($N = 34$), and Nolichucky ($N = 1$) drainages (Table 2). Twenty-four haplotypes were observed among individuals from these three drainages, six in the Powell, 18 in the Clinch, and one in the Nolichucky (Table S1). Only one haplotype was shared between the Powell and Clinch drainages, with five unique haplotypes observed in the Powell drainage, 17 in the Clinch

drainage, and one in the Nolichucky drainage. Intraspecific distances among all haplotypes ranged from 0.0011–0.0219 and averaged 0.0103.

Nine individuals of *F. masoni* were sampled from Craig Creek (Table 2), and two haplotypes were observed (Table S1). Intraspecific distances between the haplotypes was 0.0011.

One-hundred-and-four individuals of *P. oviforme* were sampled from the following drainages: Clinch ($N = 16$), North Fork Holston ($N = 32$), Middle Fork Holston ($N = 2$), Beech, Hawkins County, TN ($N = 18$), Nolichucky ($N = 3$), Little Pigeon ($N = 3$), Little, Blount County, TN ($N = 2$), Little Tennessee ($N = 13$), Hiwassee ($N = 5$), South Chickamauga ($N = 5$), Paint Rock ($N = 2$), and Duck ($N = 3$) (Table 2). Thirty-eight haplotypes were observed among individuals from these 12 drainages: eight in Clinch, nine in North Fork Holston, two in Middle Fork Holston, eight in Beech, three in Nolichucky, three in Little Pigeon, two in Little River, four in Little Tennessee, four in Hiwassee, three in South Chickamauga, two in Paint Rock, and one in Duck (Table S1). One haplotype was shared between each of the following drainages: North Fork Holston, Paint Rock and Duck; Clinch and North Fork Holston; North Fork Holston, Middle Fork Holston, and Little Pigeon; North Fork Holston, Beech, Little Tennessee, and Hiwassee; North Fork Holston and Little Tennessee; Beech, Nolichucky, and Little Tennessee. Unique haplotypes were observed for the Clinch ($N = 7$ haplotypes), North Fork Holston ($N = 4$), Middle Fork Holston ($N = 1$), Beech ($N = 6$), Nolichucky ($N = 2$), Little Pigeon ($N = 2$), Little ($N = 2$), Little Tennessee ($N = 1$), Hiwassee ($N = 3$), South Chickamauga ($N = 3$), and Paint Rock ($N = 1$) drainages. Intraspecific distances among haplotypes ranged from 0.0012–0.0181 and averaged 0.0086.

Twenty-four individuals of *P. sp. cf. oviforme* were sampled from the Little drainage, Blount County, TN (Table 2), and six haplotypes were observed (Table S1). Intraspecific distances among haplotypes ranged from 0.0011–0.0037 and averaged 0.0022.

Seventy-three individuals of *P. barnesiana* were sampled from the Powell ($N = 5$), Clinch ($N = 17$), North Fork Holston ($N = 9$), Middle Fork Holston ($N = 1$), Beech ($N = 7$), Nolichucky ($N = 6$), Little Pigeon ($N = 1$), Little ($N = 12$), Emory ($N = 5$), and Duck ($N = 10$) drainages (Table 2). Twenty-four haplotypes were observed among individuals from these ten drainages: three in Powell, five in Clinch, two in North Fork Holston, one in Middle Fork Holston, four in Beech, four in Nolichucky, one in Little Pigeon, eight in Little, one in Emory, and five in Duck. One haplotype was shared between each of the following drainages: North Fork Holston, Middle Fork Holston, Beech, Nolichucky, Little Pigeon, and Little; Powell and Clinch; Powell, Clinch, Nolichucky, and Little; North Fork Holston and Little. Unique haplotypes were observed for the Powell ($N = 1$), Clinch ($N = 3$), Beech ($N = 2$), Nolichucky ($N = 2$), Little ($N = 6$), Emory ($N = 1$), and Duck ($N = 5$) drainages. Intraspecific distances among haplotypes ranged from 0.0011–0.0200 and averaged 0.0109.

Sixty-six individuals of *P. sp. cf. barnesiana* were sampled from the Powell ($N = 1$), Clinch ($N = 64$), and South Chickamauga ($N = 1$) drainages (Table 2). Seven haplotypes were observed among individuals from these three drainages: one in Powell, six in Clinch, and one in South Chickamauga (Table S1). One haplotype was shared between Powell and Clinch drainages, with five unique haplotypes observed in the Clinch and one unique haplotype in the South Chickamauga drainages. Intraspecific distances among haplotypes ranged from 0.0011–0.0056 and averaged 0.0030.

Fifty-two individuals of *P. dolabelloides* were sampled in the Powell ($N = 2$), Clinch ($N = 17$), Middle Fork Holston ($N = 18$), Little ($N = 4$), and Duck ($N = 11$) drainages (Table 2). Twelve haplotypes were observed among individuals from these five drainages: one in Powell, five in Clinch, six in Middle Fork Holston, one in Little, and five in Duck (Table S1). One haplotype was shared between the Powell, Clinch, Middle Fork Holston, Little, and Duck drainages; two haplotypes were shared between the Clinch and Middle Fork Holston drainages. Unique haplotypes were observed for Clinch ($N = 2$), Middle Fork Holston ($N = 3$), and Duck ($N = 4$) drainages. Intraspecific distances among haplotypes ranged from 0.0011-0.0192 and averaged 0.0080.

Seven individuals of *P. sp. cf. dolabelloides* were sampled from the South Chickamauga drainage (Table 2), and two haplotypes were observed (Table S1). Intraspecific distance between the haplotypes was 0.0045.

Twenty individuals of *P. gibberum* were sampled from Collins River (Table 2), and 13 haplotypes were observed (Table S1). Intraspecific distances among haplotypes ranged from 0.0012–0.0159 and averaged 0.0085.

Three individuals of *Sintoxia rubrum* were sampled from the Clinch ($N = 1$) and Duck ($N = 2$) drainages, each river exhibiting a unique haplotype (Table S1). Intraspecific distances among haplotypes ranged from 0.0024–0.018 and averaged 0.0128.

Phylogenetic and Pairwise Genetic Analyses of ND1. – Phylogenetic analysis of ND1 DNA sequences and construction of a phylogenetic tree showed that the genera *Fusconaia*, *Pleurobema*, and *Pleuonaia* each formed monophyletic clades (Figure 2); however, *P. gibberum* was not closely associated with other *Pleuonaia* species. Although the sample size was low (N

= 3), *S. rubrum* was phylogenetically distinct from the other *Pleurobema* species. Further, pairwise genetic distances between *S. rubrum* and *P. oviforme* and *P. sp. cf. oviforme* were 13.13% and 11.54%, respectively, while the pairwise distance between the two *Pleurobema* species was 6.32%. Individuals of *P. gibberum* were phylogenetically distinct from the other *Pleurobema* species, and pairwise genetic distances between *P. gibberum* and the other members of the genus were higher than pairwise genetic distances observed among the other *Pleurobema* species. Intra-specific variation estimates were 6.62%, 6.32%, and 9.53% for *Fusconaia*, *Pleurobema*, and *Pleurobema*, respectively. Removal of *P. gibberum* haplotypes from the other sequences of *Pleurobema* reduced intra-specific variation to 6.21%.

Sequences of *F. cor*, *F. cuneolus*, *F. masoni*, *F. subrotunda*, *P. oviforme*, *P. gibberum*, *P. dolabelloides* and *P. barnesiana* formed species-specific monophyletic clades (Figure 2). Within the respective clades for *P. barnesiana*, *P. dolabelloides*, and *P. oviforme*, previously unrecognized, phylogenetically distinct sub-clades with 100% posterior probability values were identified. Estimated interspecific pairwise genetic mean distances among all species ranged from 2.85% to 17.23% (Table 4). The estimated interspecific distance between *P. barnesiana* and *P. sp. cf. barnesiana* was 2.85%, between *P. dolabelloides* and *P. sp. cf. dolabelloides* 3.17%, and between *P. oviforme* and *P. sp. cf. oviforme* 6.32%. The highest observed interspecific distance was between *F. cor* and *P. sp. cf. barnesiana* at 17.23%.

Considering variation across the species studied, mean intra-specific distances among haplotypes within species ranged from a low of 0.22% to a high of 1.09%. Mean intra-specific pairwise genetic distance within *P. barnesiana* averaged 1.09%, and the inferred phylogeny was comprised of three distinct subclades separated by genetic distances of 1.36% to 1.47%. These three distinct subclades did not reflect geographic distributions, as each subclade contained

haplotypes sampled from different drainages. The species *F. subrotunda* exhibited intraspecific distances of 1.03%, which is represented visually by the nesting of clades within one another within the main clade for the species. A mean intraspecific distance of 0.80% was observed in *P. dolabelloides*, with two haplotypes separated by approximately 1.72% from the main clade; Grobler et al. (2006) obtained similar results for this species, with one haplotype that was collected from approximately the same location in the Clinch River at Cleveland Islands; removal of the two haplotypes from the pairwise genetic analyses reduced intraspecific variation to 0.40%.

ITS1. – Approximately 520 bp of the nuclear *ITS1* gene were sequenced and analyzed for 103 individuals, a subset of those that had been sequenced for *ND1*; due to time constraints and funding limitations, select individuals were arbitrarily selected from sample sites across the distribution of the species within the UTRB and used for analysis of *ITS1*. Twenty-eight haplotypes were observed within this sample, including the outgroup sequence from *Lampsilis fasciola*. The program Clustal W produced a sequence alignment that contained 104 polymorphic nucleotide sites including indels; use of FastGap encoded 34 gap positions using these indels (Table 5). The program webPRANK produced an alignment that contained 130 polymorphic nucleotide sites including indels; FastGap encoded 46 gap positions (Table 6).

Eight individuals of *F. cor* were sequenced from the Powell ($N = 2$), Clinch ($N = 4$), and North Fork Holston ($N = 2$) drainages (Table S2), and only one haplotype was observed. Eight individuals of *F. cuneolus* were sequenced from Clinch drainage; four haplotypes were observed, one of which was shared with *F. masoni*. Eight individuals of *F. masoni* were sequenced from Craig Creek, and only one haplotype was observed. Four individuals of *F. subrotunda* were

sequenced from the Powell ($N = 2$), Clinch ($N = 1$), and Nolichucky ($N = 1$) drainages; three haplotypes were observed: one was shared between the Powell and Clinch drainages; and one was unique to each Powell and Nolichucky drainages. Thirteen individuals of *P. barnesiana* were sequenced from the Powell ($N = 2$), Clinch ($N = 2$), North Fork Holston ($N = 3$), Middle Fork Holston ($N = 1$), Little ($N = 2$), Emory ($N = 1$), and Duck ($N = 2$) drainages; three haplotypes were observed: one was shared between the Powell, Clinch, North Fork Holston, Middle Fork Holston, Little, Emory, and Duck drainages; one was shared between the Clinch, North Fork Holston, and Little drainages; and one was unique to the Middle Fork Holston drainage. Fourteen individuals of *P. sp. cf. barnesiana* were sequenced from the Powell ($N = 1$) and Clinch ($N = 13$) drainages; two haplotypes were observed: one was shared between the Powell and Clinch drainages; and one was unique to the Clinch drainage. Seven individuals of *P. dolabelloides* were sequenced from the Powell ($N = 1$), Clinch ($N = 4$), Middle Fork Holston ($N = 1$), and Duck ($N = 1$) drainages; one haplotype was observed among all four drainages and one was unique to the Clinch drainage. Five individuals of *P. sp. cf. dolabelloides* were sequenced from the South Chickamauga drainage, and two haplotypes were observed. Eight individuals of *P. gibberum* were sequenced from Collins River, and only one haplotype was observed. Seventeen individuals of *P. oviforme* were sequenced from the Clinch ($N = 2$), North Fork Holston ($N = 4$), Beech ($N = 3$), Nolichucky ($N = 3$), Little ($N = 1$), Little Tennessee ($N = 1$), South Chickamauga ($N = 2$), and Paint Rock ($N = 1$) drainages; six haplotypes were observed from the eight drainages: one haplotype was shared between the Clinch, North Fork Holston, Beech, Little, Little Tennessee, and South Chickamauga drainages; one unique haplotype was observed from each of the Clinch, South Chickamauga, and Paint Rock drainages; and the Nolichucky drainage had two unique haplotypes. Thirteen individuals of *P. sp. cf. dolabelloides*

were sequenced from the Little drainage, and two haplotypes were observed. Two individuals of *S. rubrum* were sequenced, one from each of the Clinch and Duck drainages; only one haplotype was observed.

Results of phylogenetic analysis of *ITS1* DNA sequences revealed low to moderate separation of species, e.g., by one or two nucleotide changes, but which separated many of the respective genera (Figures 3 and 4). With the gap-coded alignment produced by Clustal W, the genus *Pleuroaia* was not monophyletic, with *P. gibberum* being strongly separated from other members of the genus and placed near the *Fusconaia* clade. When the phylogenetic analysis was conducted using the gap-coded alignment created by webPRANK, *P. gibberum* grouped closer to other members of *Pleuroaia*; however, *S. rubrum* grouped within *P. oviforme*.

Estimated pairwise genetic distances among species' haplotypes using the gap-coded alignment created by Clustal W ranged from 0.00% to 3.40% for *F. cuneolus* vs. *F. masoni* and *P. sp. cf. oviforme* vs. *P. sp. cf. dolabelloides*, respectively, and intraspecific variation ranged from 0.19% to 0.71% (Table 7). Only one haplotype was observed for *F. masoni*, and it was identical to a *F. cuneolus* haplotype; when excluding interspecific variation between *F. cuneolus* and *F. masoni*, the lowest interspecific variation was 0.37% observed between *F. cor* and *F. cuneolus*/*F. masoni*. In three cases (namely, *F. cuneolus* vs. *F. masoni*; *P. dolabelloides* vs. *P. barnesiana*; and *P. dolabelloides* vs. *P. sp. cf. dolabelloides*), intraspecific variation was equal to or greater than that for interspecific variation; however, intraspecific variation was not always observed, as some species were represented by only one haplotype, i.e., *F. cor*, *F. masoni*, *P. gibberum*, and *S. rubrum*.

The estimated pairwise genetic distances among species using the gap-coded alignment created by webPRANK ranged from 0.00% to 3.45% for *F. cuneolus* vs. *F. masoni* and *P. sp. cf.*

oviforme vs. *P. barnesiana*, respectively, and intraspecific variation ranged from 0.19% to 0.75% (Table 8). When excluding interspecific variation between *F. cuneolus* and *F. masoni*, the lowest observed interspecific variation was 0.37%, which was between *F. cor* and *F. cuneolus*/*F. masoni*. The same three instances for intraspecific variation exceeding interspecific variation were observed using the webPRANK and ClustalW alignments.

DISCUSSION

Development of Molecular Markers. – Using multiple PCR primers to amplify target DNA sequences for species across several genera increased the amplification success rate in this study. The *NDI* primers created by Serb et al. (2003) did not consistently amplify target sequences for all individuals in this study, and so I aligned one or two sequences representing each species in order to identify regions suitable for annealing of new primers. One target region was identified for annealing the forward primer for all species, but no one region was identified for annealing the reverse primer. When considered independently, two groups of genera, (1) *Fusconaia* and *Pleuronaia* and (2) *Pleurobema* and *Sintoxia*, each had suitable annealing regions for a reverse primer. Hence, in order to sequence *NDI*, the DNA sequence in the forward direction was inspected first to determine the group to which it belonged, and the appropriate reverse primer was identified.

I encountered a problem regarding length differences among multiple *ITS1* sequences within an individual rendering the raw sequence data unreadable for some individuals. Elderkin (2009) cloned sequences for *Cumberlandia monodonta* in the family Margaritiferidae and found multiple *ITS1* variants in each individual. I did not characterize the *ITS1* length differences within an individual explicitly because of the large amount of time that would be required to

clone and sequence each variant. In contrast, I analyzed variation among individuals from the family Unionidae only where one *ITS1* variant was observed per individual, which was the case in 62% of the individuals screened. While cloning and analyzing all *ITS1* sequences would be appropriate for assessing variation, it should be approached with caution, as cloning itself can result in sequencing errors (Tedesoo et al. 2014).

Phylogenetic and Pairwise Analyses of NDI. – Phylogenetic and pairwise genetic analyses indicated that the six study species (*F. cor*, *F. cuneolus*, *F. subrotunda*, *P. oviforme*, *P. barnesiana*, and *P. dolabelloides*) each formed a distinct monophyletic clade. Although individuals of both species are morphologically similar, the distinctiveness of *F. cor* and *F. cuneolus* was confirmed using DNA sequences. Both species occur sympatrically in the Clinch River, and the *NDI* sequences from both species each formed distinct monophyletic clades, which were separated by 5.58% based upon pairwise genetic distances. Phylogenetic analyses also resulted in the recognition of potential cryptic species within the genera *Pleurobema* and *Pleuonaia*. *Pleurobema* sp. cf. *oviforme* collected from Little River in Blount County, TN formed a monophyletic clade distinct from *P. oviforme*; these two species were collected sympatrically in the Little River and were separated by a genetic distance of 6.32%. The *Pleuonaia* sp. cf. *barnesiana* sequences sampled in the UTRB, including individuals collected from Georgia, formed a monophyletic clade distinct from *P. barnesiana*; further, these two species were collected sympatrically in the Clinch and Powell drainages and were separated by a genetic distance of 2.85%. The *Pleuonaia* sp. cf. *dolabelloides* sequences observed in individuals collected from Georgia formed a monophyletic clade distinct from *P. dolabelloides*; these species were not collected sympatrically, but were separated by a genetic distance of

3.17%. *Pleurobema* sp. cf. *oviforme* and *Pleuonaia* sp. cf. *barnesiana* were collected in sympatry with their closest respective congeners, *P. oviforme* and *P. barnesiana*, respectively; due to the lack of gene-flow during sympatry, these species are reproductively isolated and can be recognized as species using the biological species concept. While *Pleuonaia* sp. cf. *dolabelloides* was not collected in sympatry with its closest congener, based on genetic distance it may also be reproductively isolated from *P. dolabelloides*.

My analyses generally agreed with findings from previous phylogenetic assessments on the placement of individuals in the genera *Sintoxia* and *Pleuonaia* (Campbell et al. 2005; Campbell and Lydeard 2012a). Although the sample size was low in this study, sequences of *S. rubrum* were not monophyletic within *Pleurobema*, and is likely a sister clade. These phylogenetic distinctions based on DNA sequences are congruent with those from shell morphology: *Sintoxia* spp. have thicker, more quadrate shells, and *Pleurobema* spp. typically have thinner, more compressed shells. The DNA sequences of *P. gibberum* grouped distinctly apart from the other congeners in *Pleuonaia*; therefore, noting its genetic distinctiveness, geographic isolation, and morphologically smaller size of *P. gibberum*, I recommend that other characters such as life-history traits, glochidial morphology and soft-anatomy be explored in order to determine definitively whether this species belongs in a genus other than *Pleuonaia*.

While studies list and use fixed nucleotide differences between species as an indicator of species' distinctiveness, this approach can be affected by sample size; hence, fixed nucleotide differences were not used in this study to identify species. For example, fixed differences between two species, each represented by one individual, would produce many "fixed" differences, but when more haplotypes for each species are added, the number of "fixed" differences decreases. Since previous studies (Buhay et al. 2002; Serb et al. 2003; Jones et al.

2006) used uncorrected *p*-distances to quantify genetic differentiation among species at *NDI* rather than select the best-supported nucleotide substitution model, the results from this study cannot be directly compared to those of other studies.

ITS1. – Estimated pairwise genetic distances among taxa in this study were not comparable to those of other studies due to the contrasting approach for encoding gaps. For example, other studies coded gaps as missing data (Jones et al. 2006) or as a fifth character state (Campbell 2008). Nagy (2011) illustrated the usefulness of gaps for phylogenetic inference and recommended that such coding be incorporated into future studies; however, indel evolution in DNA sequences is poorly understood, so the best approach for incorporating them is still unresolved. Hence, it was prudent for me to estimate phylogenies using two sequence alignments, and evaluate what effect the alignments had on phylogenetic results. The method for coding gaps created by Simmons (2000) encodes each indel event as a single evolutionary step. For example, a deletion event in a sequence of five nucleotides is scored as a single deletion event; a deletion event in another sequence of four nucleotides beginning at the same position would be scored as a single deletion event, but with a different code than the first deletion event in order to characterize the different size of the gap, e.g., five versus four nucleotides. Coding each gap as a fifth character state is incorrect, because it is unlikely that five separate nucleotide deletions occurred to create the pattern observed in the first sequence considered (Källersjö et al. 2005).

Against this background of encoding gaps, phylogenetic analyses of *ITS1* sequences in this study revealed slight to moderate separation of species and was more ambiguous toward delineating species and genera than the phylogenetic analyses of *NDI*. Within genera, species

typically were diverged by one or more indels. When analyses were run without the addition of these binary-coded characters added by FastGap, nucleotide positions in which a sequence contained a gap were treated as missing data by phylogenetic programs, thus phylogenetic trees and pairwise differences did not recognize gap differences between species; this outcome is similar to that of Campbell and Lydeard (2012a). While the phylogenetic results using the alignments created by Clustal W and webPRANK were similar, they differed in their relationships of *S. rubrum* and *P. gibberum* to other mussel species. For example, the alignment created by Clustal W produced a phylogram (Figure 3) that showed the nuclear *ITS1* sequence of *P. gibberum* as more related to taxa in the genus *Fusconaia* than to those in *Pleuronaia*; additionally, the phylogram illustrated *S. rubrum* as not monophyletic within *P. oviforme*. The alignment created by webPRANK, however, resulted in a phylogram (Figure 4) that placed *P. gibberum* more closely to taxa in *Pleuronaia* than to those in *Fusconaia*; however, *S. rubrum* was monophyletic within *P. oviforme*. Phylograms from both alignments indicated paraphyletic lineages of *P. dolabelloides*; the two individuals that were not monophyletic with the other *P. dolabelloides* haplotypes also were unique at the mitochondrial *ND1* gene. This paraphyletic lineage is also the reason that intraspecific variation in *ITS1* sequences for *P. dolabelloides* was greater than interspecific variation between *P. dolabelloides* and other species. The *ITS1*-based estimated pairwise genetic distances did not differ greatly between alignment algorithms. Greater intraspecific variation in *F. cuneolus* compared to interspecific variation between *F. cuneolus* vs. *F. masoni* was the result of one identical haplotype shared between these two species. This shared haplotype could be the result of nuclear gene introgression or due to shared inheritance of an ancestral lineage. Due to the geographic isolation of these two species, the most plausible explanation is that the haplotype in question represents an ancestral lineage.

Intraspecific pairwise genetic variation within *P. barnesiana* was greater than interspecific pairwise genetic variation between *P. barnesiana* and *P. dolabelloides*; the phylogram, however, showed a monophyletic clade for *P. barnesiana* produced by a fixed indel at bp 345 or bp 374 in the ClustalW and webPrank alignments, respectively.

Lower interspecific variation observed at *ITS1* within the genus *Fusconaia* could indicate a more recently diverged taxon or different population histories than genera *Pleuroaia* and *Pleurobema*. Intra-generic variation estimates from the ClustalW alignment were 0.70%, 1.05%, and 1.90% for *Fusconaia*, *Pleurobema*, and *Pleuroaia*, respectively. Removal of *P. gibberum* from *Pleuroaia* resulted in intra-generic variation of 1.66% for *Pleuroaia*.

Molecular Genetic Marker Comparison. – Results of the incongruent length differences test indicated that the mtDNA and nuclear gene trees should not be concatenated because the gene phylograms differed too greatly in branch lengths or placements of individuals within the tree. Nonetheless, the phylogenetic analyses of these two markers gave similar results. Each gene tree generally resulted in distinct clades for *Fusconaia*, *Pleurobema*, and *Pleuroaia*, but with different placements of *P. gibberum*; additionally, analyses of the nuclear *ITS1* gene did not unambiguously resolve *S. rubrum*'s affinity to other species and genera. Phylogenetic analysis of *ND1* indicated clades supporting species identifications for *F. cor*, *F. cuneolus*, *F. masoni*, *F. subrotunda*, *P. oviforme*, *P. sp. cf. oviforme*, *P. barnesiana*, *P. sp. cf. barnesiana*, *P. dolabelloides*, *P. sp. cf. dolabelloides*, *P. gibberum*, and *S. rubrum*. Results from *ITS1* differed from those of *ND1* by having similar haplotypes for *F. cuneolus* and *F. masoni*, but illustrated well-supported clades for the other species. Both genetic markers indicated slight divergence within *P. dolabelloides*, but due to the low sample sizes for the disparate haplotypes observed

within *P. dolabelloides*, further studies should explore whether this phylogenetic clade is comprised of more than one species. Based on discovery of this divergent clade, I recommend consideration of additional molecular markers and phenotypic traits to determine if a cryptic species that is phenotypically similar to *P. dolabelloides* exists in the upper Clinch River.

Management Implications. – Observation of numerous shared *NDI* intraspecific haplotypes across drainages suggest that populations at these localities were once part of a larger regional population and/or that genetic exchanges between these drainages occurred historically. Many of these drainages now are separated by large hydroelectric dams that inhibit or preclude gene flow between populations. Shared haplotypes indicate that mussel translocations likely would not adversely affect the fitness of receiving populations, but assessments including population genetic analyses at microsatellite loci and variation of life-history traits should be explored before translocations are implemented. If microsatellite loci indicate recent genetic exchange and life-history traits are similar, then mussel translocations should occur.

The three previously unrecognized cryptic species in the genera *Pleurobema* and *Pleuonaia* have limited known geographical distributions, and ultimately could warrant protection under the Endangered Species Act. *Pleurobema* sp. cf. *oviforme* was collected only in one stream, the Little River, TN. *Pleuonaia* sp. cf. *barnesiana* was collected primarily in the upper Clinch drainage in Virginia, with one individual also collected from each of the Powell and South Chickamauga drainages. *Pleuonaia* sp. cf. *dolabelloides* was collected only in the South Chickamauga drainage. Further survey work should be conducted to locate additional populations of these species, to define their distributions. However, it is likely that

anthropogenic factors have eliminated much of the suitable habitat for these species in many streams and therefore constricted their ranges.

Phylogenetic classification schemes that utilize only morphology to classify freshwater mussel taxa have the potential to overlook cryptic species. Using molecular phylogenetic approaches and the phylogenetic species concept, this study discovered three previously unrecognized freshwater mussel taxa on the basis of reciprocal monophyly of mtDNA and nuclear sequences, and morphology (see Chapter 2). Because of the high sampling intensity of this project, while focusing on relatively few streams among the many in the UTRB, it is possible that additional cryptic species may occur in this region. Further survey work is warranted in regions of the UTRB that this study did not survey. Molecular genetic approaches to clarify the phylogenetic relationships of cryptic taxa are useful, but more surveys and genetic analyses are needed for characterizing similar-looking species that may occur in the numerous small rivers and creeks of the UTRB. In addition to molecular genetics, analyses should incorporate morphology and life-history strategies in order to effectively characterize species' uniqueness.

LITERATURE CITED

- Altschul S.F., W. Gish, W. Miller, E.W. Myers, D.J. Lipman. 1990. Basic local alignment search tool. *Journal of Molecular Biology*, 215 (3):403-410.
- Arbogast B.S., S.V. Edwards, J. Wakeley, P. Beerli, J.B. Slowinski. 2002. Estimating divergence times from molecular data on phylogenetic and population genetic timescales. *Annual Review of Ecology and Systematics*, 33:707-740.
- Ballard J.W.O., M.C. Whitlock. 2004. The incomplete natural history of mitochondria. *Molecular Ecology*, 13 (4):729-744.
- Bart H.L., M.D. Clements, R.E. Blanton, K.R. Piller, D.L. Hurley. 2010. Discordant molecular and morphological evolution in buffalofishes (Actinopterygii: Catostomidae). *Molecular Phylogenetics and Evolution*, 56 (2):808-820.
- Bickford D., D.J. Lohman, N.S. Sodhi, P.K. Ng, R. Meier, K. Winker, K.K. Ingram, I. Das. 2007. Cryptic species as a window on diversity and conservation. *Trends in Ecology & Evolution*, 22 (3):148-155.
- Borchsenius F. 2009. FastGap 1.2. http://www.aubot.dk/FastGap_home.htm.
- Buhay J.E., J.M. Serb, C.R. Dean, Q. Parham, C. Lydeard. 2002. Conservation genetics of two endangered unionid bivalve species, *Epioblasma florentina walkeri* and *E. capsaeformis* (Unionidae: Lampsilini). *Journal of Molluscan Studies*, 68 (4):385-391.
- Campbell D.C., P.D. Johnson, J.D. Williams, A.K. Rindsberg, J.M. Serb, K.K. Small, C. Lydeard. 2008. Identification of 'extinct' freshwater mussel species using DNA barcoding. *Molecular Ecology Resources*, 8 (4):711-724.
- Campbell D.C., C. Lydeard. 2012a. The genera of Pleurobemini (Bivalvia: Unionidae: Amblemninae). *American Malacological Bulletin*, 30 (1):19-38.

- Campbell D.C., C. Lydeard. 2012b. Molecular systematics of *Fusconaia* (Bivalvia: Unionidae: Ambleminae). *American Malacological Bulletin*, 30 (1):1-17.
- Campbell D.C., J.M. Serb, J.E. Buhay, K.J. Roe, R.L. Minton, C. Lydeard. 2005. Phylogeny of North American amblemines (Bivalvia, Unionoida): Prodigious polyphyly proves pervasive across genera. *Invertebrate Biology*, 124 (2):131-164.
- Christian A.D., J.L. Harris, J.M. Serb. 2008. Preliminary analysis for identification, distribution, and conservation status of species of *Fusconaia* and *Pleurobema* in Arkansas. Report, Arkansas Game and Fish Commission, Perrytown, Arkansas. 40 pp.
- Darriba D., G.L. Taboada, R. Doallo, D. Posada. 2012. Jmodeltest 2: More models, new heuristics and parallel computing. *Nature Methods*, 9 (8):772-772.
- Dowton M., A.D. Austin. 2002. Increased congruence does not necessarily indicate increased phylogenetic accuracy—the behavior of the incongruence length difference test in mixed-model analyses. *Systematic Biology*, 51 (1):19-31.
- Elderkin C.L. 2009. Intragenomic variation in the rDNA internal transcribed spacer (ITS1) in the freshwater mussel *Cumberlandia monodonta* (say, 1828). *Journal of Molluscan Studies*, 75 (4):419-421.
- Gangloff M.M., J.D. Williams, J.W. Feminella. 2006. A new species of freshwater mussel (Bivalvia : Unionidae), *Pleurobema atearni*, from the Coosa River drainage of Alabama, USA. *Zootaxa*, 1118:43-56.
- Graf D.L., K.S. Cummings. 2007. Review of the systematics and global diversity of freshwater mussel species (Bivalvia: Unionoida). *Journal of Molluscan Studies*, 73 (4):291-314.
- Grobler P.J., J.W. Jones, N.A. Johnson, B. Beaty, J. Struthers, R.J. Neves, E.M. Hallerman. 2006. Patterns of genetic differentiation and conservation of the slabside pearlymussel,

- Lexingtonia dolabelloides* (Lea, 1840) in the Tennessee River drainage. *Journal of Molluscan Studies*, 72:65-75.
- Haag W., J. Williams. 2014. Biodiversity on the brink: An assessment of conservation strategies for North American freshwater mussels. *Hydrobiologia*, 735 (1):45-60.
- Haag W.R. 2012. North American freshwater mussels: Natural history, ecology, and conservation. Cambridge University Press Cambridge, UK.
- Heard W.H., R.H. Guckert. 1970. A re-evaluation of the recent unionacea (pelecypoda) of North America. *Malacologia*, 10 (2):333-355.
- Henley W.F., P.J. Grobler, R.J. Neves. 2006. Non-invasive method to obtain DNA from freshwater mussels (Bivalvia: Unionidae). *Journal of Shellfish Research*, 25 (3):975-977.
- Huelsenbeck J., F. Ronquist. 2001. MrBayes: Bayesian inference of phylogenetic trees. *Bioinformatics*, 17 (8):754-755.
- Hughes M.H., P.W. Parmalee. 1999. Prehistoric and modern freshwater mussel (Mollusca: Bivalvia: Unionoidea) faunas of the Tennessee River: Alabama, Kentucky, and Tennessee. *Regulated Rivers: Research & Management*, 15 (1-3):25-42.
- Johnson M.S. 2011. A quantitative survey of the freshwater mussel fauna in the Powell River of Virginia and Tennessee, and life history study of two endangered species, *Quadrula sparsa* and *Quadrula intermedia*. Master of Science Thesis, Virginia Polytechnic Institute and State University. 191 pp.
- Jones J.W., R.J. Neves. 2002. Life history and propagation of the endangered fanshell pearlymussel, *Cyprogenia stegaria* Rafinesque (Bivalvia:Unionidae). *Journal of the North American Benthological Society*, 21 (1):76-88.

- Jones J.W., R.J. Neves. 2007. Freshwater mussel status: Upper North Fork Holston River, Virginia. *Northeastern Naturalist*, 14 (3):471-480.
- Jones J.W., R.J. Neves. 2010. Descriptions of a new species and a new subspecies of freshwater mussels, *Epioblasma ahlstedti* and *Epioblasma florentina aureola* (Bivalvia: Unionidae), in the Tennessee River drainage, USA. *The Nautilus*, 124 (2):77.
- Jones J.W., R.J. Neves, S.A. Ahlstedt, E.M. Hallerman. 2006. A holistic approach to taxonomic evaluation of two closely related endangered freshwater mussel species, the oyster mussel *Epioblasma capsaeformis* and tan riffleshell *Epioblasma florentina walkeri* (Bivalvia: Unionidae). *Journal of Molluscan Studies*, 72 (3):267-283.
- Källersjö M., T. Von Proschwitz, S. Lundberg, P. Eldenäs, C. Erséus. 2005. Evaluation of ITS rDNA as a complement to mitochondrial gene sequences for phylogenetic studies in freshwater mussels: An example using Unionidae from north-western Europe. *Zoologica Scripta*, 34 (4):415-424.
- King T.L., M.S. Eackles, B. Gjetvaj, W.R. Hoeh. 1999. Intraspecific phylogeography of *Lasmigona subviridis* (Bivalvia: Unionidae): Conservation implications of range discontinuity. *Molecular Ecology*, 8:S65-S78.
- Langerhans R.B., C.A. Layman, A.M. Shokrollahi, T.J. Dewitt. 2004. Predator-driven phenotypic diversification in *Gambusia affinis*. *Evolution*, 58 (10):2305-2318.
- Lea I. 1836. A synopsis of the Family Naiades. Carey, Lea, and Blanchard, Philadelphia, Pennsylvania and John Miller, London, UK.
- Librado P., J. Rozas. 2009. DnaSP v5: A software for comprehensive analysis of DNA polymorphism data. *Bioinformatics*, 25:1451-1452.

- Löytynoja A., N. Goldman. 2010. webPRANK: A phylogeny-aware multiple sequence aligner with interactive alignment browser. *BMC Bioinformatics*, 11 (1):579.
- Miyatake T., T. Shimizu. 1999. Genetic correlations between life-history and behavioral traits can cause reproductive isolation. *Evolution*, 53 (1):201-208.
- Moyer G.R., E. Díaz-Ferguson. 2012. Identification of endangered Alabama lampmussel (*Lampsilis virescens*) specimens collected in the Emory River, Tennessee, USA via DNA barcoding. *Conservation Genetics*, 13 (2):885-889.
- Nagy L.G., S. Kocsubé, Z. Csanádi, G.M. Kovács, T. Petkovits, C. Vágvölgyi, T. Papp. 2012. Re-mind the gap! Insertion–deletion data reveal neglected phylogenetic potential of the nuclear ribosomal internal transcribed spacer (ITS) of fungi. *PloS One*, 7 (11):e49794.
- Neves R.J., A.E. Bogan, J.D. Williams, S.A. Ahlstedt, P.W. Hartfield. 1997. Status of aquatic mollusks in the southeastern United States: A downward spiral of diversity. Pages 43-86 in G. W. Benz and D. E. Collins, editors. *Aquatic Fauna in Peril: The Southeastern Perspective*. Lenz Design and Communications, Decatur, GA, Special Publication 1, Southeast Aquatic Research Institute.
- Ortmann A.E. 1912. Notes upon the families and genera of the najades. *Annals of the Carnegie Museum*, 8 (2):222-365.
- Ortmann A.E. 1918. The nayades (freshwater mussels) of the upper Tennessee drainage. With notes on synonymy and distribution. *Proceedings of the American Philosophical Society*, 57 (6):521-626.
- Ostby B.J., P.L. Angermeier, R.J. Neves. 2010. Freshwater mussel survey in the North Fork Holston River, Virginia. Final Report, United States Fish and Wildlife Service, Abingdon, Virginia. 58 pp.

- Parmalee P.W., A.E. Bogan. 1998. The Freshwater Mussels of Tennessee. The University of Tennessee Press, Knoxville, Tennessee, USA.
- Rambaut A. 2007. FigTree, a graphical viewer of phylogenetic trees. Downloaded from: <http://tree.bio.ed.ac.uk/software/figtree>.
- Ricciardi A., J.B. Rasmussen. 1999. Extinction rates of North American freshwater fauna. *Conservation Biology*, 13 (5):1220-1222.
- Scheiner S.M. 1993. Genetics and evolution of phenotypic plasticity. *Annual Review of Ecology and Systematics*, 24:35-68.
- Serb J.M., J.E. Buhay, C. Lydeard. 2003. Molecular systematics of the North American freshwater bivalve genus *Quadrula* (Unionidae: Ambleminae) based on mitochondrial *NDI* sequences. *Molecular Phylogenetics and Evolution*, 28 (1):1-11.
- Simmons M.P., H. Ochoterena. 2000. Gaps as characters in sequence-based phylogenetic analyses. *Systematic Biology*, 49 (2):369-381.
- Simpson C.T. 1900. Synopsis of the naiades, or pearly fresh-water mussels. *Proceedings of the United States National Museum*, 22:501-1044.
- Spooner D.E., C.C. Vaughn. 2006. Context-dependent effects of freshwater mussels on stream benthic communities. *Freshwater Biology*, 51 (6):1016-1024.
- Swofford D. 2002. PAUP*: Phylogenetic analysis using parsimony (*and other methods), version 4.0b10. Sunderland, Massachusetts: Sinauer Associates, Inc. <http://paup.csit.fsu.edu/>.
- Tamura K., D. Peterson, N. Peterson, G. Stecher, M. Nei, S. Kumar. 2011. MEGA5: Molecular evolutionary genetics analysis using maximum likelihood, evolutionary distance, and maximum parsimony methods. *Molecular Biology and Evolution*, 28 (10):2731-2739.

- Tedersoo L., M. Bahram, M. Ryberg, E. Otsing, U. Kõljalg, K. Abarenkov. 2014. Global biogeography of the ectomycorrhizal/sebacina lineage (fungi, Sebaciniales) as revealed from comparative phylogenetic analyses. *Molecular Ecology*, 23 (16):4168-4183.
- Thompson J.D., D.G. Higgins, T.J. Gibson. 1994. Clustal W: Improving the sensitivity of progressive multiple sequence alignment through sequence weighting, position-specific gap penalties and weight matrix choice. *Nucleic Acids Research*, 22 (22):4673-4680.
- United States Fish and Wildlife Service (USFWS). 1975. Proposed endangered status for 216 species on convention on international trade. *Federal Register* 40:(188): 44329-44333.
- United States Fish and Wildlife Service (USFWS). 1991. Endangered and threatened wildlife and plants; determination of endangered status for the cumberland pigtoe mussel. *Federal Register* 56:(88): 21084-21087.
- United States Fish and Wildlife Service (USFWS). 2013. Endangered and threatened wildlife and plants; endangered species status for the fluted kidneyshell and slabside pearlymussel and designation of critical habitat. *Federal Register* 78:(187): 59269-59287.
- Vaughn C.C., S.J. Nichols, D.E. Spooner. 2008. Community and foodweb ecology of freshwater mussels. *Journal of the North American Benthological Society*, 27 (2):409-423.
- Vences M., F. Andreone, F. Glaw, J. Kosuch, A. Meyer, H.C. Schaefer, M. Veith. 2002. Exploring the potential of life-history key innovation: Brook breeding in the radiation of the malagasy treefrog genus *Boophis*. *Molecular Ecology*, 11 (8):1453-1463.
- Watters G.T. 1996. Small dams as barriers to freshwater mussels (*Bivalvia*, *Unionoida*) and their hosts. *Biological Conservation*, 75 (1):79-85.
- Watters G.T., M.A. Hoggarth, D.H. Stansbery. 2009. *The Freshwater Mussels of Ohio*. Ohio State University Press Columbus, Ohio.

Williams J.D., A.E. Bogan, J.T. Garner. 2008. Freshwater Mussels of Alabama and the Mobile Basin in Georgia, Mississippi and Tennessee. The University of Alabama Press, Tuscaloosa, Alabama.

Williams J.D., M.L. Warren, K.S. Cummings, J.L. Harris, R.J. Neves. 1993. Conservation status of freshwater mussels of the United States and Canada. *Fisheries*, 18 (9):6-22.

Zanatta D.T., R.W. Murphy. 2006. Evolution of active host-attraction strategies in the freshwater mussel tribe Lampsilini (Bivalvia: Unionidae). *Molecular Phylogenetics and Evolution*, 41 (1):195-208.

Table 1. Site numbers and locality information for sites sampled for freshwater mussels primarily in the Tennessee River basin from 2012 through 2014. NA = information not available.

Site Number	Drainage	Stream	River km	River Mile	Collection Site	County	State	Latitude	Longitude
1	Powell	Powell River	214.0	133.0	Towell Ford	Lee	Virginia	36.63330	-83.17429
2	Powell	Powell River	210.5	130.8	Flanary Bridge	Lee	Virginia	36.64306	-83.20391
3	Powell	Powell River	199.5	124.0	Snodgrass Ford	Lee	Virginia	36.61873	-83.24799
4	Powell	Powell River	185.9	115.5	Baldwin Ford	Hancock	Tennessee	36.59530	-83.30549
5	Powell	Powell River	180.6	112.2	Bales Ford	Hancock	Tennessee	36.58230	-83.33289
6	Powell	Powell River	164.8	102.4	Alanthus Hill	Hancock	Tennessee	36.56082	-83.39177
7	Powell	Powell River	144.4	89.7	Wellness Center	Claiborne	Tennessee	36.53511	-83.46728
8	Powell	Indian Creek	24.6	15.3	Machine Branch	Lee	Virginia	36.62099	-83.53786
9	Powell	Indian Creek	0.3	0.2	Aggy Vanderpool's	Claiborne	Tennessee	36.55992	-83.60705
10	Clinch	Indian Creek	0.8	0.5	631 Bridge	Tazewell	Virginia	37.08773	-81.75887
11	Clinch	Little River	48.9	30.4	Ostby Sites 12&13	Tazewell	Virginia	37.03010	-81.78014
12	Clinch	Clinch River	447.5	278.1	Bennet Property	Russell	Virginia	36.96063	-82.09579
13	Clinch	Clinch River	441.9	274.6	Artrip	Russell	Virginia	36.96229	-82.12002
14	Clinch	Clinch River	437.9	272.1	Cleveland Elementary	Russell	Virginia	36.94473	-82.14821
15	Clinch	Clinch River	435.8	270.8	Cleveland	Russell	Virginia	36.93711	-82.16432
16	Clinch	Clinch River	401.7	249.6	Burtions Ford	Wise	Virginia	36.89224	-82.33993
17	Clinch	Clinch River	378.3	235.1	Semones	Scott	Virginia	36.80936	-82.48399
18	Clinch	Clinch River	339.9	211.2	Spears Ferry	Scott	Virginia	36.65007	-82.74842
19	Clinch	Clinch River	309.8	192.5	Wallen Bend	Hancock	Tennessee	36.57927	-83.00404
20	Clinch	Clinch River	305.4	189.8	Kyle's Ford	Hancock	Tennessee	36.56953	-83.04100
21	Clinch	Clinch River	291.8	181.3	Frost Ford	Hancock	Tennessee	36.53077	-83.15085
22	Clinch	Clinch River	287.6	178.7	Garland Hollow	Hancock	Tennessee	36.52171	-83.19388
23	Clinch	Clinch River	277.1	172.2	Swan Island	Hancock	Tennessee	36.47349	-83.28995
24	Clinch	Copper Creek	87.2	54.2	Parsonage	Russell	Virginia	36.82027	-82.23781
25	Clinch	Copper Creek	24.1	15.0	Holland Property	Scott	Virginia	36.69179	-82.54093
26	Clinch	Copper Creek	21.7	13.5	Williams Mill	Scott	Virginia	36.67833	-82.55828
27	Clinch	Copper Creek	4.2	2.6	Jennings Ford	Scott	Virginia	36.65792	-82.71182
28	Holston	North Fork Holston River	191.7	119.1	619 Bridge	Smyth	Virginia	36.94680	-81.42096
29	Holston	North Fork Holston River	175.2	108.9	Chatham Hill	Smyth	Virginia	36.95545	-81.52300
30	Holston	North Fork Holston River	142.7	88.7	Possom Hollow Rd	Smyth	Virginia	36.90987	-81.69957
31	Holston	Possom Creek	12.2	7.6	Route 637	Scott	Virginia	36.59568	-82.65532
32	Holston	Middle Fork Holston River	16.3	10.1	Neff	Washington	Virginia	36.70459	-81.86119
33	Holston	Middle Fork Holston River	15.4	9.6	Lower Neff	Washington	Virginia	36.69940	-81.85765
34	Holston	Beech Creek	25.6	15.9	Ball Cemetary	Hawkins	Tennessee	36.40276	-82.77281
35	Holston	Beech Creek	20.6	12.8	Van Hill	Hawkins	Tennessee	36.38576	-82.81234
36	Holston	Beech Creek	17.7	11.0	Private Bridge	Hawkins	Tennessee	36.39561	-82.82597
37	Holston	Beech Creek	10.8	6.7	Keplar Bridge	Hawkins	Tennessee	36.40076	-82.88415
38	Holston	Beech Creek	3.9	2.4	Tunnel Hill Church	Hawkins	Tennessee	36.38951	-82.91663
39	Nolichucky	Nolichucky River	47.2	29.3	Pate Hill	Greene	Tennessee	36.09284	-83.03545
40	Nolichucky	Little Chucky Creek	14.0	8.7	Sinking Springs Road	Greene	Tennessee	36.12375	-83.01076
41	French Broad	Little Pigeon River	9.8	6.1	Sevierville	Sevier	Tennessee	35.87317	-83.57164
42	Tennessee	Little River	47.6	29.6	Apple Store	Blount	Tennessee	35.68228	-83.78775
43	Tennessee	Little River	33.2	20.6	Coulter's Bridge	Blount	Tennessee	35.76385	-83.85273
44	Tennessee	Little River	23.8	14.8	River Jon's	Blount	Tennessee	35.79638	-83.88515
45	Tennessee	Little River	20.0	12.4	Brakebill Island	Blount	Tennessee	35.81021	-83.89966
46	Little Tennessee	Little Tennessee River	167.0	103.8	McCoy Bridge	Macon	North Carolina	35.27178	-83.44036
47	Little Tennessee	Little Tennessee River	144.4	89.7	Halls Ford	Swain	North Carolina	35.35550	-83.50662
48	Emory	Emory River	62.8	39.0	Gobey	Morgan	Tennessee	36.14942	-84.60550
49	Hiwassee	Hiwassee River	96.6	60.0	Turtletown	Polk	Tennessee	35.16777	-84.35236
50	South Chickamauga	South Chickamauga Creek	24.8	15.4	Ringgold	Catoosa	Georgia	34.91496	-85.12300
51	South Chickamauga	East Fork Chickamauga Creek	50.4	31.3	Freeman Springs Rd	Whitfield	Georgia	34.76076	-85.08174
52	Paint Rock	Paint Rock River	53.6	33.3	TNC Property	Jackson	Alabama	34.68748	-86.31015
53	Duck	Duck River	288.2	179.1	Lillards Mill	Marshall	Tennessee	35.58595	-86.78707
54	Collins	Collins River	5.6	3.5	Shellsford	Warren	Tennessee	35.67563	-85.71016
55	Craig's	Craig's Creek	NA	NA	Anderson Ford	Botetourt	Virginia	37.61234	-79.98054
56	Craig's	Craig's Creek	NA	NA	Carter Ford	Botetourt	Virginia	37.63418	-79.95854
57	Craig's	Craig's Creek	NA	NA	Swinging Bridge	Botetourt	Virginia	37.61502	-79.98830

Table 2. Sample sizes for freshwater mussels collected at sites from 2012-2014, with species identifications confirmed by analysis of the mitochondrial gene region *ND1*.

Drainage	Stream	Site Name	Site Number	<i>F. cor</i>	<i>F. cuneolus</i>	<i>F. masoni</i>	<i>F. subrotunda</i>	<i>P. oviforme</i>	<i>P. sp. oviforme</i>	<i>P. bamesiana</i>	<i>P. sp. bamesiana</i>	<i>P. dolabelloides</i>	<i>P. sp. dolabelloides</i>	<i>P. gibberum</i>	<i>S. rubrum</i>	Grand Total		
<u>Powell Drainage</u>	Powell River	Towell Ford	1	3			9			5	1	2				20		
		Flanary Bridge	2	3			9			4		2					18	
		Snodgrass Ford	3	1			1						2				2	
		Baldwin Ford	4	1				5			3						11	
		Bales Ford	5				1				1						1	
		Alanthus Hill	6				1										1	
		Wellness Center	7	1				1									1	
		Indian Creek	Machine Branch	8								1	1					2
			Aggy Vanderpool	9								1						1
<u>Clinch Drainage</u>	Indian Creek	631 Bridge	10	41	27		34	16		17	64	17			1	217		
		Little River	Ostby Sites 12&13	11				4				2					6	
	Clinch River		Bennet Property	12				4				2					6	
		Artrip	13				4				2					6		
		Cleveland Elementary	14	41	27		34	4			52	17			1	177		
		Cleveland	15	5			1	2			1		7			1		
		Burtens Ford	16	1							21					1		
		Semones	17	31			13	1			27	10				82		
		Spears Ferry	18				1									3		
		Wallen Bend	19		2		1									1		
		Kyle's Ford	20		1	7		2								1		
		Frost Ford	21					10	1			3				1		
		Garland Hollow	22					1								2		
		Swan Island	23					3								1		
		Copper Creek	Parsonage	24						4		17	8				29	
			Holland Property	25						1		2					3	
			Williams Mill	26						2			1				3	
	Jennings Ford		27						1		12	7				20		
											3					3		
	<u>North Fork Holston River Drainage</u>	North Fork Holston River	619 Bridge	28	2				32		9						43	
			Chatham Hill	29	2				2								35	
			Possum Hollow Rd.	30					30								2	
			Possum Creek	Route 637	31	2							9					9
													9					9
			<u>Middle Fork Holston River Drainage</u>	Middle Fork Holston River	Neff	32					2		1		18			
	Lower Neff	33							2		1		18				21	
													13				16	
											5				5			

Table 2. Continued.

Drainage	Stream	Site Name	Site Number	<i>F. cor</i>	<i>F. cuneolus</i>	<i>F. masoni</i>	<i>F. subrotunda</i>	<i>P. oviforme</i>	<i>P. sp. oviforme</i>	<i>P. barnesiana</i>	<i>P. sp. barnesiana</i>	<i>P. dolabelloides</i>	<i>P. sp. dolabelloides</i>	<i>P. gibberum</i>	<i>S. rubrum</i>	Grand Total	
<u>Holston Drainage</u>	Beech Creek							<u>18</u>		<u>7</u>						<u>25</u>	
		Ball Cemetary	34					10		3							13
		Van Hill	35					2									2
		Private Bridge	36					1									1
		Keplar Bridge	37					4		4							8
	Tunnel Hill Church	38					1									1	
<u>Nolichucky Drainage</u>	Nolichucky River						<u>1</u>	<u>2</u>		<u>6</u>						<u>10</u>	
		Pate Hill	39				1			5							6
		Little Chucky Creek						3		1							4
	Sinking Springs Road	40					3		1							4	
<u>French Broad Drainage</u>	Little Pigeon River							<u>2</u>		<u>1</u>						<u>4</u>	
		Sevierville	41					3		1							4
<u>Tennessee Drainage</u>	Little River				<u>1</u>			<u>2</u>	<u>24</u>	<u>12</u>		<u>4</u>				<u>43</u>	
		Apple Store	42		1			2	24	12		4					38
		Coulter's Bridge	43						20								20
		River Jon's	44					2	4	11							17
		Brakebill Island	45		1						1		4				5
<u>Little Tennessee Drainage</u>	Little Tennessee River															<u>13</u>	
McCoy Bridge		46						13								13	
Halls Ford		47						10								10	
<u>Emory Drainage</u>	Emory River									<u>5</u>						<u>5</u>	
Gobey		48								5						5	
<u>Hiwassee Drainage</u>	Hiwassee River							<u>5</u>								<u>5</u>	
Turtletown		49						5								5	
<u>South Chickamauga Drainage</u>	South Chickamauga Creek							<u>2</u>			<u>1</u>		<u>2</u>			<u>13</u>	
		Ringgold	50					1									1
		East Fork Chickamauga Creek							4		1		7				12
	Freeman Springs Rd	51					4			1		7				12	
<u>Paint Rock Drainage</u>	Paint Rock River							<u>2</u>								<u>2</u>	
		TNC Property	52					2									2
<u>Duck Drainage</u>	Duck River							<u>3</u>		<u>10</u>		<u>11</u>			<u>2</u>	<u>26</u>	
		Lillard's Mill	53					3		10		11			2		26
<u>Collins Drainage</u>	Collins River													<u>20</u>		<u>20</u>	
Shellsford		54												20		20	
<u>Craig's Creek Drainage</u>	Craig's Creek															<u>9</u>	
		Anderson Ford	55														9
		Carter Ford	56														5
		Swinging Bridge	57														1
Grand Total																3	
				46	28	9	44	104	24	73	66	52	7	20	3	476	

Table 3. Variable nucleotide sites for haplotypes at the mitochondrial gene *ND1*, where species abbreviations are: Fcor = *Fusconaia cor*; Fcun = *F. cuneolus*; Fmas = *F. masoni*; Fsub = *F. subrotunda*; Pbar = *Pleuroaia barnesiana*; PcfB = *P. sp. cf. barnesiana*; Pdol = *P. dolabelloides*; PcfD = *P. sp. cf. dolabelloides*; Pgib = *P. gibberum*; Povi = *Pleurobema oviforme*; PcfO = *P. sp. cf. oviforme*; Srub = *Sintoxia rubrum*. Identical nucleotide sites to the first sequence are indicated by "." and missing data is indicated by "-".

Table 3. Extended.

Table 3. Continued.

Table 3. Extended and continued.

Table 4. Pairwise nucleotide distances between species' haplotypes at the mitochondrial gene *ND1*. Pairwise differences were calculated using the general time reversible model with rates gamma (GTR+G) in PAUP. Bold numbers indicate intraspecific variation. Species abbreviations are defined in Table 3.

	Fcor	Fcun	Fmas	Fsub	Pbar	PcfB	Pdol	PcfD	Pgib	Povi	PcfO	Srub
Fcor	0.0042											
Fcun	0.0558	0.0055										
Fmas	0.0620	0.0570	0.0011									
Fsub	0.0714	0.0671	0.0680	0.0103								
Pbar	0.1561	0.1317	0.1307	0.1454	0.0109							
PcfB	0.1723	0.1502	0.1426	0.1647	0.0285	0.0030						
Pdol	0.1456	0.1387	0.1214	0.1503	0.0738	0.0796	0.0080					
PcfD	0.1722	0.1441	0.1432	0.1713	0.0843	0.0957	0.0317	0.0045				
Pgib	0.1552	0.1455	0.1447	0.1542	0.1335	0.1462	0.1176	0.1234	0.0085			
Povi	0.1299	0.1131	0.1372	0.1256	0.1594	0.1710	0.1526	0.1615	0.1460	0.0086		
PcfO	0.1214	0.1226	0.1226	0.1300	0.1307	0.1418	0.1437	0.1484	0.1344	0.0632	0.0022	
Srub	0.1275	0.1190	0.1212	0.1361	0.1264	0.1322	0.1140	0.1228	0.1312	0.1313	0.1154	0.0128

Table 6. Variable nucleotide sites for haplotypes at the nuclear gene region *ITS1* using the alignment algorithm from webPRANK. A blank at a nucleotide site indicates identical nucleotide as first sequence. Haplotype numbers do not correspond with those for mitochondrial DNA data. Species abbreviations are defined in Table 3. Insertions or gaps are indicated by "-"; identical nucleotide positions to the first sequence are blank.

Haplotype	N	Base Pairs																																																		Coded Index																																																																																																																																																																																																																																																																																																																																																																																																																																																																																																																																																																																																																																																																																																																																																																																																																																																																																																																																																																																																																																																																																																																																																																																																																																																																																																																																																																																																																																																																													
		1	2	3	4	5	6	7	8	9	10	11	12	13	14	15	16	17	18	19	20	21	22	23	24	25	26	27	28	29	30	31	32	33	34	35	36	37	38	39	40	41	42	43	44	45	46	47	48	49	50	51	52	53	54	55	56	57	58	59	60	61	62	63	64	65	66	67	68	69	70	71	72	73	74	75	76	77	78	79	80	81	82	83	84	85	86	87	88	89	90	91	92	93	94	95	96	97	98	99	100	101	102	103	104	105	106	107	108	109	110	111	112	113	114	115	116	117	118	119	120	121	122	123	124	125	126	127	128	129	130	131	132	133	134	135	136	137	138	139	140	141	142	143	144	145	146	147	148	149	150	151	152	153	154	155	156	157	158	159	160	161	162	163	164	165	166	167	168	169	170	171	172	173	174	175	176	177	178	179	180	181	182	183	184	185	186	187	188	189	190	191	192	193	194	195	196	197	198	199	200	201	202	203	204	205	206	207	208	209	210	211	212	213	214	215	216	217	218	219	220	221	222	223	224	225	226	227	228	229	230	231	232	233	234	235	236	237	238	239	240	241	242	243	244	245	246	247	248	249	250	251	252	253	254	255	256	257	258	259	260	261	262	263	264	265	266	267	268	269	270	271	272	273	274	275	276	277	278	279	280	281	282	283	284	285	286	287	288	289	290	291	292	293	294	295	296	297	298	299	300	301	302	303	304	305	306	307	308	309	310	311	312	313	314	315	316	317	318	319	320	321	322	323	324	325	326	327	328	329	330	331	332	333	334	335	336	337	338	339	340	341	342	343	344	345	346	347	348	349	350	351	352	353	354	355	356	357	358	359	360	361	362	363	364	365	366	367	368	369	370	371	372	373	374	375	376	377	378	379	380	381	382	383	384	385	386	387	388	389	390	391	392	393	394	395	396	397	398	399	400	401	402	403	404	405	406	407	408	409	410	411	412	413	414	415	416	417	418	419	420	421	422	423	424	425	426	427	428	429	430	431	432	433	434	435	436	437	438	439	440	441	442	443	444	445	446	447	448	449	450	451	452	453	454	455	456	457	458	459	460	461	462	463	464	465	466	467	468	469	470	471	472	473	474	475	476	477	478	479	480	481	482	483	484	485	486	487	488	489	490	491	492	493	494	495	496	497	498	499	500	501	502	503	504	505	506	507	508	509	510	511	512	513	514	515	516	517	518	519	520	521	522	523	524	525	526	527	528	529	530	531	532	533	534	535	536	537	538	539	540	541	542	543	544	545	546	547	548	549	550	551	552	553	554	555	556	557	558	559	560	561	562	563	564	565	566	567	568	569	570	571	572	573	574	575	576	577	578	579	580	581	582	583	584	585	586	587	588	589	590	591	592	593	594	595	596	597	598	599	600	601	602	603	604	605	606	607	608	609	610	611	612	613	614	615	616	617	618	619	620	621	622	623	624	625	626	627	628	629	630	631	632	633	634	635	636	637	638	639	640	641	642	643	644	645	646	647	648	649	650	651	652	653	654	655	656	657	658	659	660	661	662	663	664	665	666	667	668	669	670	671	672	673	674	675	676	677	678	679	680	681	682	683	684	685	686	687	688	689	690	691	692	693	694	695	696	697	698	699	700	701	702	703	704	705	706	707	708	709	710	711	712	713	714	715	716	717	718	719	720	721	722	723	724	725	726	727	728	729	730	731	732	733	734	735	736	737	738	739	740	741	742	743	744	745	746	747	748	749	750	751	752	753	754	755	756	757	758	759	760	761	762	763	764	765	766	767	768	769	770	771	772	773	774	775	776	777	778	779	780	781	782	783	784	785	786	787	788	789	790	791	792	793	794	795	796	797	798	799	800	801	802	803	804	805	806	807	808	809	810	811	812	813	814	815	816	817	818	819	820	821	822	823	824	825	826	827	828	829	830	831	832	833	834	835	836	837	838	839	840	841	842	843	844	845	846	847	848	849	850	851	852	853	854	855	856	857	858	859	860	861	862	863	864	865	866	867	868	869	870	871	872	873	874	875	876	877	878	879	880	881	882	883	884	885	886	887	888	889	890	891	892	893	894	895	896	897	898	899	900	901	902	903	904	905	906	907	908	909	910	911	912	913	914	915	916	917	918	919	920	921	922	923	924	925	926	927	928	929	930	931	932	933	934	935	936	937	938	939	940	941	942	943	944	945	946	947	948	949	950	951	952	953	954	955	956	957	958	959	960	961	962	963	964	965	966	967	968	969	970	971	972	973	974	975	976	977	978	979	980	981	982	983	984	985	986	987	988	989	990	991	992	993	994	995	996	997	998	999	1000	1001	1002	1003	1004	1005	1006	1007	1008	1009	1010	1011	1012	1013	1014	1015	1016	1017	1018	1019	1020	1021	1022	1023	1024	1025	1026	1027	1028	1029	1030	1031	1032	1033	1034	1035	1036	1037	1038	1039	1040	1041	1042	1043	1044	1045	1046	1047	1048	1049	1050	1051	1052	1053	1054	1055	1056	1057	1058	1059	1060	1061	1062	1063	1064	1065	1066	1067	1068	1069	1070	1071	1072	1073	1074	1075	1076	1077	1078	1079	1080	1081	1082	1083	1084	1085	1086	1087	1088	1089	1090	1091	1092	1093	1094	1095	1096	1097	1098	1099	1100	1101	1102	1103	1104	1105	1106	1107	1108	1109	1110	1111	1112	1113	1114	1115	1116	1117	1118	1119	1120	1121	1122	1123	1124	1125	1126	1127	1128	1129	1130	1131	1132	1133	1134	1135	1136	1137	1138	1139	1140	1141	1142	1143	1144	1145	1146	1147	1148	1149	1150	1151	1152	1153	1154	1155	1156	1157	1158	1159	1160	1161	1162	1163	1164	1165	1166	1167	1168	1169	1170	1171	1172	1173	1174	1175	1176	1177	1178	1179	1180	1181	1182	1183	1184	1185	1186	1187	1188	1189	1190	1191	1192	1193	1194	1195	1196	1197	1198	1199	1200	1201	1202	1203	1204	1205	1206	1207	1208	1209	1210	1211	1212	1213	1214	1215	1216	1217	1218	1219	1220	1221	1222	1223	1224	1225	1226	1227	1228	1229	1230	1231	1232	1233	1234	1235	1236	1237	1238	1239	1240	1241	1242	1243	1244	1245	1246	1247	1248	1249	1250	1251	1252	1253	1254	1255	1256	1257	1258	1259	1260	1261	1262	1263	1264	1265	1266	1267	1268	1269	1270	1271	1272	1273	1274	1275	1276	1277	1278	1279	1280	1281	1282	1283	1284	1285	1286	1287	1288	1289	1290	1291	1292	1293	1294	1295	1296	1297	1298	1299	1300	1301	1302	1303	1304	1305	1306	1307	1308	1309	1310	1311	1312	1313	1314	1315	1316	1317	1318	1319	1320	1321	1322	1323	1324	1325	1326	1327	1328	1329	1330	1331	1332	1333	1334	1335	1336	1337	1338	1339	1340	1341	1342	1343	1344	1345	1346	1347	1348	1349	1350	1351	1352	1353	1354	1355	1356	1357	1358	1359	1360	1361	1362	1363	1364	1365	1366	1367	1368	1369	1370	1371	1372	1373	1374	1375	1376	1377	1378	1379	1380	1381	1382	1383	1384	1385	1386	1387	1388	1389	1390	1391	1392	1393	1394	1395	1396	1397	1398	1399	1400	1401	1402	1403	1404	1405	1406	1407	1408	1409	1410	1411	1412	1413	1414	1415	1416	1417	1418	1419	1420	1421	1422	1423	1424	1425	1426	1427	1428	1429	1430	1431	1432	1433	1434	1435	1436	1437	1438	1439	1440	1441	1442	1443	1444	1445	1446	1447	1448	1449	1450	1451	1452	1453	1454	1455	1456	1457	1458	1459	1460	1461	1462	1463	1464	1465	1466	1467	1468	1469	1470	1471	1472

Table 7. Pairwise nucleotide distances between species' haplotypes at the nuclear gene *ITS1* using the alignment algorithm from Clustal W. Pairwise distances were calculated using uncorrected *p*-distances in PAUP. Species abbreviations are defined in Table 3. Bold numbers indicate intraspecific variation; *N*=1 indicates that only one haplotype was recovered for the species, thus intraspecific variation cannot be computed.

	Fcor	Fcun	FcunMas	Fsub	Pbar	PcfB	Pdol	PcfD	Pgib	Povi	PcfO	Srub	Lfas
Fcor	N=1												
Fcun	0.0056	0.0037											
FcunMas	0.0037	0.0019	N=1										
Fsub	0.0043	0.0100	0.0081	0.0037									
Pbar	0.0232	0.0204	0.0194	0.0269	0.0025								
PcfB	0.0239	0.0233	0.0220	0.0258	0.0266	0.0019							
Pdol	0.0199	0.0192	0.0180	0.0236	0.0095	0.0201	0.0133						
PcfD	0.0236	0.0230	0.0218	0.0277	0.0097	0.0250	0.0104	0.0056					
Pgib	0.0151	0.0151	0.0132	0.0169	0.0309	0.0219	0.0256	0.0284	N=1				
Povi	0.0223	0.0198	0.0186	0.0216	0.0306	0.0252	0.0280	0.0337	0.0281	0.0071			
PcfO	0.0208	0.0182	0.0170	0.0205	0.0318	0.0238	0.0255	0.0340	0.0264	0.0105	0.0036		
Srub	0.0189	0.0183	0.0170	0.0194	0.0311	0.0221	0.0248	0.0296	0.0247	0.0091	0.0112	N=1	
Lfas	0.1048	0.1040	0.1029	0.1076	0.0999	0.1012	0.0980	0.1002	0.1101	0.1061	0.1058	0.1069	N=1

Table 8. Pairwise nucleotide differences between species' haplotypes at the nuclear gene *ITS1* using the alignment algorithm from webPRANK. Pairwise distances were calculated using uncorrected *p*-distances in PAUP. Species abbreviations are defined in Table 3. Bold numbers indicate intraspecific variation; *N*=1 indicates that only one haplotype was recovered for the species, thus intraspecific variation cannot be computed.

	Fcor	Fcun	FcunMas	Fsub	Pbar	PcfB	Pdol	PcfD	Pgib	Povi	PcfO	Srub	Lfas
Fcor	N=1												
Fcun	0.0055	0.0037											
FcunMas	0.0037	0.0018	N=1										
Fsub	0.0043	0.0098	0.0080	0.0036									
Pbar	0.0325	0.0301	0.0288	0.0343	0.0025								
PcfB	0.0216	0.0191	0.0179	0.0241	0.0205	0.0019							
Pdol	0.0263	0.0238	0.0226	0.0282	0.0065	0.0161	0.0075						
PcfD	0.0291	0.0266	0.0254	0.0310	0.0090	0.0170	0.0065	0.0056					
Pgib	0.0167	0.0148	0.0130	0.0191	0.0287	0.0197	0.0225	0.0234	N=1				
Povi	0.0217	0.0192	0.0180	0.0260	0.0339	0.0229	0.0295	0.0304	0.0286	0.0064			
PcfO	0.0186	0.0161	0.0149	0.0229	0.0345	0.0235	0.0282	0.0310	0.0260	0.0088	0.0036		
Srub	0.0243	0.0218	0.0205	0.0286	0.0327	0.0217	0.0283	0.0292	0.0281	0.0092	0.0110	N=1	
Lfas	0.0913	0.0887	0.0875	0.0929	0.0790	0.0800	0.0746	0.0755	0.0894	0.0892	0.0897	0.0900	N=1

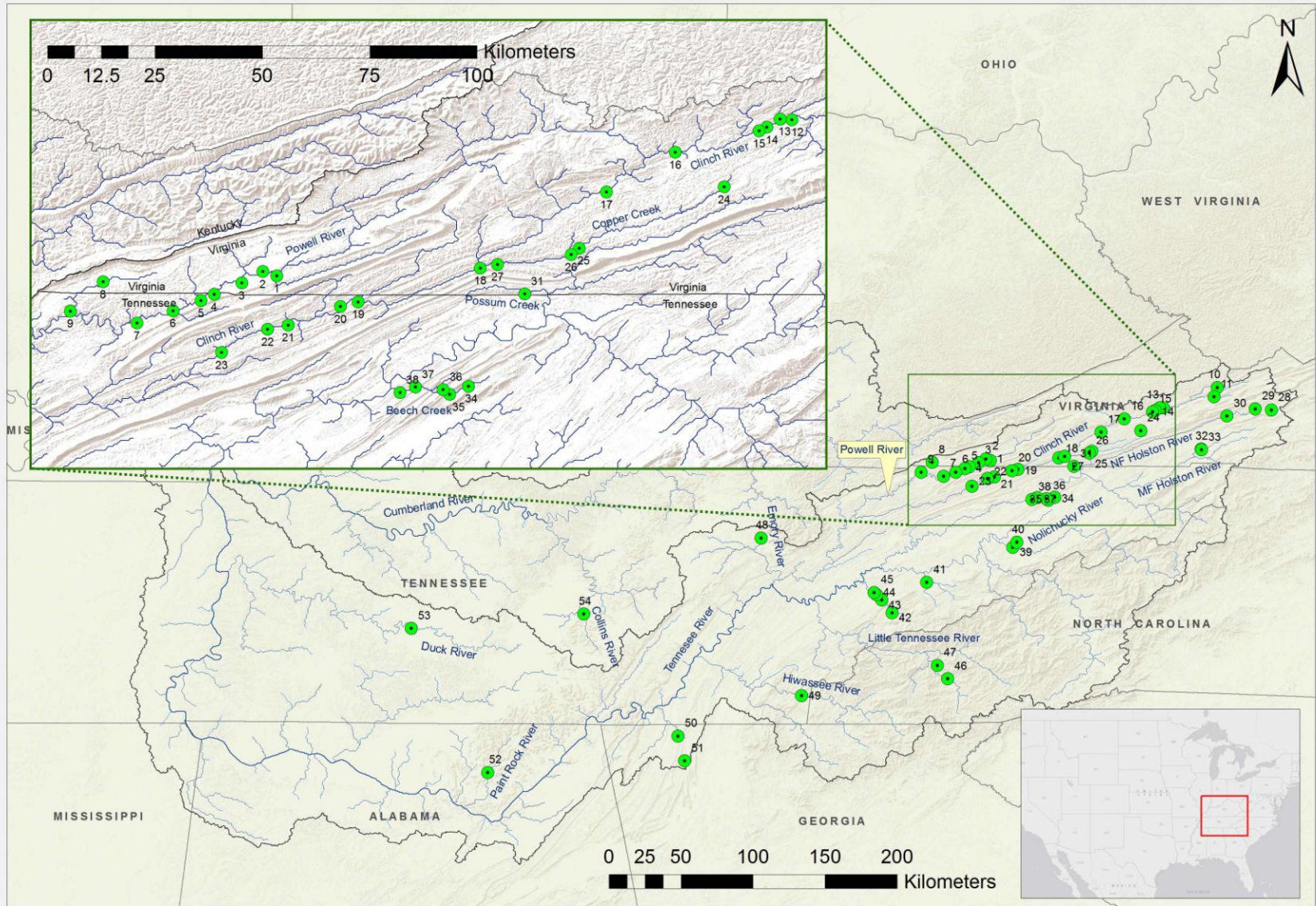


Figure 1. Sampling localities and site numbers for freshwater mussels collected primarily in the Tennessee River basin from 2012 through 2014. Craig Creek collection localities are not shown.

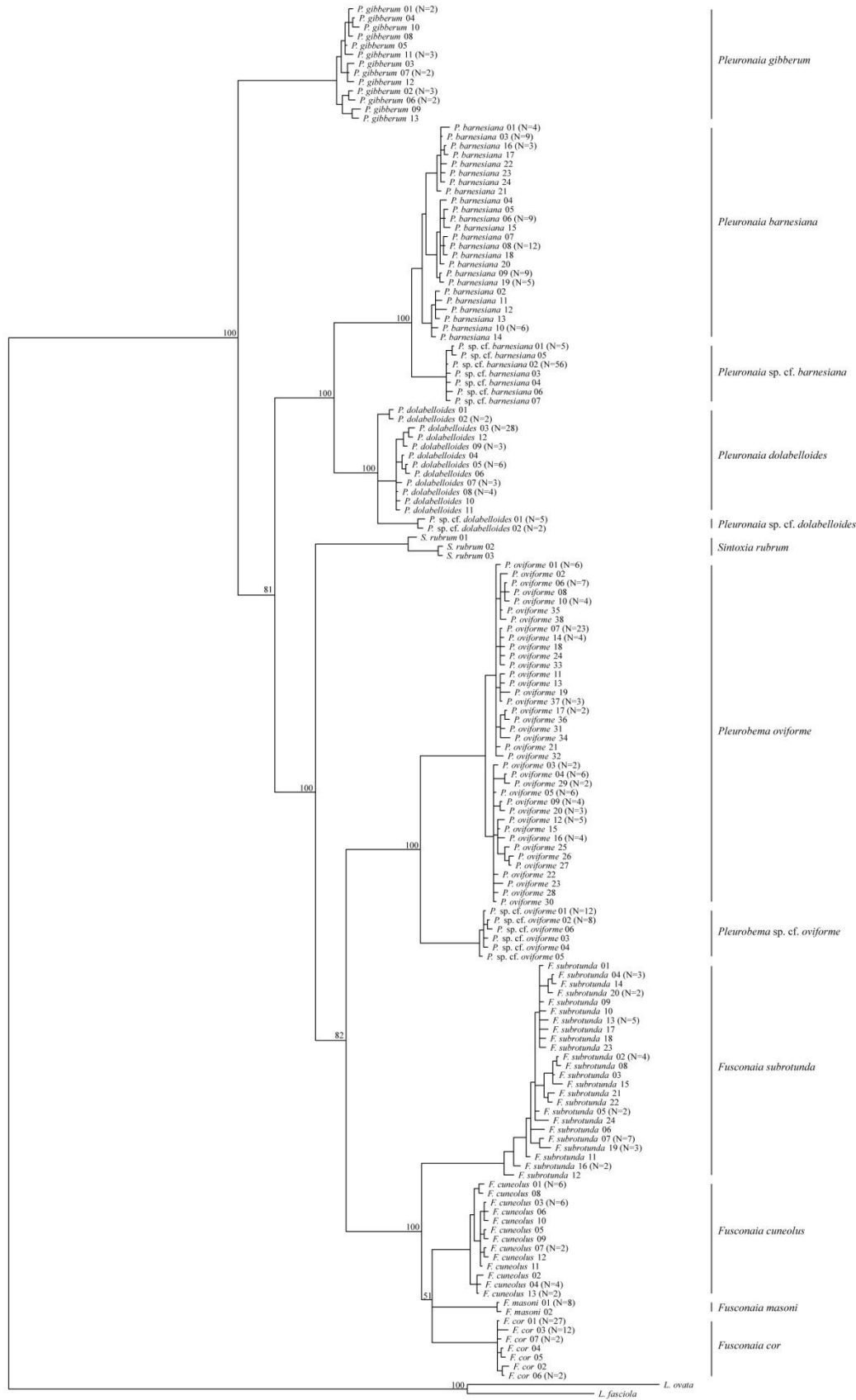
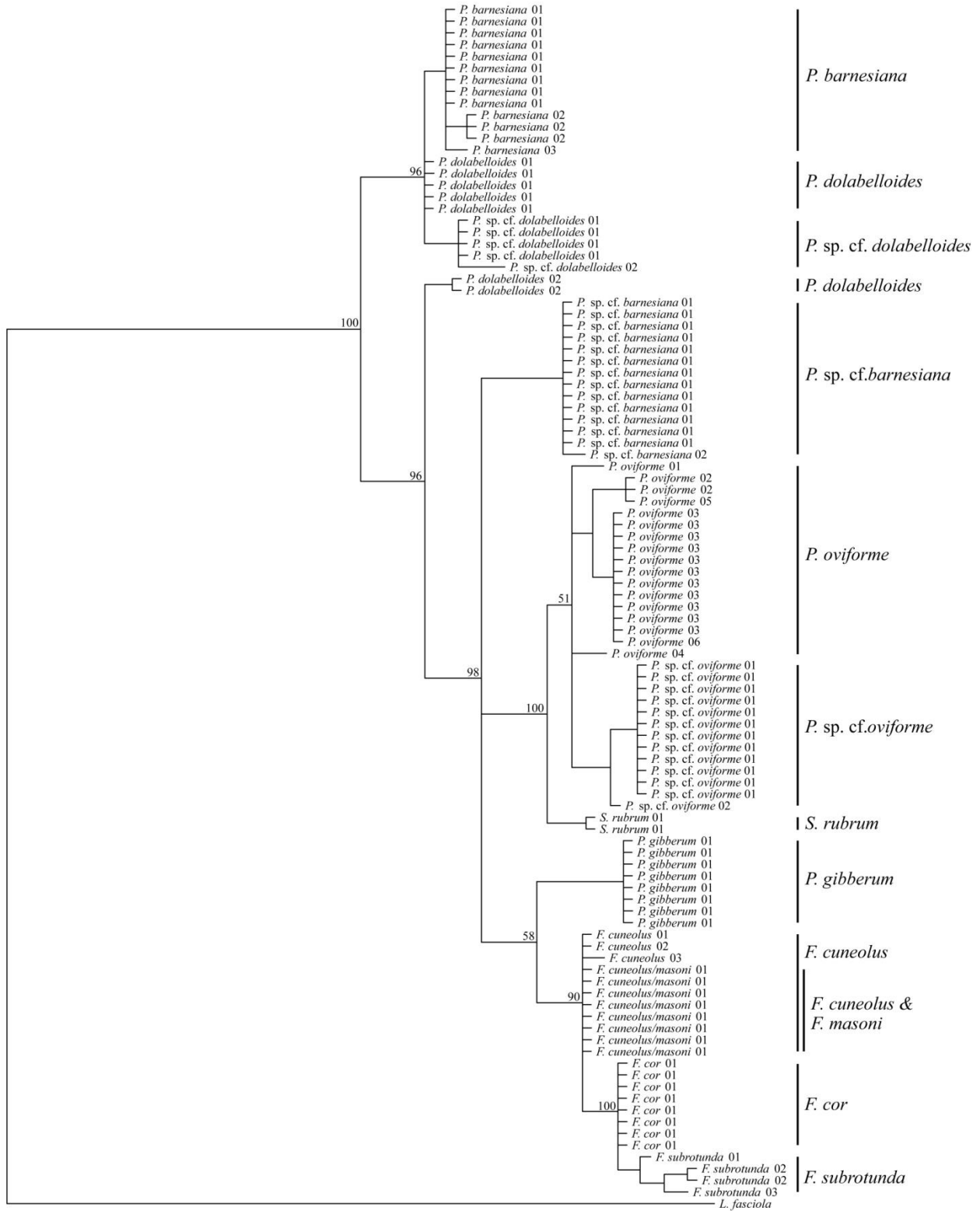


Figure 2. Phylogenetic relationships showing Bayesian consensus tree for freshwater mussels inferred from the mitochondrial gene region *ND1*. Numbers on branches are posterior probabilities of tree topology. The analysis was run for 10 million generations with split frequencies of 0.0065, with the most likely tree possessing a $-\ln$ likelihood of -6286.032 and the mean $-\ln$ likelihood of -6367.785.



0.01

Figure 3. Phylogenetic relationships showing the Bayesian consensus tree for freshwater mussels inferred from the nuclear gene *ITS1* using the alignment algorithm from Clustal W. Numbers on branches are posterior probabilities of tree topology. The analysis was run for 2 million generations with split frequencies of 0.0067, with the most likely tree possessing a -ln likelihood of -1514.34 and the mean -ln likelihood of -1566.02.

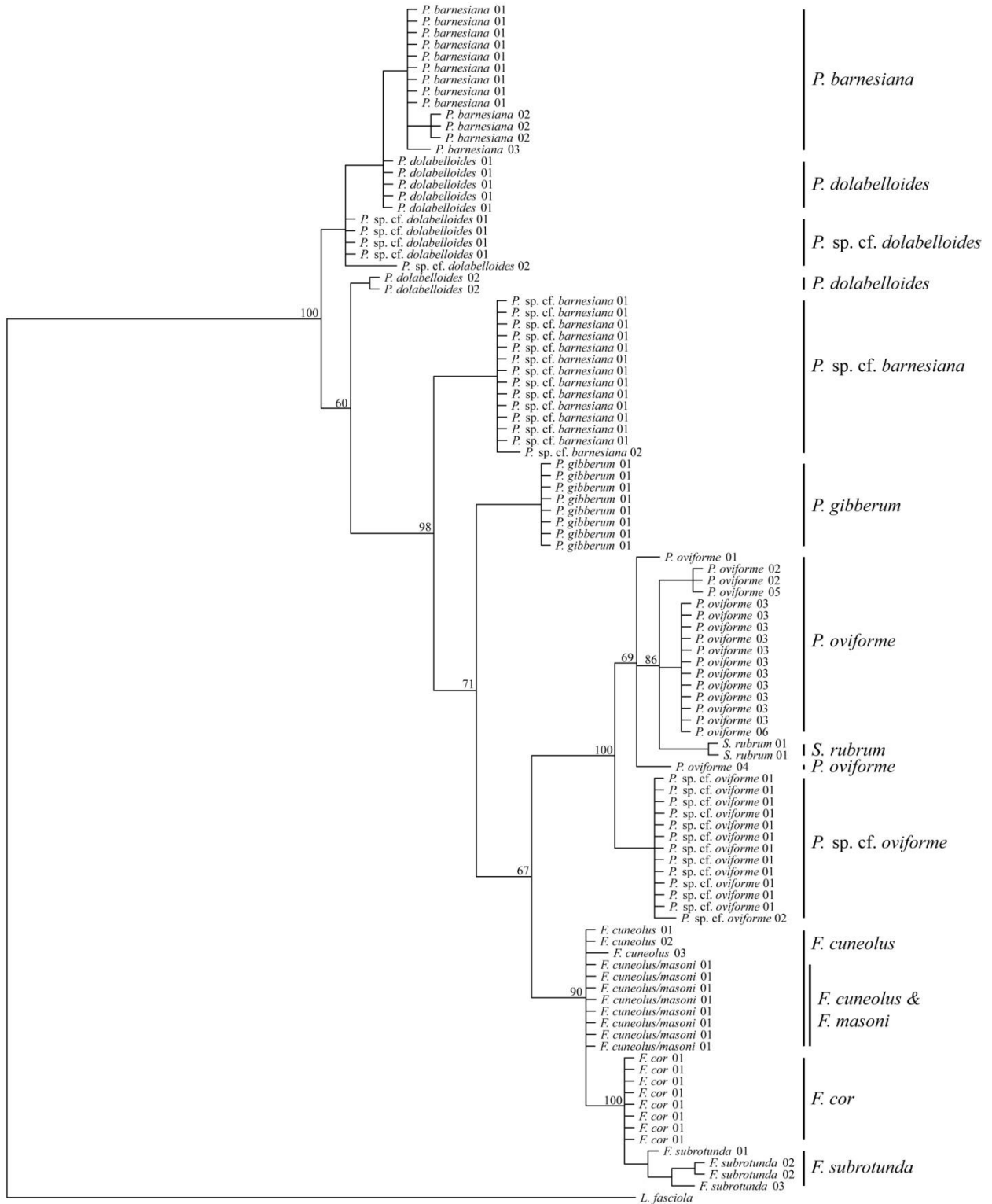


Figure 4. Phylogenetic relationships showing the Bayesian consensus tree for freshwater mussels inferred from the nuclear gene *ITS1* using the alignment algorithm from webPRANK. Numbers on branches are posterior probabilities of tree topology. The analysis was run for 2 million generations with split frequencies of 0.0065, with the most likely tree possessing a -ln likelihood of -1487.89 and the mean -ln likelihood of -1539.72.

APPENDIX A: Haplotype Collections

Table A. 1. Site numbers and counts of haplotypes analyzed for the mitochondrial gene region *ND1*. Species abbreviations are defined in Table 3.

Table A. 1. Extended.

Table A. 2. Site numbers and counts of haplotypes analyzed for the nuclear gene region *ITS1*.

Species abbreviations are defined in Table 3.

Drainage	Collection Site	Fcor01	Fcun01	Fcun02	Fcun03	FCunMas01	Fsub01	Fsub02	Fsub03	Pbar01	Pbar02	Pbar03	Pdol01	Pdol02	PcfB01	PcfB02	Pgib01	PcfD01	PcfD02	Povi01	Povi02	Povi03	Povi04	Povi05	Povi06	PcfO01	PcfO02	Strub01	Grand Total	
Powell	1	1					1																						2	
	2	1						1		2																			5	
	9														1														1	
Clinch	10														1							1							2	
	13	1												2	4	1													8	
	15	1												2	3														6	
	18				1																								1	
	19	2	1	1		5																							9	
	20							1																				1	2	
	24																					1							1	
	25															1														1
26									1	1					3														5	
North Fork Holston	29																				4								4	
	30	2																											2	
	31									2	1																		3	
Middle Fork Holston	32										1	1																	2	
Holston	34																					1							1	
	36																					1							1	
	38																					1							1	
Nolichucky	39							1																					1	
	40																				2			1					3	
Little River	42																								11	1			12	
	43									1	1											1				1			4	
Little Tennessee	46																				1								1	
Emory	48									1																			1	
South Chickamauga	51																	4	1			1		1					7	
Paint Rock	52																				1								1	
Duck	53									2			1														1		4	
Collins	54																8												8	
Craig Creek	55					1																							1	
	57					2																							2	
Total		8	1	1	1	8	1	2	1	9	3	1	5	2	13	1	8	4	1	1	2	11	1	1	1	1	12	1	2	102

CHAPTER 2

Identification of morphological characters for use in taxonomic delineation of selected mussel species in the genera *Fusconaia*, *Pleurobema*, and *Pleuonaia* in the upper Tennessee River basin of Tennessee and Virginia

ABSTRACT

The purpose of this study was to analyze the morphological variation of eight difficult-to-identify freshwater mussel species, including *Fusconaia cor*, *F. cuneolus*, *F. subrotunda*, *Pleurobema oviforme*, *Pleurobema barnesiana*, *P. dolabelloides*, and two unrecognized taxa, *Pleurobema* sp. cf. *oviforme* and *Pleurobema* sp. cf. *barnesiana*. These mussels are conchologically similar in external appearance. Hence, species-specific shell and soft-anatomy traits were characterized so that each species could be identified reliably in the field. Mussels were collected from 2012 through 2014, primarily in streams of the upper Tennessee River basin in Tennessee and Virginia, where sample sizes for each species ranged from 27 to 84 for continuous variables (e.g., length, height, and width) and 8 to 49 individuals for categorical variables (e.g., periostracum color, ray pattern, and depth of beak cavity). Three classification and regression tree analyses were conducted, with the best-performing tree the one that analyzed only the categorical shell characters, exhibiting an overall accuracy of 80.63% on terminal nodes. Although canonical variates analysis and Goodall's *F*-test conducted on geometric morphometric data showed statistically significant differences in external shell shape between most species, the large overlap among species made these results only statistically significant, but not practical for field identifications. Morphological overlap of continuous and categorical variables among investigated species made unambiguous identifications of shells and live individuals difficult. Thus, if a mussel is thought to be a new distribution record for one of these species or its occurrence at a site could affect implementation of a project, its species identity should be verified using molecular genetic techniques.

KEYWORDS: Freshwater mussels, *Fusconaia*, *Pleurobema*, *Pleuronaia*, Morphometrics, Classification and regression tree, Geometric morphometrics

INTRODUCTION

Freshwater mussels are considered the most imperiled taxonomic group in North America (Williams et al. 1993; Neves et al. 1997). Of the 297 recognized species in the families Unionidae and Margaritiferidae in North America, 213 – or approximately 70% – are considered endangered, threatened or of special concern (Williams et al. 1993). Extinction rates for freshwater taxa are five times greater than those for terrestrial fauna and similar to rates estimated for tropical rainforest communities (Ricciardi and Rasmussen 1999). Freshwater mussel habitat has been lost, fragmented, and degraded due to anthropogenic effects from dam construction, sedimentation, and water pollution (Williams et al. 1993; Watters 1996; Hughes and Parmalee 1999; Haag 2012). The sedentary nature of adult unionid mussels and their general reliance on fish hosts to disperse their glochidia makes recolonization of isolated stream reaches difficult, especially those blocked by dams. Ongoing translocation and propagation efforts for mussels aim to restore mussels to rivers with suitable water and habitat quality (Jones and Neves 2002; Haag and Williams 2014). Protection and restoration of habitat is important for freshwater mussels, not only to address their imperiled status, but also because they serve valuable functional roles in stream ecosystems (Spooner and Vaughn 2006; Vaughn et al. 2008).

The Tennessee and Cumberland River basins, major tributaries of the Ohio River, collectively hold the highest diversity of freshwater mussel species in North America (Haag 2012). Several mussel species of interest in this study, shiny pigtoe (*Fusconaia cor*), fine-rayed pigtoe (*Fusconaia cuneolus*), and Tennessee pigtoe (*Pleuronaia barnesiana*), are endemic to the Tennessee River basin, whereas Tennessee clubshell (*Pleurobema oviforme*) and slabside pearlymussel (*Pleuronaia dolabelloides*) are endemic to the Tennessee and Cumberland River basins, and longsolid (*Fusconaia subrotunda*) occurs broadly throughout the Ohio River basin

(Parmalee and Bogan 1998; Watters et al. 2009). The United States Fish and Wildlife Service (USFWS) listed *F. cor* and *F. cuneolus* as endangered in 1975 (USFWS 1975), *P. gibberum* as endangered in 1991 (USFWS 1991), *P. dolabelloides* as endangered in 2013 (USFWS 2013) and *P. oviforme* as a species of concern. These species are morphologically very similar, leading field biologists to be concerned about correct identification of an individual, with species identifications often varying among biologists. Correct identifications are necessary to understand species distributions and design effective management and recovery strategies. Misidentification of individuals could result in incorrect determination of population status for species, leading to improper management actions.

Identification of freshwater mussel species requires use of morphological characters such as shell shape, periostracum texture and color, ray patterns, foot color, nacre color, number of gills charged when gravid, and alignment and structure of pseudocardinal and lateral teeth patterns (Figure 1) (Parmalee and Bogan 1998; Williams et al. 2008; Jones and Neves 2010). Some soft-part and internal shell characters cannot be readily utilized without sacrificing the individual; thus, field identifications of live mussels mainly utilize external shell characters that can be difficult to distinguish between similar looking species.

Traditional morphometric analyses rely on a limited set of measurements, to include lengths, angles and length ratios (Adams et al. 2004; Slice 2007). Traditional shell measurements – such as ratios of maximum length, height and width – were heavily relied upon for describing freshwater mussel species, but rarely provided a suite of diagnostic traits to definitively identify species (Parmalee and Bogan 1998; Williams et al. 2008). However, geometric morphometrics can analyze and resolve differences in external shell shape between species that biologists often struggle to quantify (Bogan and Roe 2008). Geometric

morphometrics can analyze more than distances between two points because it retains the geometry of the specimen and can analyze distances and angles between any set of landmarks (Slice 2007). Modern geometric morphometric programs use photographs from the user to digitize and analyze points, but for accurate analysis, unbiased photographs are needed. Therefore, because this analytical approach has the potential to discriminate between subtle morphological differences among specimens, it was used to assess shells of my study species.

The purpose of this study was to assess phenotypic variation of mussels in the genera *Fusconaia*, *Pleurobema*, and *Pleuronaia* in the upper Tennessee River basin (UTRB) using both traditional measurements of shell and soft-anatomy and geometric morphometric analysis of the external shell. I analyzed phenotypic variation among my eight study species using statistical testing of data, including classification and regression trees and canonical variance analysis.

METHODS

Species Collection. – Freshwater mussels were collected from 2012 through 2014 in the Upper Tennessee River Basin (UTRB) primarily in three areas, the upper Clinch, Holston and Powell river watersheds, and also in select tributaries of the Tennessee River downstream of that region (Table 1, Figure 2). Once individuals were identified to species with genetic markers (Chapter 1), they were used for morphometric analyses. Using genetically identified individuals ensured that misidentified individuals would not affect morphology-based analyses.

Morphology. – Mussels were measured to the nearest tenth of a millimeter (mm) with digital calipers. A total of five measurements were made, including: (1) maximum length, (2) maximum height perpendicular to maximum length, (3) height posterior to umbo perpendicular

to maximum length, (4) maximum width, and (5) hinge length (Figure 1). Traditional morphological characteristics, such as foot color and gravidity, were recorded. When gravid individuals were encountered, the number of charged gills, location of conglomerates in the gills, and color of charged gills were recorded. Additionally, gravid individuals were transported to and held in the laboratory at the Freshwater Mussel Conservation Center (FMCC) until conglomerates were discharged. Photographs were taken of conglomerates, and their general shape and color were recorded.

Glochidia were measured from discharged conglomerates using an ocular micrometer in a compound microscope. Grains of salt were added to the water near glochidia to close them for more accurate measurements; this also ensured that the glochidia were viable. A total of ten glochidia per mussel were measured for: height, length, and hinge length. Tukey's comparisons from analysis of variance (ANOVA) was conducted on each measurement to determine if significant differences occurred among species.

Traditional categorical and quantitative characters were assessed for sacrificed, genetically-identified individuals of non-listed species. Categorical characters recorded included: shell outline (elongate, quadrate, or round); umbo position (anterior or posterior), periostracum color (yellow, light brown, brown, or dark brown); periostracum texture (dull, satiny, or shiny); ray pattern (no rays, continuous, or discontinuous, i.e., rays broken or interrupted); ray length (extending to shell margin or cessation before shell margin); ray width (narrow < 1 mm or wide > 1 mm); shape of posterior ridge (angular or rounded); presence of sulcus (present or absent); sulcus length (short, extending < 2/3 of shell length from ventral margin towards umbo; or long, extending > 2/3 of shell length from ventral margin towards umbo). Due to low sample sizes of shells for endangered species, non-genetically identified

specimens were selected from the FMCC shell collection based on characters generally observed on genetically-verified individuals. Umbo elevation was measured using digital calipers to the nearest 0.1 mm. For many of the sacrificed individuals, I possessed data for foot color; therefore, this data was concatenated into the database for shells. Photographs of all mussels were taken as voucher pictures and for use in geometric morphometric programs. A Pentax Optio WG1 compact camera was used with settings at macro focus and with a two-second photograph delay. The delay ensured that vibrations caused from focusing the camera would not result in poor image quality. Bias can be introduced into photographs in various ways, such as inconsistent lighting, focal length, tilt and distance between lens and specimen (Zelditch et al. 2004). Hence, a light box (Figure 3) was used to ensure consistent light, distance between camera lens and specimen, stabilization of camera, and leveling of specimens. Calipers located 220 mm below the camera lens in the light box were used to hold the specimens; the calipers held the individuals at the posterior and anterior intersections of the left and right valves (Figure 4). Calipers held individuals so that the shell valve was parallel to the camera lens and provided a measurement reference if digital re-measuring was needed.

Classification and Regression Tree Analysis of Morphological Data. – Both categorical and continuous morphological variables from live individuals and their shells were analyzed using a classification and regression tree (CART) procedure in the graphic user interface package rattle (Williams 2009) that summons rpart (Therneau et al. 2010) implemented in the program R version 2.14.1 (R Development Core Team, 2011); data were not partitioned due to low sample sizes for endangered species. Correlations between variables were analyzed to determine whether CART could use categorical and continuous morphological characters to consistently

separate species. Three CART analyses were conducted: (1) using data collected from live mussels, including traditional continuously distributed variables of shell length, maximum height, height at umbo, width, and hinge length, plus one categorical variable, foot color, which were analyzed together, (2) using data collected from shells of the genetically identified, sacrificed non-endangered mussels, and from the sub-set of shells of endangered mussels maintained in the FMCC shell collection, including the whole suite of continuous and categorical variables previously mentioned, but lacking beak cavity depth, and (3) from the same shell data and variable set as in analysis two, but with beak cavity depth included and minus foot color. Data were not scaled or transformed, as combinations of variables in subsequent steps should adjust for differing mussel sizes. The package rattle can accommodate missing values in the data set, but assigns the modal value observed from all species; thus, the modal value for each species was used to address missing values for foot color. Trees were built using a minimum split and minimum bucket of 12 and 4, respectively, to accommodate low sample sizes observed in endangered species; setting minimum bucket too low may over-fit the data, with each bucket representing an individual mussel. The minimum split is the minimum number of observations necessary to create a split or node in the decision tree; the minimum bucket is the minimum number of observations necessary to create a group after a split that is either terminal or non-terminal. Overall tree accuracy was determined as the percent correct classification of species on terminal nodes. A confusion matrix was created for each of the three CART trees to show species predictions based on morphological characters. A confusion matrix illustrates the true identity of the species in the rows and the predicted classification in the columns. The matrix allows for comparison of correct classification, false negatives or type two errors (the species in

question labeled as different species), and false positives or type one errors (other species labeled as the species in question).

Geometric Morphometrics. – A transparent radial graph with lines at 15-degree increments was overlain onto photographs of mussel shells (Figure 4). Two homologous locations, the posterior termination of the hinge ligament and the anterior intersection of the hinge ligament and umbo, were used to align the radial graph; an additional nine semi-sliding landmarks were used for analysis (Figure 4). Photographs were loaded into the program tpsdig2 (Rohlf 2005) to digitize points; the two homologous points were used to align the 15° overlay grid, and the remaining nine points were digitized where the radial grid intersects the margin of the shell. Digitized points were resized using one of several superimposition methods to eliminate size and orientation bias, but the shape of the digitization remained the same. The most fundamental superimposition method uses Bookstein shape coordinates, also referred to as the two-point registration (Zelditch et al. 2004). This method uses two homologous points shared between individuals as the baseline for superimposition. These points were digitized as 0,0 and 0,1 so that the baseline was consistent between all individuals; thus, only shape differences remained. Another, more favored approach to eliminating size and orientation bias is the generalized least squares Procrustes superimposition (Zelditch et al. 2004). Rather than using a baseline, Procrustes superimposition uses the summed squared distances between analogous landmarks to minimize differences. The advantage of using Procrustes superimposition is that the combination of translation, scaling, and rotation removes all information that is not related to shape (Zelditch et al. 2004). Data then were exported into the

program CoordGen6f (Sheets 2000), and the digitized points were translated into Procrustes coordinate systems.

Shape variation was analyzed using Canonical Variates Analysis (CVA) (Zelditch et al. 2004). The CVA used priors, such as species identification, to analyze morphological differences that consistently reproduced variability between the species (Christian et al. 2008). The CVA determined axes that maximize differences between group means (i.e., species) relative to within-group mean variation (Zelditch et al. 2004). Differences among species were tested using Goodall's *F*-test using Procrustes superimposition; Goodall's *F*-test analyzes the difference in mean shape between two species relative to shape variation within all samples of each species. Geometric morphometric data produced from CoordGen6f were analyzed using CVA in the program CVAGen6k (Sheets 2000). The program TwoGroup6h (Sheets 2000) was used to conduct Goodall's *F*-test between pairs of species and to illustrate differences between species using vector grids; deformations illustrated the movement of landmarks to highlight key areas of shell variation between species.

RESULTS

Morphological Assessment and Species Descriptions. – A total of 414 individuals representing eight difficult-to-identify mussel species distributed in the upper Tennessee River system were photographed. A series of photographs were organized to illustrate variation within species across sampling locations (Figures 5–12). Traditional shell measurements for live mussels were recorded for 384 individuals across the eight species and foot color was recorded for 377 of these individuals (Tables 2 and 3). Additional characters for sacrificed individuals were recorded for 160 individuals of these eight species (Table 4); of these, a total of 39

individuals were non-genetically identified shells from the FMCC collection, to include: nine *F. cor*, eight *F. cuneolus*, four *F. subrotunda*, nine *P. dolabelloides*, and nine sacrificed individuals of *P. sp. cf. oviforme* from the Little River, TN. Gravid condition was recorded for 50 individuals of seven species (Table 5), and conglomerates and glochidia were photographed to illustrate size and color differences between species (Figures 13 and 14).

Morphological variation and measured variables were summarized for each species in the following descriptions.

Fusconaia cor – The shell outline is quadrate to elongate; smaller individuals <50 mm are generally quadrate, but can occasionally appear elongated posteriorly. Periostracum color in young individuals can range from yellow, light brown to dark brown, whereas larger older individuals typically are dark brown (Figure 5). The periostracum rays are conspicuously wide, 1–2 mm or wider. Rays typically extend to the shell margin continuously, but occasionally they are interrupted or broken. The sheen of the periostracum is shiny, but can occasionally appear satiny or dull in older individuals. The posterior ridge of the shell is angular. A shallow depression or sulcus is present on the mid-section of the shell, typically extending from the ventral margin to 3/4 the length of the shell toward the umbo, occasionally extending onto umbo. The height of the umbo is moderate to high (2–4 mm). The position of the umbo is central to anterior in young individuals, but generally located anteriorly in older and larger individuals. The beak cavities are deep and angular. Foot color is pale orange to orange, but can be white in smaller individuals <50 mm. Only one individual was collected gravid during this study, with all four gills charged and appearing pink in color; conglomerates also are pink, appearing like a "+" symbol from the side (Figure 13). The species is most similar in appearance to *F. cuneolus*, but differs by having a shiny periostracum, wider rays, and slightly deeper and longer sulcus.

Fusconaia cuneolus – The shell outline is elongate, even in smaller individuals <50 mm, but can occasionally appear quadrate. The periostracum color in young individuals can range from yellow, light brown to dark brown, whereas larger older individuals typically are dark brown (Figure 6). The periostracum rays are conspicuously narrow or fine, 1 mm or less. Rays typically extend to the shell margin continuously, but occasionally they are interrupted or broken. The sheen of the periostracum is satiny or dull. The posterior ridge of the shell is angular. A shallow depression or sulcus is present on the mid-section of the shell, typically extending from the ventral margin to 2/3 the length of the shell but not onto the umbo. The height of the umbo is moderate to high (2–4 mm). The position of the umbo is predominantly anterior. The beak cavities are deep and angular. Foot color can vary from orange to cream white, occasionally appearing light pink. No individuals were collected gravid. The species is most similar in appearance to *F. cor*, but differs by having a duller periostracum, finer rays and a shallower and shorter sulcus.

Fusconaia subrotunda – The shell outline is predominantly elongate, especially in larger individuals >70 mm, but smaller individuals are variable, appearing rounded, quadrate to elongated. The periostracum color is chestnut brown to dark brown (Figure 7). The periostracum rays are narrow, typically 1 mm. Rays typically extend to the shell margin continuously, but occasionally they are interrupted or broken. The sheen of the periostracum is satiny in small individuals, becoming dull in larger individuals. The posterior ridge of the shell is rounded, occasionally appearing flat. The shell lacks a sulcus. The height of the umbo is typically moderate (~2 mm). The position of the umbo is predominantly anterior, occasionally centrally located. The beak cavities are deep and angular. Foot color varies from orange to white. Only one individual was observed gravid; all four gills were charged and red in color. Conglutinates

were red, elongate, slender and conical, sometimes being bifurcate, trifurcate, or multi-furcate (Figure 13). The species can resemble *F. cor* and *F. cuneolus*, but differs by lacking a sulcus. When young and <50 mm, it can be confused with *P. barnesiana*, appearing compressed and quadrate, but with a darker-brown periostracum.

Pleurobema oviforme – The shell outline is predominantly elongate, even in smaller individuals <50 mm. The periostracum color is light brown when young, fading to dark brown in older individuals (Figure 8). The periostracum rays are narrow to wide, typically 1–2 mm wide, but occasionally wider. The rays typically extend to the shell margin continuously, but occasionally they are interrupted or broken. The sheen of the periostracum is dull to satiny. The posterior ridge of the shell is rounded. The shell lacks a sulcus. The height of umbo is typically low to moderate, 1 mm or less. The position of the umbo is predominantly anteriorly located, occasionally central. The beak cavities are shallow and rounded. Foot color typically is white to cream-white, occasionally pale-orange to orange. In gravid individuals, the outer two gills are charged and white to pale-orange in color. The conglutinates are white to pale orange, sometimes bifurcate, but when flat, appear like a football in outline (Figure 13). The species is most similar in appearance to *Pleurobema barnesiana* and *P. sp. cf. barnesiana*; the shell traits are nearly indistinguishable, but larger individuals are typically elongate. Further, the white-colored conglutinates and two charged gills of gravid individuals are diagnostic.

Pleurobema sp. cf. oviforme – The shell outline is predominantly elongate, even in smaller individuals <50 mm. The periostracum color is brown to dark brown (Figure 9). The periostracum rays are narrow, typically 1 mm or less; younger individuals are faintly rayed to ray-less. The rays typically extend to the shell margin continuously. The sheen of the periostracum is very satiny. The posterior ridge of the shell is rounded. The shell lacks a sulcus.

The height of the umbo is typically very low, 1 mm or less, occasionally flush with or below the shell margin. The position of the umbo is predominantly anteriorly located. The beak cavities are shallow to very shallow and rounded. The foot color is orange. In gravid individuals, the outer two gills are charged and orange in color. The conglutinates are orange, sometimes bifurcate, but when flat, appear like a football in outline (Figure 13). The species generally is distinctive from the other study species by an elongate shell, satiny periostracum, low umbo and orange foot.

Pleuroaia barnesiana – The shell outline is predominantly quadrate, especially in smaller individuals <50 mm; larger individuals occasionally are elongate. The periostracum color is light brown when young, fading to dark brown in older individuals (Figure 10). The periostracum rays are typically narrow, 1–2 mm wide, with occasional finer rays. The rays typically extend to the shell margin continuously, but occasionally they are interrupted or broken. The sheen of the periostracum is dull to satiny. The posterior ridge of the shell is rounded to occasionally angular. The shell lacks a sulcus. The height of the umbo typically is low to moderate, 1 mm or less. The position of the umbo is predominantly centrally located, occasionally anterior in elongated individuals. The beak cavities are shallow and rounded. Foot color typically is white to cream white. In gravid individuals, all four gills are charged, but the conglutinates are small, slender and conical, and light tan in color, making them difficult to see when inspecting gravid individuals. The species is most similar in appearance to *Pleuroaia* sp. cf. *barnesiana*; the shell traits are nearly indistinguishable, but differ by typically having a white-colored foot, and tan-colored conglutinates that are slender (Figure 14).

Pleuroaia sp. cf. *barnesiana* – The shell outline is predominantly elongate, even in smaller individuals <50 mm. The periostracum color is light brown when young, fading to dark brown in older individuals (Figure 11). The periostracum rays are typically narrow, 1–2 mm

wide, occasionally with finer or broader rays. The rays typically extend to the shell margin continuously, but occasionally they are interrupted or broken. The sheen of the periostracum is dull to satiny. The posterior ridge of the shell is rounded. The shell lacks a sulcus. The height of the umbo is typically low to moderate, 1 mm or less. The position of the umbo is predominantly anteriorly located, especially in elongated individuals. The beak cavities are shallow and rounded. Foot color is orange to pale orange. In gravid individuals, all four gills are charged and orange in color. The conglutinates are pale orange, sometimes bifurcate, but when flat, appear like a football in outline (Figure 14). The species is most similar in appearance to *Pleuonaia barnesiana*; the shell traits are nearly indistinguishable, but differ by typically having an orange-colored foot and conglutinates.

Pleuonaia dolabelloides – The shell outline is predominantly rounded to elongate, occasionally quadrate, sometimes appearing truncated on the posterior end. The periostracum color is predominantly yellow, occasionally light brown (Figure 12). The periostracum rays are typically >1–2 mm wide. The rays typically extend to the shell margin in small individuals <50 mm; however, in older and larger individuals, the rays rarely extend to the margin, only to 1/2 the shell height. The rays are interrupted or broken, especially in larger individuals. The sheen of the periostracum is dull. The posterior ridge of the shell is angular. The shell lacks a sulcus. The height of the umbo is typically low to moderate, 1 mm or less. The position of the umbo is predominantly centrally located, occasionally anterior in older individuals. The beak cavities are shallow and rounded. Foot color is typically orange, varying from red-orange to pale-orange, rarely cream-white. In gravid individuals, the outer two gills are charged and pink in color. The conglutinates are elongate, slender and conical, sometimes being bifurcate, trifurcate, or multi-

furcate (Figure 14). The species generally is distinctive from the other study species by its shell outline, yellow periostracum with rays that are short, wide and interrupted.

Assessment of Glochidia Dimensions among Species – Mean measurements of glochidia for gravid mussels collected in this study are reported in Table 6. Tukey's pairwise comparisons of height, length, and hinge length revealed significant differences among species (Table 7). At $\alpha=0.05$, the following comparisons between species were significantly different at all three measurements: *F. cor* and *P. sp. cf. oviforme*; *F. cor* and *P. sp. cf. barnesiana*; *F. subrotunda* and *P. sp. cf. oviforme*; *F. subrotunda* and *P. sp. cf. barnesiana*; *P. oviforme* and *P. sp. cf. barnesiana*; *P. barnesiana* and *P. sp. cf. oviforme*; and *P. barnesiana* and *P. sp. cf. barnesiana*.

Classification and Regression Tree Analysis of Morphological Data – The CART analysis of live individuals using traditional morphological measurements (continuous variables) plus foot color produced a decision tree with 22 splits, 23 terminal nodes, and an overall classification accuracy of 62.0% on terminal nodes (Figure 15). All measurements were utilized in the decision tree, except for maximum height perpendicular to maximum length. The classification accuracy on terminal nodes ranged from 32.0% to 100%, with three nodes achieving 100% accuracy, including *F. cuneolus* and two groups of *P. oviforme*; due to the CART analysis attempting to classify species based on the best way to separate species, some species have multiple terminal nodes. However, terminal nodes with 100% accuracy do not reflect the species' overall accuracy. A confusion matrix (Table 8) gives the tree's misidentification rates for each species, and showed that *F. subrotunda* was most likely to be confused as another species (31.0% correct or 69.0% error), and other species were most likely

to be confused as *F. subrotunda* (41.9% correct or 58.1% error). *Pleuonaia barnesiana* was most likely to not be confused as another species (84.5% correct) and other species were least likely to be confused as *Pleuonaia dolabelloides* (84.2% correct).

The CART analysis incorporating continuous and categorical variables for "live" individuals from sacrificed individuals and FMCC shells produced a decision tree with 15 splits, 16 terminal nodes and an overall accuracy of 77.5% on the terminal nodes (Figure 16). The analysis utilized the following variables to construct the decision tree: foot color; maximum height perpendicular to maximum length; maximum height at umbo perpendicular to maximum length, maximum length, umbo elevation, periostracum color, periostracum sheen, posterior ridge, ray length, and ray pattern. The accuracy on terminal nodes ranged from 50.0% to 100%, with four nodes achieving 100% accuracy, including nodes for *F. cor*, *F. subrotunda*, *P. oviforme*, and *P. barnesiana*. A confusion matrix (Table 9) gives the tree's misidentification rates for each species, and showed that *Pleurobema oviforme* was the most likely to be confused as another species (65.3% correct or 34.7% error), and other species were most likely to be confused with *Pleuonaia barnesiana* (65.5% correct or 34.5% error). *Pleurobema* sp. cf. *oviforme* was the least likely to be confused as another species (100% correct), and other species were least likely to be confused as *Fusconaia cor* (100% correct).

The CART analysis of continuous and categorical variables for shell-only material from sacrificed individuals and FMCC shells produced a decision tree with 13 splits, 14 terminal nodes, and an overall accuracy of 80.6% on the terminal nodes (Figure 17). The analysis utilized the following variables: beak cavity, hinge length, maximum length, umbo elevation, periostracum color, periostracum sheen, posterior ridge, ray pattern, ray width, and presence of sulcus. Accuracy on terminal nodes ranged from 50% to 100%, with two nodes achieving 100%

accuracy, *F. cor* and *P. oviforme*. A confusion matrix (Table 10) gives the tree's misidentification rates for each species, and showed that *Pleuroaia* sp. cf. *barnesiana* was the most likely to be confused as another species (71.4% correct or 28.6% error) and other species were most likely to be confused with *Pleuroaia* sp. cf. *barnesiana* (62.5% correct or 37.5% error). *Fusconaia subrotunda* was least likely to be confused as another species (95.2% correct) and other species were least likely to be confused as *Fusconaia cor* (100% correct).

Geometric Morphometrics – Photographs for 414 individuals of 8 species were digitized for geometric morphometric analyses (Table 2). The CVA yielded four distinct canonical variates, but the plot illustrated overlap of individuals between species (Figure 18). Groupings by CVA produced 44.7% accuracy in assigning individuals to their respective species (Table 11). *Pleurobema* sp. cf. *oviforme* was least likely to be confused as another species (87.5% correct) and other species were least likely to be confused with *Pleurobema oviforme* (57.8% correct). Goodall's *F*-tests produced significant differences between all groups of species except when analyzing *Pleurobema oviforme* vs. *Pleuroaia* sp. cf. *barnesiana* (Table 11); while there were significant differences between mean shapes of species, overlap of shell shape between individuals of different species was observed. Mean shapes of each species were visually compared to determine extent of differences, but similarity was too great to make meaningful distinctions among species (Figure 19).

DISCUSSION

Classification and Regression Tree Analysis of Morphological Data – In this study, quantitative variables were easy to measure, while categorical variables were more difficult to

measure, and often individuals possessed characters that were intermediate between two categories. These judgment decisions could prove difficult to biologists that wish to identify species without error. The most accurate decision tree produced from CART analysis was for the analysis of shells from non-living mussels using categorical variables. Accuracy of this decision tree likely would decrease if categorical variables were classified incorrectly in the development of the study or by future users of the decision tree. Incorrect assessment of categorical variables could affect any species' assignment, beginning with beak cavity depth; if beak cavity depth was not assessed in the same manner as the key was built, the subsequent steps would lead to incorrect species assignment. Other characters that could proved difficult to assess were shape of posterior ridge, length and pattern of periostracum rays, periostracum color, and presence or absence of sulcus. Thus, adequate training is required to score categorical variables as accurately as possible. A benefit of the CART approach is the ability of the program to use variables from multiple categories (e.g., continuous and categorical variables) to identify species. A drawback, however, is that CART uses a "greedy" algorithm; i.e., this algorithm makes categorical splits that best discriminate species early on in the identification process, but does not find the overall best algorithm that reduces error on terminal nodes.

The least accurate CART analysis used traditional quantitative morphometric and foot color data, and achieved an overall accuracy of 62.0% on terminal nodes. Foot color was the root, or first split, but varied within species; only for *P. sp. cf. oviforme* did all individuals have the same foot color. Eight individuals of *F. cuneolus* were identified with 100% accuracy, as these were the only mussels to have pink-colored feet. Terminal nodes were reached by combinations of foot color and quantitative variables. The lower accuracy of this analysis was due to overlap of traditional quantitative measurements among species.

The second-best performing CART analysis used quantitative and categorical variables from sacrificed live individuals and achieved an overall accuracy of 77.5% on terminal nodes; this data set included individuals from the FMCC collection that were not genetically verified. Foot color was the root, and varied less in this analysis than in the previous one due to using the modal value of this trait, which was orange. The modal value was applied to all individuals used from the FMCC collection, which resulted in specimens of *F. cor*, *F. cuneolus*, *P. sp. cf. oviforme*, and *P. dolabelloides* from the collection being coded with the same foot color. Since these species generally have an orange foot, applying the modal value for foot color likely did not greatly affect the analysis and classification rates for these species. Terminal nodes were determined by combinations of quantitative and categorical variables. The lower accuracy of this analysis was due to morphological overlap between species, but the categorical variables improved accuracy of species identifications.

The best-performing CART analysis used shell-only quantitative and categorical variables from sacrificed individuals, and achieved an overall accuracy of 80.6% on terminal nodes. This data set also included individuals from the FMCC shell collection that were not genetically verified. Beak cavity depth was the root, which varied minimally among species and was deeper for species of *Fusconaia* compared to species of *Pleurobema* and *Pleuonaia*. Terminal nodes were reached by combinations of quantitative and categorical variables. Increased accuracy of this tree is due to use of categorical variables, namely beak cavity. Categorical variables improved accuracy of decision trees and often are used by field biologists. While categorical traits proved useful for identifying species, they can overlap among species and categories, leading to judgment decisions being made by the practitioner. Further, such

judgment decisions can vary among biologists, making transmission of species identifications knowledge difficult.

Including categorical variables in the decision tree analysis increased accuracy, but – perhaps paradoxically – smaller sample sizes may have been a contributing factor in the increased accuracy. Lacourse and May (2012) found that decreasing sample sizes for pollen identification increased CART accuracy using morphological features. Smaller sample sizes are less likely to capture a broader range of morphological variation; in addition, localized collections not encompassing species' ranges also will not capture regional morphological differences. Larger sample sizes from entire species' ranges will more accurately capture morphological variation than smaller, more localized collections; however, the decision trees in these analyses were created for the UTRB. Categorical data used in CART analysis using shells from the FMCC collection did not encompass the species' ranges from the UTRB, with individuals coming from few sites, and did not include many individuals; additionally, the shells that were selected for analysis were typical individuals for each species; thus, potential morphological variations were not captured.

Geometric Morphometrics – The CVA using geometric morphometric data exhibited a high amount of morphological overlap among species and thus consistent patterns to separate species were not found when all species were analyzed together. Analyses for pairs of species using Goodall's *F*-test demonstrated that statistically significant morphometric differences occurred between all species pair but one; however, these morphometric traits overlapped between individuals and among species. Significant differences were not observed between *P. oviforme* and *P. sp. cf. barnesiana*, which is consistent with difficulties in identifying these two

species in the field without knowledge of foot color. While these results are statistically significant, the morphological differences cannot be applied by field biologists due to the high morphological overlap among species.

I chose to use only 11 shell landmarks for geometric morphometric analyses under the assumption that fewer landmarks could illustrate more visually obvious changes that could be incorporated into field-level identification characters. However, future studies, should explore more landmarks, as they have the benefit of recognizing differences in curvature of external margins, especially where the landmarks are not close together (e.g., the posterior margin). Even if statistical differences occur between species with minimal morphological overlap, geometric morphometrics are not useful for field biologists; direct comparison would require precise photographs and digitization of specimens in question. Although geometric morphometrics should be used to determine if significant differences exist between species, and then used to determine the best solution (e.g., measurements or traits) that will help field biologists separate the species in question.

Cryptic Species Discovered – Molecular genetic analyses of freshwater mussels (Chapter 1) revealed three currently unrecognized taxa. Morphological analyses were conducted on two of these species, *P. sp. cf. oviforme* and *P. sp. cf. barnesiana*, to determine differences and similarities among the study taxa. Morphological traits were not recorded for *P. sp. cf. dolabelloides* from South Chickamauga Creek so distinguishing traits are not currently available or discussed further herein. While large morphological overlap occurred among these species, and therefore they were unrecognized due to similarity of appearance with other species, some general traits can help correctly identify them. Currently, *P. sp. cf. oviforme* is considered

endemic to Little River, Blount County, Tennessee, where it co-occurs with *P. oviforme* and *P. barnesiana*. Typically, *P. oviforme* and *P. barnesiana* have a white-colored foot, with the former occasionally having a pale-orange foot; all individuals of *P. sp. cf. oviforme* had an orange-colored foot. Additionally, these species can easily be distinguished when in gravid condition, with *P. barnesiana* having all four gills charged and tan in color, *P. oviforme* having the outer two gills charged, typically white and occasionally pale-orange in color, while *P. sp. cf. oviforme* having the outer two gills charged and orange in color. These morphological characters can help distinguish *P. sp. cf. oviforme* from congeners within its known range in the Little River, TN.

The known distribution of *P. sp. cf. barnesiana* is more sporadic. It has been found in one location each in the Powell River and South Chickamauga Creek drainages, and it occurs throughout the Clinch River and its tributaries. Thus, it could occur in many of the streams of the Upper Tennessee River Basin. It was found to co-occur with *F. cor*, *F. cuneolus*, *F. subrotunda*, *P. oviforme*, *P. barnesiana*, *P. dolabelloides*, and *P. sp. cf. dolabelloides*. Leaving aside molecular genetic markers (Chapter 1), it typically is distinguished from *F. cor* and *F. cuneolus* by its lack of a sulcus and shallow beak cavity, from *F. subrotunda* by its shallow beak cavity, from *P. barnesiana* and *P. oviforme* by its pale-orange foot and from *P. dolabelloides* by continuous and finer rays. The most difficult identifications typically occurs between *P. sp. cf. barnesiana* and *P. oviforme* or *P. barnesiana* due to similar size and shape of the shell, as well as needing to determine foot color. However, *P. sp. cf. barnesiana* is unique in its gravid state, with all four gills charged and orange in color.

Morphological Similarities – Variations in shell morphology in freshwater mussels has challenged taxonomists throughout the centuries. Many described species were later found to be the same and synonymized, for example with *Pyganadon grandis* having approximately 78 synonymous names (Williams et al. 2008). Incorporating soft-anatomy into species descriptions assisted with developing a more accurate taxonomy, but molecular genetic approaches also have improved the understanding of taxonomy and phylogeny of freshwater mussels.

Species identifications and morphological analyses across size-classes of mussels also are challenging because mussel shape changes with size. Further, environmental factors influence how mussels grow. Results from morphological analyses could be obscured due to inconsistent shell growth due to habitat influences; mussels in swifter waters or coarser substrates may not grow the same as conspecific mussels in slower water, with finer substrates (Zieritz et al. 2010; Inoue et al. 2013). Congruent with Ortmann's law of stream position (Ortmann 1920), individuals living in headwater streams are elongate and compressed, while individuals living in larger streams are round and inflated (Hornbach et al. 2010).

Collection of each species from differing habitats in the UTRB may have provided too much morphological overlap between conchologically similar species in the genera *Fusconaia*, *Pleurobema*, and *Pleuronaia*. While future studies should attempt to classify the microhabitat from which each individual was collected, it is important to note that these often-sedentary animals can move or be washed into sections of the stream from which they did not originally settle and grow in. While developmental genetics influences the typical shape into which the shell should grow, environmental factors obviously can affect shell shape and lead to phenotypic plasticity.

Although sample sizes were not adequate to include gravidity into the CART analyses, this trait is valuable for field identification of freshwater mussels. Assessment of gravidity would require biologists to obtain mussels during the breeding season and assess the gravid traits without injuring the mussel. Of all the species examined, only *F. cuneolus* was not observed gravid; however, all species examined were distinct in their gravid state using a combination of number, location and color of charged gills.

Management Implications – While the most accurate CART analysis improved the classification of individuals from random chance (1/8 or 12.5%) to 80.6%, the classification error is too great for field biologists to reliably use the decision tree to identify all species; 100% classification rates would be ideal, but future studies should explore the minimum classification rate that would not hinder management objectives. Additionally, because the data were not partitioned for the CART analyses, the presented error rates may be optimistic. Further, this decision tree requires shells rather than live individuals, which is not always practical. Species' distributions and abundances play important roles in management decisions, and 80.6% accuracy level would still lead to incorrect species records and possibly incorrect management decisions. However, some species such as *F. cor* (91.7%), *F. cuneolus* (87.5%), *F. subrotunda* (95.2%), and *P. sp. cf. oviforme* (87.5%) had higher classification rates for the shell analysis; similarly for the live analysis, *F. cor* (91.7%), *F. cuneolus* (87.5%), *P. sp. cf. oviforme* (100%), *P. sp. cf. barnesiana* (85.7%), and *P. dolabelloides* (84.6%) had higher classification rates. These species can be more reliably identified in the field than other species. When utilizing gravid mussels, identifying individuals correctly in the genera *Fusconaia*, *Pleurobema*, and *Pleuronaia* in the

UTRB may be possible for field biologists, and thus leading to more accurate species identifications and field records of species occurrences.

While this study did not find shell and soft-anatomy traits to unequivocally identify freshwater mussels in the genera *Fusconaia*, *Pleurobema*, and *Pleuronaia*, there are still various approaches and characters that expert mussel taxonomists use. Many begin with the question: Where did the shell come from? This question can be valid, but relies on previous species distribution knowledge to narrow the possible species to which the shell could belong. Then biologists attempt to identify the species based upon a variety of categorical traits, i.e., traits that can be difficult to accurately assess. These characters can include presence/absence of sulcus, shape and position of posterior ridge, shape and position of posterior margin, variations of periostracum color, distance between external annuli, minor striations, and position and size of rays on the shell. Field biologists are able to incorporate many qualitative characters, many of which are ambiguous, into identification schemes that are not easy to quantitatively assess. Critically, this specialized knowledge and its application for reaching decisions on categories for characters is difficult to teach others.

I recommend that species occurrences outside known ranges be confirmed using mitochondrial DNA markers. For example, if a live mussel is thought to be a new distributional record for the species or its occurrence could affect implementation of a project, its species identity should be verified using molecular genetic techniques. Using DNA as a basis, future surveys can identify field-collected individuals and verify whether the species is known to occur near the survey site; if surveyors believe the occurrence of the mussel may be a range extension, they should recommend a genetic identification. While this may sound impractical, contracts between state agencies and universities pose reasonable costs, and field surveyors would only

need to carry buccal swabs in order to collect tissue material for isolation of DNA. This approach will increase our understanding of species distributions and abundance, as well as assist in possibly discovering unrecognized taxa.

LITERATURE CITED

- Adams D.C., F.J. Rohlf, D.E. Slice. 2004. Geometric morphometrics: Ten years of progress following the 'revolution'. *Italian Journal of Zoology*, 71 (1):5-16.
- Bogan A.E., K.J. Roe. 2008. Freshwater bivalve (Unioniformes) diversity, systematics, and evolution: Status and future directions. *Journal of the North American Benthological Society*, 27 (2):349-369.
- Christian A.D., J.L. Harris, J.M. Serb. 2008. Preliminary analysis for identification, distribution, and conservation status of species of *Fusconaia* and *Pleurobema* in Arkansas. Report, Arkansas Game and Fish Commission, Perrytown, Arkansas. 40 pp.
- Haag W.R. 2012. *North American Freshwater Mussels: Natural History, Ecology, and Conservation*. Cambridge University Press Cambridge, UK.
- Haag W., J. Williams. 2014. Biodiversity on the brink: An assessment of conservation strategies for North American freshwater mussels. *Hydrobiologia*, 735 (1):45-60.
- Hornbach D.J., V.J. Kurth, M.C. Hove. 2010. Variation in freshwater mussel shell sculpture and shape along a river gradient. *American Midland Naturalist*, 164 (1):22-36.
- Hughes M.H., P.W. Parmalee. 1999. Prehistoric and modern freshwater mussel (mollusca: Bivalvia: Unionoidea) faunas of the Tennessee River: Alabama, Kentucky, and Tennessee. *Regulated Rivers: Research & Management*, 15 (1-3):25-42.
- Inoue K., D.M. Hayes, J.L. Harris, A.D. Christian. 2013. Phylogenetic and morphometric analyses reveal ecophenotypic plasticity in freshwater mussels *Obovaria jacksoniana* and *Villosa arkansasensis* (Bivalvia: Unionidae). *Ecology and Evolution*, 3 (8):2670-2683.

- Jones J.W., R.J. Neves. 2002. Life history and propagation of the endangered fanshell pearl mussel, *Cyprogenia stegaria* Rafinesque (Bivalvia:Unionidae). *Journal of the North American Benthological Society*, 21 (1):76-88.
- Jones J.W., R.J. Neves. 2010. Descriptions of a new species and a new subspecies of freshwater mussels, *Epioblasma ahlstedti* and *Epioblasma florentina aureola* (Bivalvia: Unionidae), in the Tennessee River drainage, USA. *The Nautilus*, 124 (2):77.
- Lacourse T., L. May. 2012. Increasing taxonomic resolution in pollen identification: Sample size, spatial sampling bias and implications for palaeoecology. *Review of Palaeobotany and Palynology*, 182:55-64.
- Neves R.J., A.E. Bogan, J.D. Williams, S.A. Ahlstedt, P.W. Hartfield. 1997. Status of aquatic mollusks in the southeastern United States: A downward spiral of diversity. Pages 43-86 in G. W. Benz and D. E. Collins, editors. *Aquatic fauna in peril: The southeastern perspective*. Lenz Design and Communications, Decatur, GA, Special Publication 1, Southeast Aquatic Research Institute.
- Ortmann A.E. 1920. Correlation of shape and station in fresh-water mussels (naiades). *Proceedings of the American Philosophical Society*, 59 (4):269-312.
- Parmalee P.W., A.E. Bogan. 1998. *The Freshwater Mussels of Tennessee*. The University of Tennessee Press, Knoxville, Tennessee, USA.
- R Development Core Team. 2011. *R: A language and environment for statistical computing*. R foundation for statistical computing, vienna, austria. ISBN 3-900051-07-0. <http://www.R-project.org>.
- Ricciardi A., J.B. Rasmussen. 1999. Extinction rates of North American freshwater fauna. *Conservation Biology*, 13 (5):1220-1222.

- Rohlf F.J. 2005. Tpsdig2, version 2.0. Department of Ecology and Evolution, State University of New York, Stony Brook.
- Sheets D.H. 2000. Integrated morphometrics software (IMP) - mathworks, matlab6. The Mathworks, Natick, Massachusetts <http://www.canisius.edu/~sheets/morphsoft.html>.
- Slice D.E. 2007. Geometric morphometrics. *Annual Review of Anthropology*, 36 (1):261-281.
- Spooner D.E., C.C. Vaughn. 2006. Context-dependent effects of freshwater mussels on stream benthic communities. *Freshwater Biology*, 51 (6):1016-1024.
- Therneau T.M., B. Atkinson, B. Ripley. 2010. Rpart: Recursive partitioning. R package version, 3:1-46.
- United States Fish and Wildlife Service (USFWS). 1975. Proposed endangered status for 216 species on convention on international trade. *Federal Register* 40:(188): 44329-44333.
- United States Fish and Wildlife Service (USFWS). 1991. Endangered and threatened wildlife and plants; determination of endangered status for the cumberland pigtoe mussel. *Federal Register* 56:(88): 21084-21087.
- United States Fish and Wildlife Service (USFWS). 2013. Endangered and threatened wildlife and plants; endangered species status for the fluted kidneyshell and slabside pearlymussel and designation of critical habitat. *Federal Register* 78:(187): 59269-59287.
- Vaughn C.C., S.J. Nichols, D.E. Spooner. 2008. Community and foodweb ecology of freshwater mussels. *Journal of the North American Benthological Society*, 27 (2):409-423.
- Watters G.T. 1996. Small dams as barriers to freshwater mussels (Bivalvia, Unionoida) and their hosts. *Biological Conservation*, 75 (1):79-85.
- Watters G.T., M.A. Hoggarth, D.H. Stansbery. 2009. *The Freshwater Mussels of Ohio*. Ohio State University Press Columbus, Ohio.

- Williams G.J. 2009. Rattle: A data mining guide for R. *The R Journal*, 1 (2):45-55.
- Williams J.D., M.L. Warren, K.S. Cummings, J.L. Harris, R.J. Neves. 1993. Conservation status of freshwater mussels of the United States and Canada. *Fisheries*, 18 (9):6-22.
- Williams J.D., A.E. Bogan, J.T. Garner. 2008. *Freshwater Mussels of Alabama and the Mobile Basin in Georgia, Mississippi and Tennessee*. The University of Alabama Press, Tuscaloosa, Alabama.
- Zelditch M.L., D.L. Swiderski, H.D. Sheets. 2004. *Geometric Morphometrics for Biologists: A Primer*. Academic Press, New York.
- Zieritz A., J.I. Hoffman, W. Amos, D.C. Aldridge. 2010. Phenotypic plasticity and genetic isolation-by-distance in the freshwater mussel *unio pictorum* (Mollusca: Unionoida). *Evolutionary Ecology*, 24 (4):923-938.

Table 1. Locality information for sites sampled for freshwater mussels in the Tennessee River basin from 2012 through 2014. Data from live mussels collected at these sites were used to conduct the morphological analyses in this study.

Site Number	Drainage	Stream	River km	River Mile	Collection Site	County	State	Latitude	Longitude
1	Powell	Powell River	214.0	133.0	Towell Ford	Lee	Virginia	36.63330	-83.17429
2	Powell	Powell River	210.5	130.8	Flanary Bridge	Lee	Virginia	36.64306	-83.20391
3	Powell	Powell River	199.5	124.0	Snodgrass Ford	Lee	Virginia	36.61873	-83.24799
4	Powell	Powell River	185.9	115.5	Baldwin Ford	Hancock	Tennessee	36.59530	-83.30549
5	Powell	Powell River	180.6	112.2	Bales Ford	Hancock	Tennessee	36.58230	-83.33289
6	Powell	Powell River	164.8	102.4	Alanthus Hill	Hancock	Tennessee	36.56082	-83.39177
7	Powell	Powell River	144.4	89.7	Wellness Center	Claiborne	Tennessee	36.53511	-83.46728
8	Powell	Indian Creek	24.6	15.3	Machine Branch	Lee	Virginia	36.62099	-83.53786
9	Powell	Indian Creek	0.3	0.2	Aggy Vanderpool's	Claiborne	Tennessee	36.55992	-83.60705
10	Clinch	Indian Creek	0.8	0.5	631 Bridge	Tazewell	Virginia	37.08773	-81.75887
11	Clinch	Little River	48.9	30.4	Ostby Sites 12&13	Tazewell	Virginia	37.03010	-81.78014
12	Clinch	Clinch River	447.5	278.1	Bennet Property	Russell	Virginia	36.96063	-82.09579
13	Clinch	Clinch River	441.9	274.6	Artrip	Russell	Virginia	36.96229	-82.12002
14	Clinch	Clinch River	437.9	272.1	Cleveland Elementary	Russell	Virginia	36.94473	-82.14821
15	Clinch	Clinch River	435.8	270.8	Cleveland	Russell	Virginia	36.93711	-82.16432
16	Clinch	Clinch River	401.7	249.6	Burtens Ford	Wise	Virginia	36.89224	-82.33993
17	Clinch	Clinch River	378.3	235.1	Semones	Scott	Virginia	36.80936	-82.48399
18	Clinch	Clinch River	339.9	211.2	Spears Ferry	Scott	Virginia	36.65007	-82.74842
19	Clinch	Clinch River	309.8	192.5	Wallen Bend	Hancock	Tennessee	36.57927	-83.00404
20	Clinch	Clinch River	305.4	189.8	Kyle's Ford	Hancock	Tennessee	36.56953	-83.04100
21	Clinch	Clinch River	291.8	181.3	Frost Ford	Hancock	Tennessee	36.53077	-83.15085
22	Clinch	Clinch River	287.6	178.7	Garland Hollow	Hancock	Tennessee	36.52171	-83.19388
23	Clinch	Clinch River	277.1	172.2	Swan Island	Hancock	Tennessee	36.47349	-83.28995
24	Clinch	Copper Creek	87.2	54.2	Parsonage	Russell	Virginia	36.82027	-82.23781
25	Clinch	Copper Creek	24.1	15.0	Holland Property	Scott	Virginia	36.69179	-82.54093
26	Clinch	Copper Creek	21.7	13.5	Williams Mill	Scott	Virginia	36.67833	-82.55828
27	Clinch	Copper Creek	4.2	2.6	Jennings Ford	Scott	Virginia	36.65792	-82.71182
28	Holston	North Fork Holston River	191.7	119.1	619 Bridge	Smyth	Virginia	36.94680	-81.42096
29	Holston	North Fork Holston River	175.2	108.9	Chatham Hill	Smyth	Virginia	36.95545	-81.52300
30	Holston	North Fork Holston River	142.7	88.7	Possum Hollow Rd	Smyth	Virginia	36.90987	-81.69957
31	Holston	Possum Creek	12.2	7.6	Route 637	Scott	Virginia	36.59568	-82.65532
32	Holston	Middle Fork Holston River	16.3	10.1	Neff	Washington	Virginia	36.70459	-81.86119
33	Holston	Middle Fork Holston River	15.4	9.6	Lower Neff	Washington	Virginia	36.69940	-81.85765
34	Holston	Beech Creek	25.6	15.9	Ball Cemetary	Hawkins	Tennessee	36.40276	-82.77281
35	Holston	Beech Creek	20.6	12.8	Van Hill	Hawkins	Tennessee	36.38576	-82.81234
36	Holston	Beech Creek	17.7	11.0	Private Bridge	Hawkins	Tennessee	36.39561	-82.82597
37	Holston	Beech Creek	10.8	6.7	Keplar Bridge	Hawkins	Tennessee	36.40076	-82.88415
38	Holston	Beech Creek	3.9	2.4	Tunnel Hill Church	Hawkins	Tennessee	36.38951	-82.91663
39	Nolichucky	Nolichucky River	47.2	29.3	Pate Hill	Greene	Tennessee	36.09284	-83.03545
40	Nolichucky	Little Chucky Creek	14.0	8.7	Sinking Springs Road	Greene	Tennessee	36.12375	-83.01076
41	French Broad	Little Pigeon River	9.8	6.1	Sevierville	Sevier	Tennessee	35.87317	-83.57164
42	Tennessee	Little River	47.6	29.6	Apple Store	Blount	Tennessee	35.68228	-83.78775
43	Tennessee	Little River	33.2	20.6	Coulter's Bridge	Blount	Tennessee	35.76385	-83.85273
44	Tennessee	Little River	23.8	14.8	River Jon's	Blount	Tennessee	35.79638	-83.88515
45	Tennessee	Little River	20.0	12.4	Brakebill Island	Blount	Tennessee	35.81021	-83.89966
46	Little Tennessee	Little Tennessee River	167.0	103.8	McCoy Bridge	Macon	North Carolina	35.27178	-83.44036
47	Little Tennessee	Little Tennessee River	144.4	89.7	Halls Ford	Swain	North Carolina	35.35550	-83.50662
48	Emory	Emory River	62.8	39.0	Gobey	Morgan	Tennessee	36.14942	-84.60550
49	Hiwassee	Hiwassee River	96.6	60.0	Turtletown	Polk	Tennessee	35.16777	-84.35236
50	South Chickamauga	South Chickamauga Creek	24.8	15.4	Ringgold	Catoosa	Georgia	34.91496	-85.12300
51	South Chickamauga	East Fork Chickamauga Creek	50.4	31.3	Freeman Springs Rd	Whitfield	Georgia	34.76076	-85.08174
52	Duck	Duck River	288.2	179.1	Lillard's Mill	Marshall	Tennessee	35.58595	-86.78707

Table 2. Sample sizes for live individuals identified to species using mitochondrial DNA (mtDNA), and for observations of morphological traits for specimens sampled in Upper Tennessee River basin from 2012-2014. Sample sizes of non-genetically identified shells from the FMCC collection also are included.

Mussel Species	mtDNA	Foot Color	Gravid	Shell Measurements	Geometric Morphometric	Shells	FMCC Shells
<i>Fusconaia cor</i>	46	40	1	40	43	3	9
<i>Fusconaia cuneolus</i>	28	27	0	27	27	0	8
<i>Fusconaia subrotunda</i>	44	42	1	42	44	17	4
<i>Pleurobema oviforme</i>	104	81	15	84	97	49	0
<i>P. sp. cf. oviforme</i>	24	24	5	24	24	7	9
<i>Pleuronaia barnesiana</i>	73	69	13	71	73	27	0
<i>P. sp. cf. barnesiana</i>	66	48	9	50	58	14	0
<i>Pleuronaia dolabelloides</i>	52	46	6	46	48	4	9
Grand Total	437	377	50	384	414	121	39

Table 3. Sample sizes of foot-color observations on live mussels of each species collected in the Upper Tennessee River basin from 2012-2014.

Mussel Species	Foot Color				Grand Total
	White	Pale Orange	Orange	Light Pink	
<i>Fusconaia cor</i>	2	29	9	0	40
<i>Fusconaia cuneolus</i>	2	14	3	8	27
<i>Fusconaia subrotunda</i>	28	10	4	0	42
<i>Pleurobema oviforme</i>	56	23	2	0	81
<i>P. sp. cf. oviforme</i>	0	0	24	0	24
<i>Pleuonaia barnesiana</i>	68	1	0	0	69
<i>P. sp. cf. barnesiana</i>	0	33	15	0	48
<i>Pleuonaia dolabelloides</i>	2	15	29	0	46
Grand Total	158	125	86	8	377

Table 4. Categorical variables for shell traits and respective sample sizes per species.

Species	Count	<u>Outline</u>			<u>Umbo Position</u>		<u>Ray Width</u>			<u>Ray Length</u>			<u>Ray Pattern</u>			<u>Ridge</u>	
		Elongate	Quadrata	Round	Anterior	Central	Fine	Wide	None	Margin	Short	None	Broken	Continuous	None	Angular	Round
<i>Fusconaia cor</i>	12	7	5	0	7	5	0	12	0	12	0	0	1	11	0	12	0
<i>Fusconaia cuneolus</i>	8	6	2	0	6	2	1	7	0	7	1	0	0	8	0	7	1
<i>Fusconaia subrotunda</i>	21	16	4	1	15	6	5	5	11	4	6	11	0	10	11	2	19
<i>Pleurobema oviforme</i>	49	41	7	1	44	5	7	17	25	14	10	25	7	17	25	4	45
<i>Pleurobema</i> sp. cf. <i>oviforme</i>	16	15	1	0	15	1	6	5	5	11	0	5	0	11	5	0	16
<i>Pleuonaia barnesiana</i>	27	16	11	0	16	11	11	8	8	11	8	8	3	16	8	8	19
<i>Pleuonaia</i> sp. cf. <i>barnesiana</i>	14	12	2	0	12	2	1	8	5	7	2	5	1	8	5	1	13
<i>Pleuonaia dolabelloides</i>	13	3	10	0	4	9	0	13	0	2	11	0	12	1	0	12	1
Grand Total	160	116	42	2	119	41	31	75	54	68	38	54	24	82	54	46	114

Table 4. Extended.

Species	<u>Color</u>				<u>Sheen</u>			<u>Sulcus</u>			<u>Beak</u>		<u>Foot Color</u>		
	Dark Brown	Brown	Light Brown	Yellow	Dull	Satiny	Shiny	Long	Short	None	Deep	Shallow	Orange	Pale Orange	White
<i>Fusconaia cor</i>	3	5	4	0	0	1	11	6	6	0	12	0	0	12	0
<i>Fusconaia cuneolus</i>	0	1	7	0	1	7	0	1	6	1	8	0	0	8	0
<i>Fusconaia subrotunda</i>	13	5	3	0	13	8	0	0	1	20	21	0	3	1	17
<i>Pleurobema oviforme</i>	13	8	28	0	36	13	0	0	1	48	0	49	2	13	34
<i>Pleurobema</i> sp. cf. <i>oviforme</i>	5	2	9	0	2	14	0	0	0	16	0	16	16	0	0
<i>Pleuonaia barnesiana</i>	15	3	8	1	12	15	0	0	1	26	0	27	0	0	27
<i>Pleuonaia</i> sp. cf. <i>barnesiana</i>	5	2	6	1	9	5	0	0	0	14	0	14	9	5	0
<i>Pleuonaia dolabelloides</i>	0	0	5	8	9	4	0	0	1	12	0	13	10	3	0
Grand Total	54	26	70	10	82	67	11	7	16	137	41	119	40	42	78

Table 5. Number of charged gills and their color for gravid mussels sampled in the Upper Tennessee River basin from 2012-2014. *No specimens were observed gravid during study; thus, number of charged gills is based on observations reported in literature.

<u>Mussel Species</u>	<u>No. Charged Gills</u>	<u>Color of Charged Gills</u>					<u>Grand Total</u>
		<u>Orange</u>	<u>Pink</u>	<u>Red</u>	<u>Tan</u>	<u>White</u>	
<i>Fusconaia cor</i>	4	0	1	0	0	0	1
<i>Fusconaia cuneolus*</i>	4	0	0	0	0	0	0
<i>Fusconaia subrotunda</i>	4	0	0	1	0	0	1
<i>Pleurobema oviforme</i>	2	4	0	0	0	11	15
<i>P. sp. cf. oviforme</i>	2	5	0	0	0	0	5
<i>Pleurobema barnesiana</i>	4	0	0	0	13	0	13
<i>P. sp. cf. barnesiana</i>	4	9	0	0	0	0	9
<i>Pleurobema dolabelloides</i>	2	0	6	0	0	0	6
Grand Total	NA	18	7	1	13	11	50

Table 6. Mean height, length, and hinge length of glochidia for species observed gravid. No individuals of *Fusconaia cuneolus* were observed gravid during this study.

Species	No. of Glochidea Measured	Height	Length	Hinge
<i>Fusconaia cor</i>	10	6.80	5.90	4.50
<i>Fusconaia cuneolus</i>	-	-	-	-
<i>Fusconaia subrotunda</i>	10	6.50	6.00	4.50
<i>Pleurobema oviforme</i>	110	6.97	7.47	5.59
<i>Pleurobema</i> sp. cf. <i>oviforme</i>	50	7.98	8.66	5.98
<i>Pleuronaia barnesiana</i>	100	6.92	6.95	5.39
<i>Pleuronaia</i> sp. cf. <i>barnesiana</i>	70	7.85	8.31	5.96
<i>Pleuronaia dolabelloides</i>	40	7.70	6.54	5.35

Table 7. Tukey's comparisons for glochidia measurements of species observed gravid. *P*-values are listed in the order of height, length, and hinge length.

<u>Species</u>	<i>Fusconaia</i> <u>cor</u>	<i>Fusconaia</i> <u>subrotunda</u>	<i>Pleurobema</i> <u>oviforme</u>	<i>Pleurobema</i> sp. cf. <u>oviforme</u>	<i>Pleurobema</i> <u>barnesiana</u>	<i>Pleurobema</i> sp. cf. <u>barnesiana</u>	<i>Pleurobema</i> <u>dolabelloides</u>
<i>Fusconaia cor</i>							
	0.985						
<i>Fusconaia subrotunda</i>	1.000						
	1.000						
	0.996	0.646					
<i>Pleurobema oviforme</i>	0.004	0.009					
	0.002	0.002					
	0.007	<0.001	<0.001				
<i>Pleurobema</i> sp. cf. <i>oviforme</i>	<0.001	<0.001	<0.001				
	<0.001	<0.001	0.056				
	1.000	0.770	0.999	<0.001			
<i>Pleurobema barnesiana</i>	0.117	0.194	0.034	<0.001			
	0.015	0.016	0.446	0.001			
	0.018	0.001	<0.001	0.981	<0.001		
<i>Pleurobema</i> sp. cf. <i>barnesiana</i>	<0.001	<0.001	<0.001	0.636	<0.001		
	<0.001	<0.001	0.034	1.000	<0.001		
	0.080	0.008	0.001	0.725	<0.001	0.973	
<i>Pleurobema dolabelloides</i>	0.691	0.828	0.002	<0.001	0.486	<0.001	
	0.038	0.039	0.571	0.006	1.000	0.004	

Table 8. Species predictions ($N=384$) using classification and regression tree analysis of traditional shell measurements and foot color data. Actual species identifications are reported in the rows and predictions made by the Classification and Regression Tree Analysis (CART) are reported in the columns.

<u>Species</u>	Species Predicted by CART for Traditional Shell Measurements and Foot Color								<u>% Correct Classification</u>
	<u><i>Fusconaia cor</i></u>	<u><i>Fusconaia cuneolus</i></u>	<u><i>Fusconaia subrotunda</i></u>	<u><i>Pleurobema oviforme</i></u>	<u><i>Pleurobema</i> sp. cf. <i>oviforme</i></u>	<u><i>Pleurobema barnesiana</i></u>	<u><i>Pleurobema</i> sp. cf. <i>barnesiana</i></u>	<u><i>Pleurobema dolabelloides</i></u>	
<i>Fusconaia cor</i>	24	2	2	0	1	2	9	0	0.6000
<i>Fusconaia cuneolus</i>	6	12	2	0	0	2	4	1	0.4444
<i>Fusconaia subrotunda</i>	2	0	13	8	0	15	3	1	0.3095
<i>Pleurobema oviforme</i>	1	3	6	56	2	10	6	0	0.6667
<i>Pleurobema</i> sp. cf. <i>oviforme</i>	0	0	0	0	20	0	3	1	0.8333
<i>Pleurobema barnesiana</i>	0	1	0	10	0	60	0	0	0.8451
<i>Pleurobema</i> sp. cf. <i>barnesiana</i>	4	3	1	2	3	0	37	0	0.7400
<i>Pleurobema dolabelloides</i>	9	1	7	0	3	1	9	16	0.3478
% Correct Classification	0.5217	0.5455	0.4194	0.7368	0.6897	0.6667	0.5211	0.8421	

Table 9. Species predictions ($N=160$) using classification and regression tree analysis of quantitative, foot color, and categorical variables from sacrificed live individuals. These data include non-genetically identified individuals from the FMCC shell collection. Actual species identifications are reported in the rows and predictions made by the Classification and Regression Tree Analysis (CART) are reported in the columns.

<u>Species</u>	Species Predicted by CART for Live Individuals								<u>% Correct Classification</u>
	<u><i>Fusconaia cor</i></u>	<u><i>Fusconaia cuneolus</i></u>	<u><i>Fusconaia subrotunda</i></u>	<u><i>Pleurobema oviforme</i></u>	<u><i>Pleurobema</i> sp. cf. <i>oviforme</i></u>	<u><i>Pleurobema barnesiana</i></u>	<u><i>Pleurobema</i> sp. cf. <i>barnesiana</i></u>	<u><i>Pleurobema dolabelloides</i></u>	
<i>Fusconaia cor</i>	11	1	0	0	0	0	0	0	0.9167
<i>Fusconaia cuneolus</i>	0	7	0	1	0	0	0	0	0.8750
<i>Fusconaia subrotunda</i>	0	0	16	4	0	1	0	0	0.7619
<i>Pleurobema oviforme</i>	0	0	1	32	2	9	5	0	0.6531
<i>Pleurobema</i> sp. cf. <i>oviforme</i>	0	0	0	0	16	0	0	0	1.0000
<i>Pleurobema barnesiana</i>	0	0	2	6	0	19	0	0	0.7037
<i>Pleurobema</i> sp. cf. <i>barnesiana</i>	0	0	0	0	1	0	12	1	0.8571
<i>Pleurobema dolabelloides</i>	0	0	0	1	0	0	1	11	0.8462
% Correct Classification	1.0000	0.8750	0.8421	0.7273	0.8421	0.6552	0.6667	0.9167	

Table 10. Species predictions ($N=160$) using classification and regression tree analysis of shell-only quantitative and categorical variables from sacrificed individuals. These data include non-genetically identified individuals from the FMCC shell collection. Actual species identifications are reported in the rows and predictions made by the Classification and Regression Tree Analysis (CART) are reported in the columns.

<u>Species</u>	Species Predicted by CART for Shells								<u>% Correct Classification</u>
	<i>Fusconaia</i> <u>cor</u>	<i>Fusconaia</i> <u>cuneolus</u>	<i>Fusconaia</i> <u>subrotunda</u>	<i>Pleurobema</i> <u>oviforme</u>	<i>Pleurobema</i> sp. cf. <u>oviforme</u>	<i>Pleurobema</i> <u>barnesiana</u>	<i>Pleurobema</i> sp. cf. <u>barnesiana</u>	<i>Pleurobema</i> <u>dolabelloides</u>	
<i>Fusconaia cor</i>	11	1	0	0	0	0	0	0	0.9167
<i>Fusconaia cuneolus</i>	0	7	1	0	0	0	0	0	0.8750
<i>Fusconaia subrotunda</i>	0	1	20	0	0	0	0	0	0.9524
<i>Pleurobema oviforme</i>	0	0	0	37	1	6	3	2	0.7551
<i>Pleurobema</i> sp. cf. <i>oviforme</i>	0	0	0	2	14	0	0	0	0.8750
<i>Pleurobema barnesiana</i>	0	0	0	3	2	20	2	0	0.7407
<i>Pleurobema</i> sp. cf. <i>barnesiana</i>	0	0	0	1	0	2	10	1	0.7143
<i>Pleurobema dolabelloides</i>	0	0	0	1	0	1	1	10	0.7692
% Correct Classification	1.0000	0.7778	0.9524	0.8409	0.8235	0.6897	0.6250	0.7692	

Table 11. Species predictions using canonical variates analysis (CVA) of geometric morphometric data.

<u>Species</u>	Species Predicted by CVA								<u>% Correct Classification</u>
	<i>Fusconaia</i> <u>cor</u>	<i>Fusconaia</i> <u>cuneolus</u>	<i>Fusconaia</i> <u>subrotunda</u>	<i>Pleurobema</i> <u>oviforme</u>	<i>Pleurobema</i> sp. cf. <u>oviforme</u>	<i>Pleurobema</i> <u>barnesiana</u>	<i>Pleurobema</i> sp. cf. <u>barnesiana</u>	<i>Pleurobema</i> <u>dolabelloides</u>	
<i>Fusconaia cor</i>	21	11	5	1	1	2	0	2	0.4884
<i>Fusconaia cuneolus</i>	6	14	1	0	0	1	0	5	0.5185
<i>Fusconaia subrotunda</i>	2	1	15	3	5	7	3	8	0.3409
<i>Pleurobema oviforme</i>	4	1	4	37	11	9	30	1	0.3814
<i>Pleurobema</i> sp. cf. <i>oviforme</i>	0	0	0	1	21	1	1	0	0.8750
<i>Pleurobema barnesiana</i>	8	0	10	4	1	36	11	3	0.4932
<i>Pleurobema</i> sp. cf. <i>barnesiana</i>	5	0	3	18	1	12	18	1	0.3103
<i>Pleurobema dolabelloides</i>	3	8	8	0	0	4	2	23	0.4792
Correct Classification	0.4286	0.4000	0.3261	0.5781	0.5250	0.5000	0.2769	0.5349	

Table 12. Goodall's *F*-test for morphological differences using geometric morphometric data. All pairwise comparisons between species are significantly different ($p < 0.05$), except between *Pleurobema oviforme* and *Pleuonaia* sp. cf. *barnesiana*.

<u>Species</u>	<u><i>Fusconaia cor</i></u>	<u><i>Fusconaia cuneolus</i></u>	<u><i>Fusconaia subrotunda</i></u>	<u><i>Pleurobema oviforme</i></u>	<u><i>Pleurobema</i> sp. <u><i>cf. oviforme</i></u></u>	<u><i>Pleuonaia barnesiana</i></u>	<u><i>Pleuonaia</i> sp. <u><i>cf. barnesiana</i></u></u>	<u><i>Pleuonaia dolabelloides</i></u>
<i>Fusconaia cor</i>	n=43 <i>F</i> -Score=2.07							
<i>Fusconaia cuneolus</i>	$p = 5.323E-3$ <i>F</i> -Score=3.23	n=27 <i>F</i> -Score=4.43						
<i>Fusconaia subrotunda</i>	$p = 5.334E-6$ <i>F</i> -Score=26.51	$p = 2.071E-9$ <i>F</i> -Score=23.26	n=44 <i>F</i> -Score=16.26					
<i>Pleurobema oviforme</i>	$p = 0$ <i>F</i> -Score=20.92	$p = 0$ <i>F</i> -Score=24.79	$p = 0$ <i>F</i> -Score=13.30	n=97 <i>F</i> -Score=16.95				
<i>Pleurobema</i> sp. cf. <i>oviforme</i>	$p = 0$ <i>F</i> -Score=15.21	$p = 0$ <i>F</i> -Score=11.96	$p = 0$ <i>F</i> -Score=7.88	$p = 0$ <i>F</i> -Score=18.80	n=24 <i>F</i> -Score=29.88			
<i>Pleuonaia barnesiana</i>	$p = 0$ <i>F</i> -Score=21.67	$p = 0$ <i>F</i> -Score=20.25	$p = 0$ <i>F</i> -Score=11.83	$p = 0$ <i>F</i> -Score=0.90	$p = 0$ <i>F</i> -Score=18.71	n=73 <i>F</i> -Score=9.77		
<i>Pleuonaia</i> sp. cf. <i>barnesiana</i>	$p = 0$ <i>F</i> -Score=1.96	$p = 0$ <i>F</i> -Score=2.11	$p = 0$ <i>F</i> -Score=4.98	$p = 0.5782$ <i>F</i> -Score=39.38	$p = 0$ <i>F</i> -Score=23.31	$p = 0$ <i>F</i> -Score=22.50	n=58 <i>F</i> -Score=30.96	
<i>Pleuonaia dolabelloides</i>	$p = 9.345E-3$	$p = 4.390E-3$	$p = 3.772E-11$	$p = 0$	$p = 0$	$p = 0$	$p = 0$	n=48

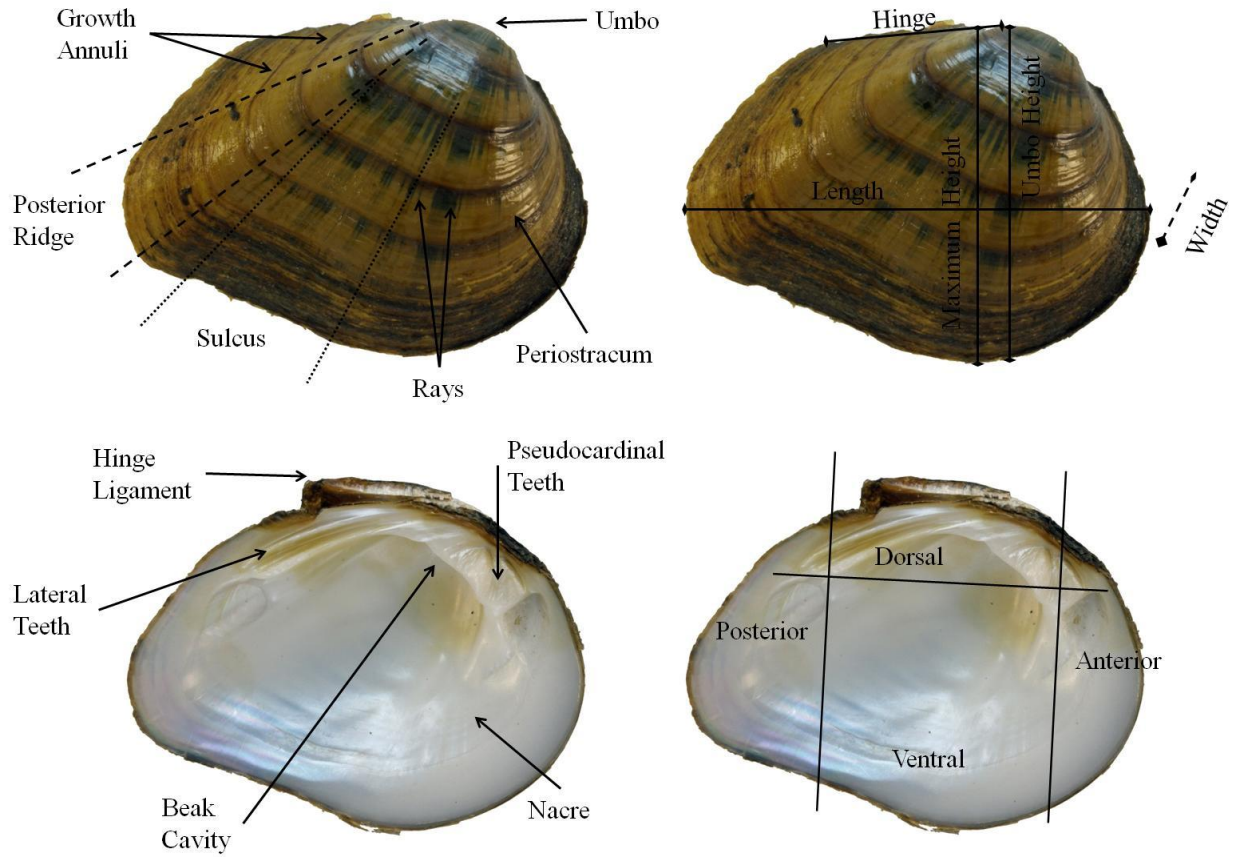


Figure 1. External (top) and internal (bottom left) shell characters investigated in this study, including anatomical regions (bottom right) of the shell.

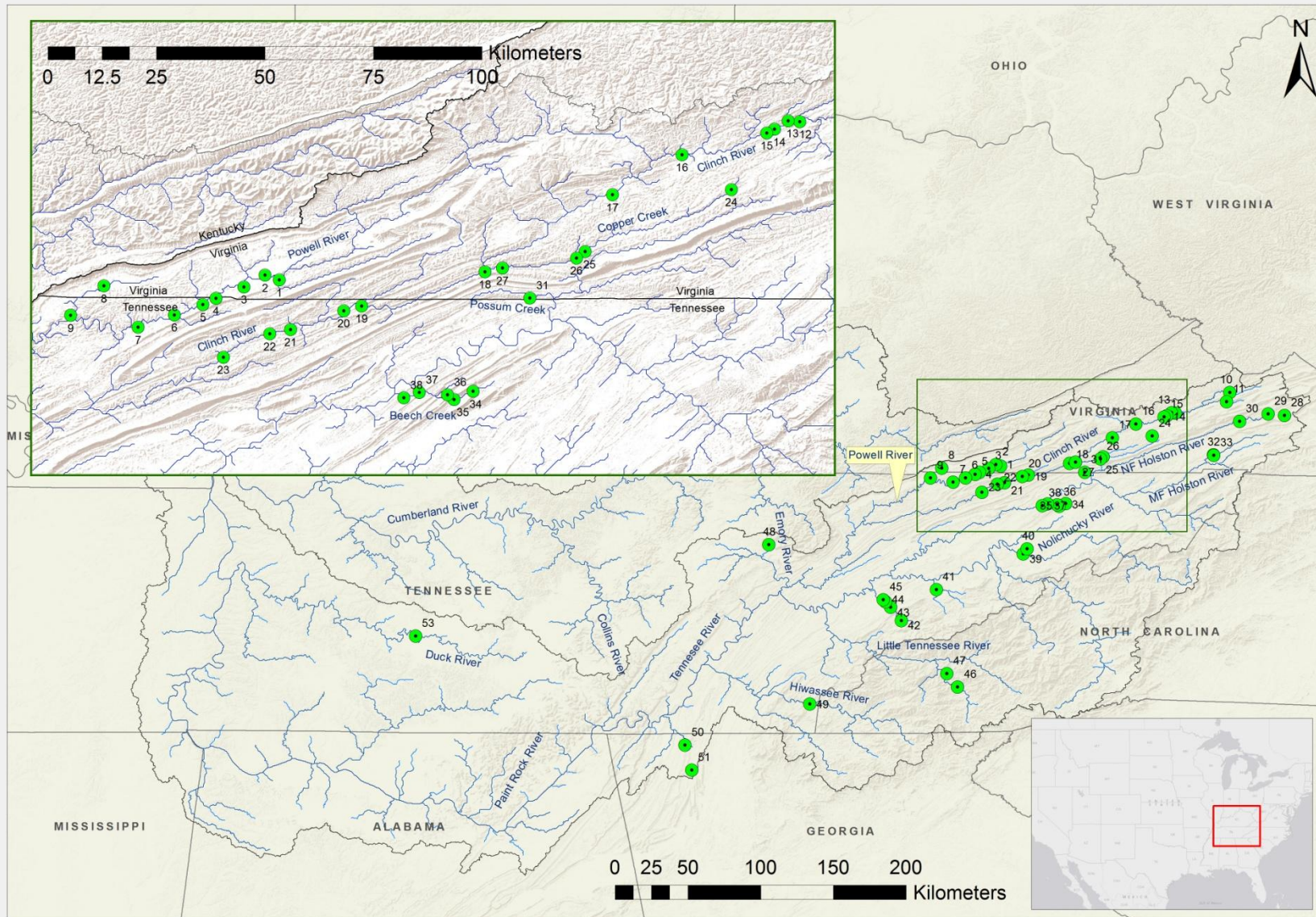


Figure 2. Sampling localities and site numbers for freshwater mussels collected primarily in the Tennessee River basin from 2012 through 2014.



Figure 3. Light-box used to hold specimens while photographs were taken; lid not shown.

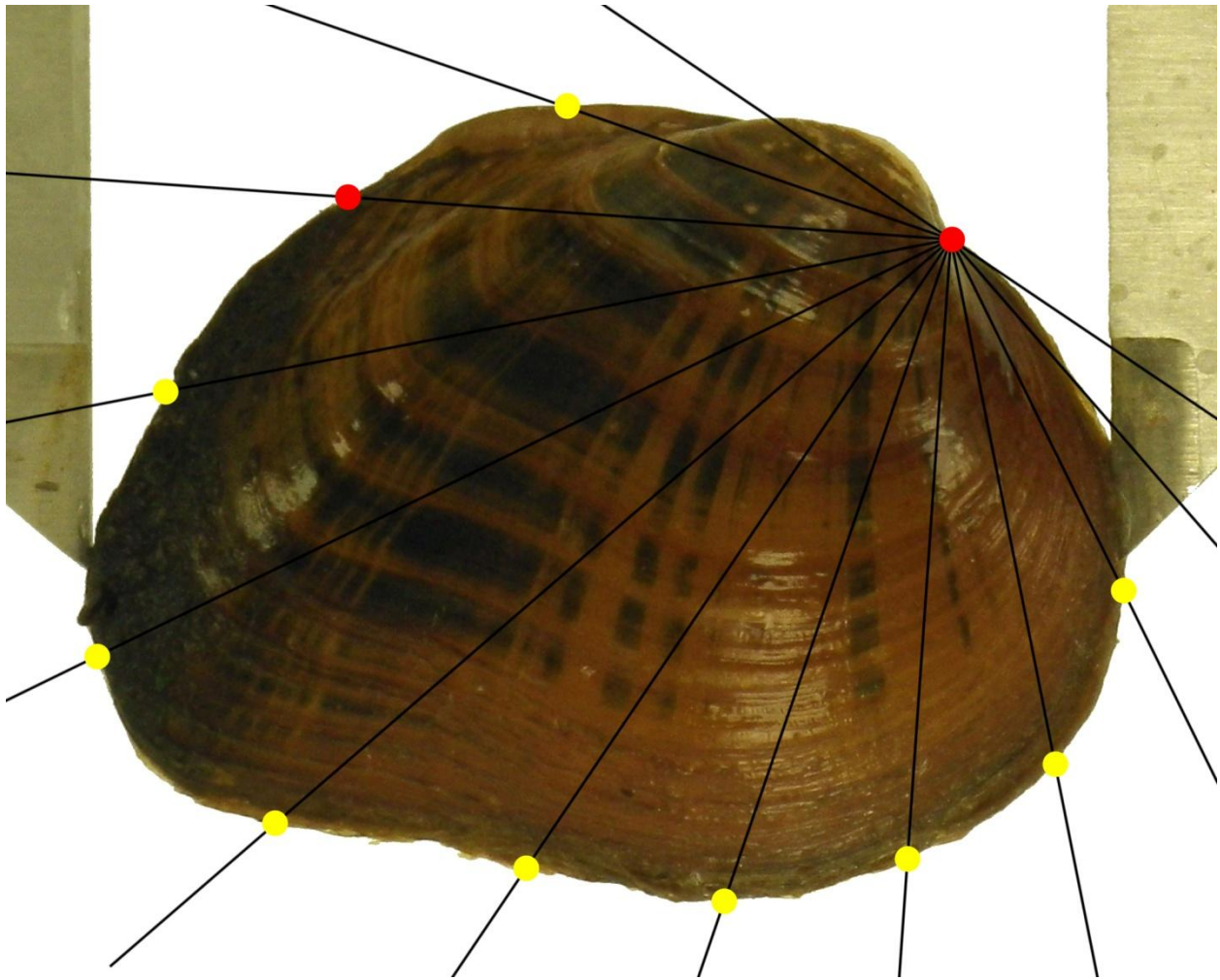


Figure 4. Geometric morphometric measurements of freshwater mussel shells. Calipers held specimens parallel to the camera lens in order to standardize all photographs. A radial overlay was superimposed on the photograph, aligning the terminating segments of the hinge ligament to serve as a baseline (red dots). Nine semi-sliding landmarks (yellow dots) were digitized where the radial overlay intersected the shell margin.

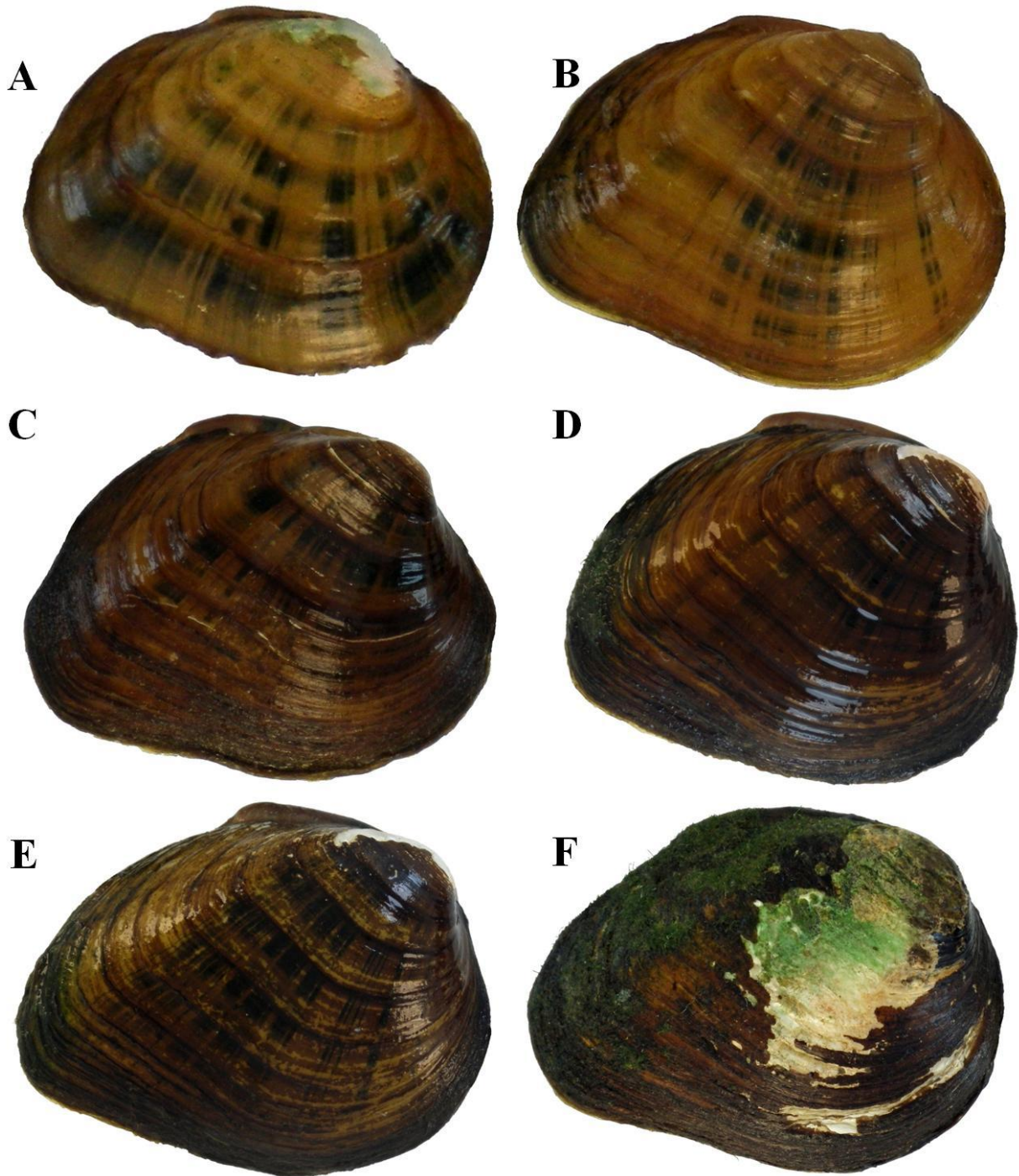


Figure 5. Individuals of *Fusconaia cor* depicting size classes and variation in periostracum color and ray patterns: (A) 23 mm from North Fork Holston River, km 142.7; (B) 35 mm from Clinch River, km 435.8; (C) 49 mm from Clinch River, km 435.8; (D) 53 mm from Clinch River, km 435.8; (E) 61 mm from Clinch River, km 437.9; (F) 79 mm from Powell River, km 214.0.

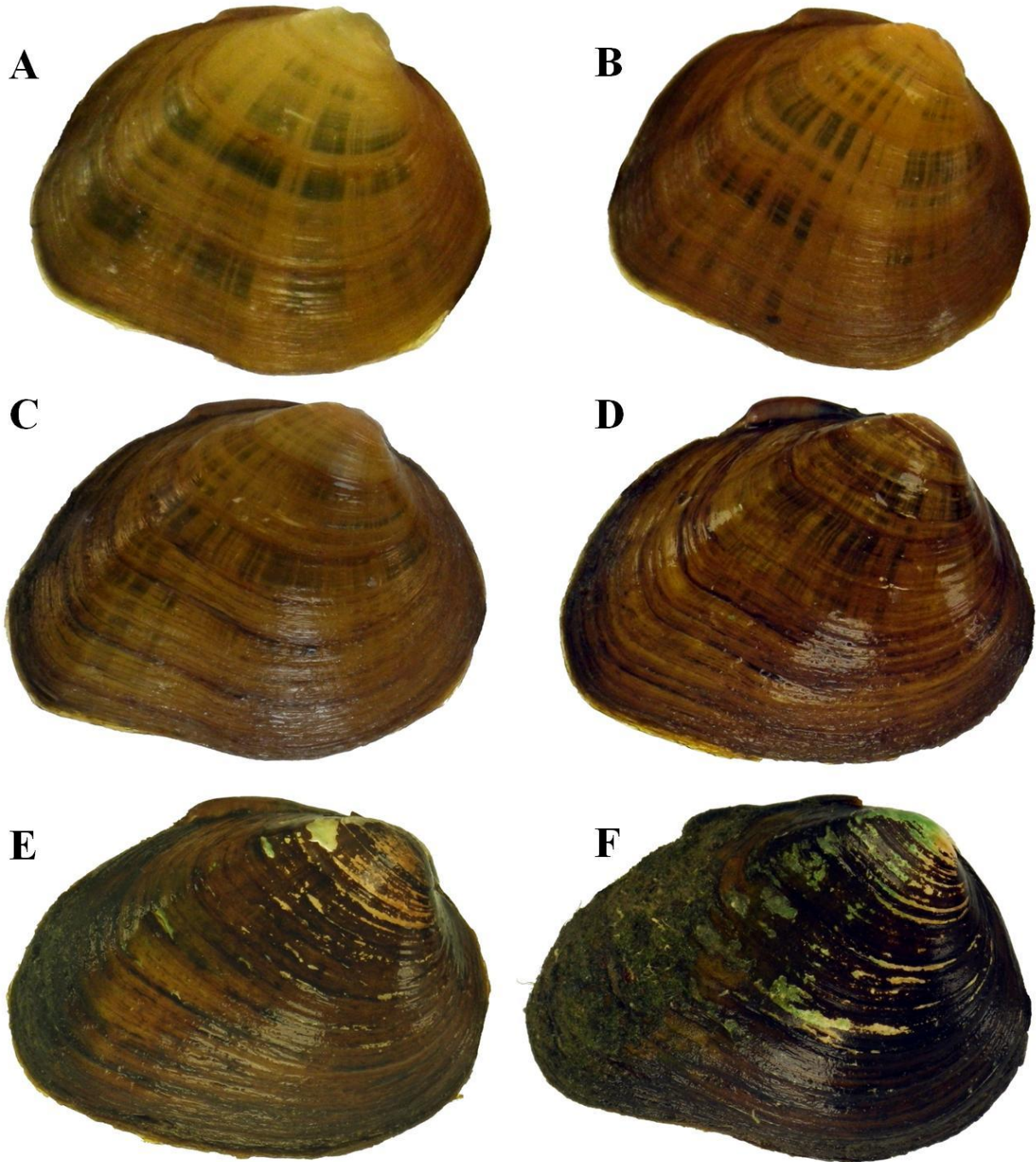


Figure 6. Individuals of *Fusconaia cuneolus* depicting size classes and variation in periostracum color and ray patterns: (A) 27 mm from Clinch River, km 309.8; (B) 32 mm from Clinch River, km 309.8; (C) 41 mm from Clinch River, km 309.8; (D) 51 mm from Clinch River, km 309.8; (E) 65 mm from Clinch River, km 401.7; (F) 75 mm from Clinch River, km 401.7.

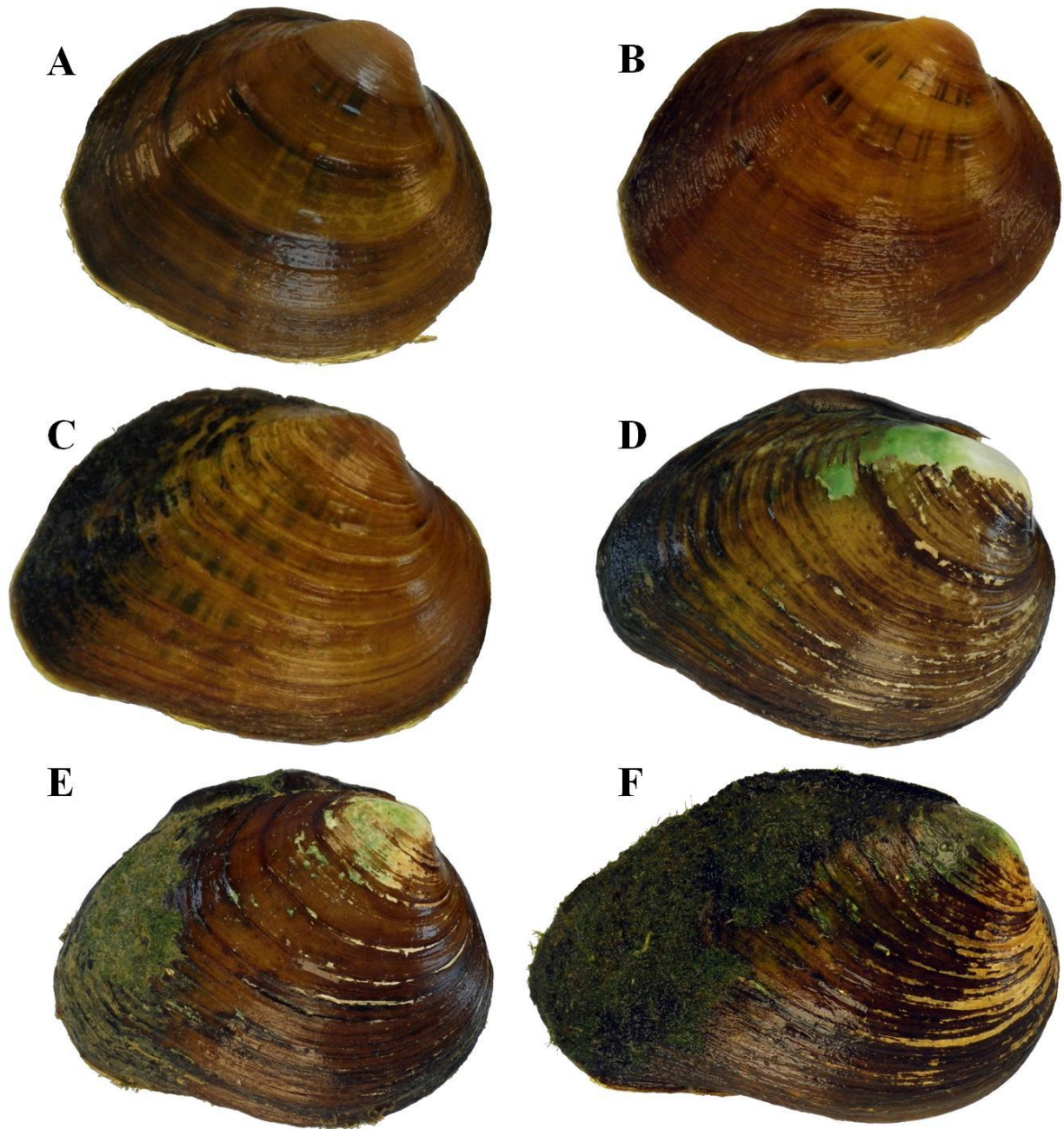


Figure 7. Individuals of *Fusconaia subrotunda* depicting size classes and variation in periostracum color and ray patterns: (A) 37 mm from Clinch River, km 305.4; (B) 42 mm from Clinch River, km 305.4; (C) 53 mm from Clinch River, km 435.8; (D) 75 mm from Clinch River, km 435.8; (E) 84 mm from Clinch River, km 435.8; (F) 97 mm from Clinch River, km 378.3.

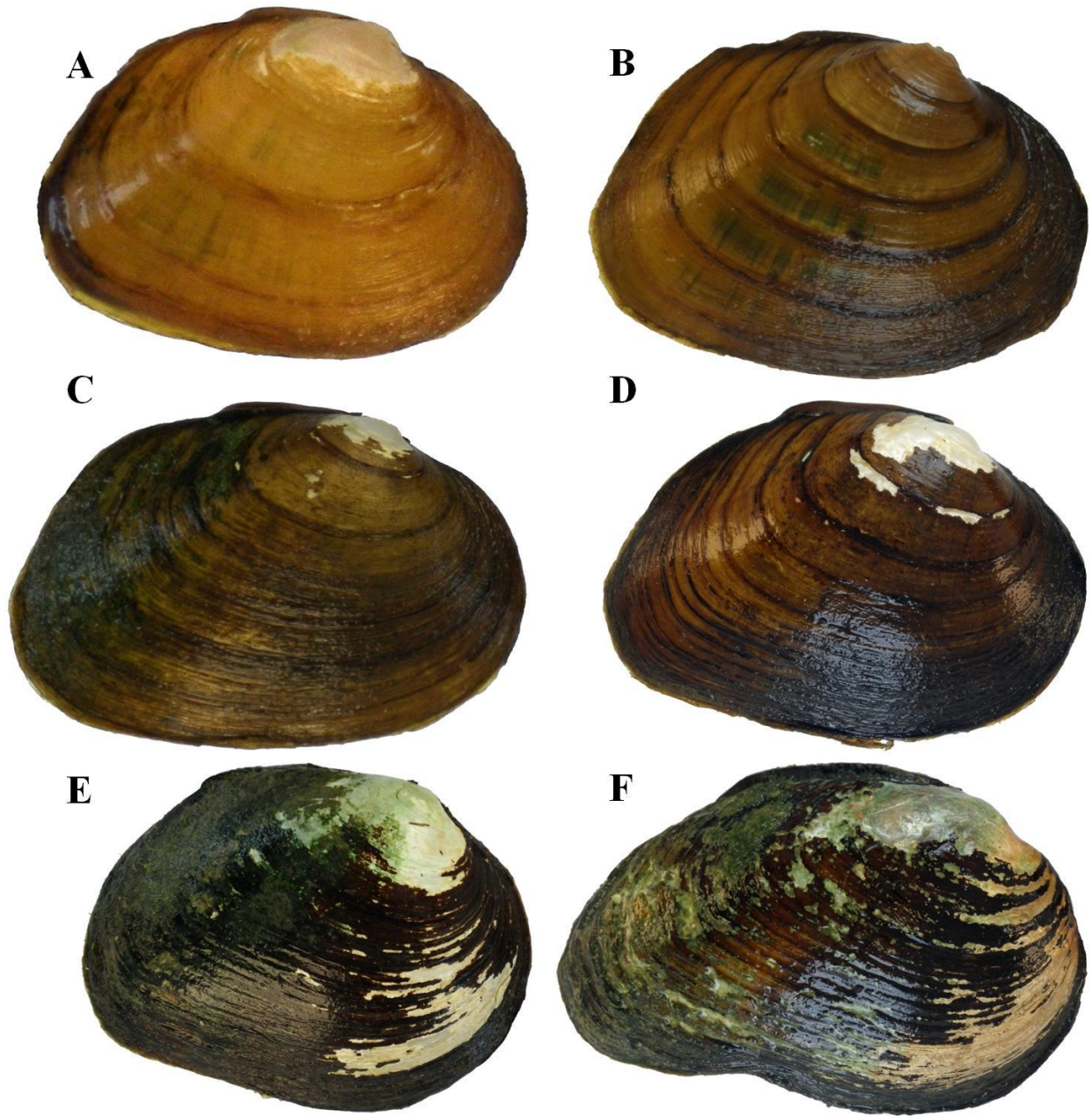


Figure 8. Individuals of *Pleurobema oviforme* depicting size classes and variation in periostracum color and ray patterns: (A) 27 mm from North Fork Holston River, km 175.2; (B) 38 mm from Copper Creek, km 24.1; (C) 52 mm from Beech Creek, km 10.8; (D) 71 mm from Indian Creek (Clinch Drainage), km 0.8; (E) 80 mm from Beech Creek, km 25.6; (F) 93 mm from North Fork Holston River, km 191.7.

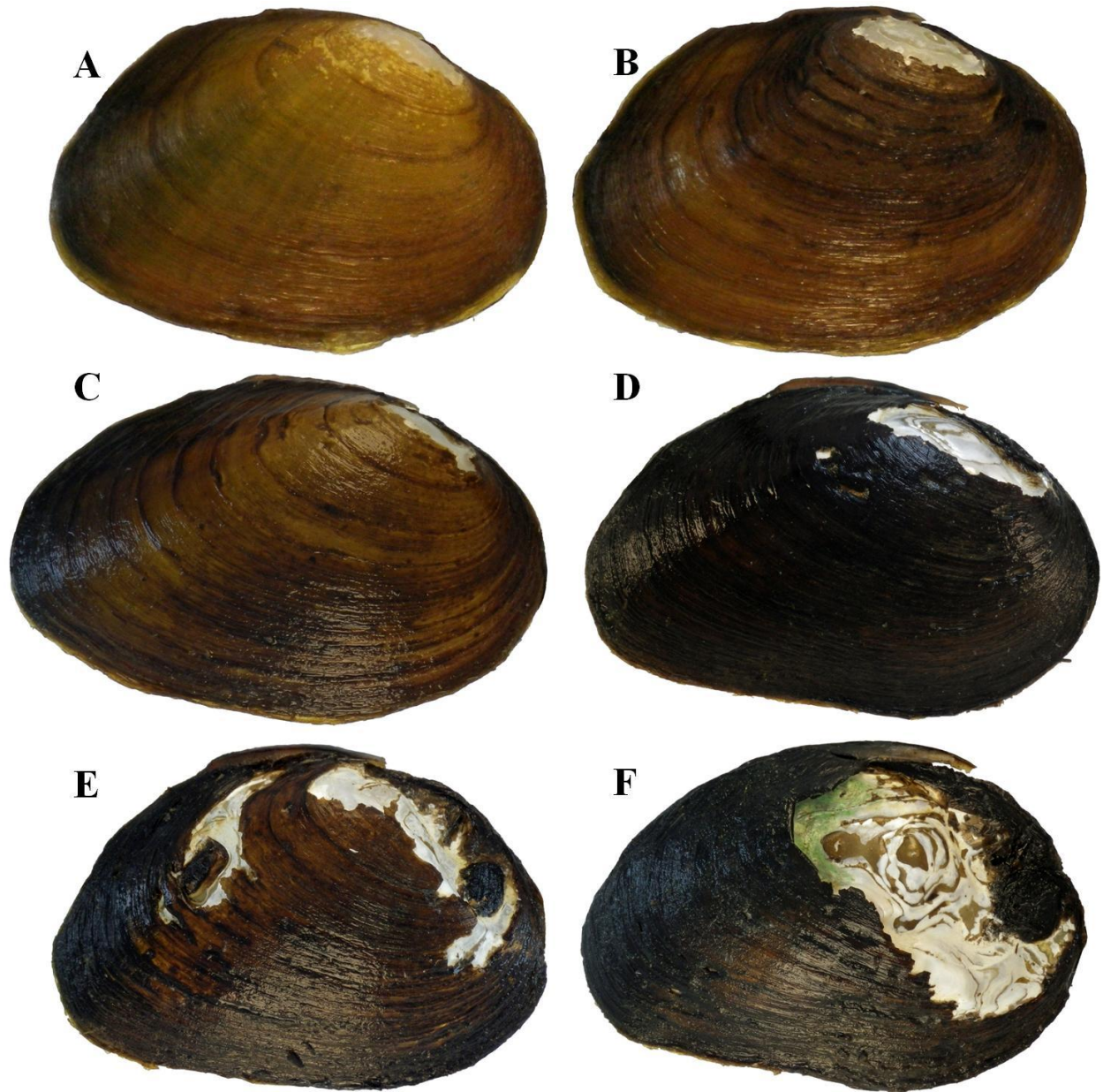


Figure 9. Individuals of *Pleurobema* sp. cf. *oviforme* depicting size classes and variation in periostracum color and ray patterns: (A) 37 mm from Little River, km 47.6; (B) 44 mm from Little River, km 47.6; (C) 65 mm from Little River, km 47.6; (D) 79 mm from Little River, km 33.2; (E) 89 mm from Little River, km 47.6; (F) 104 mm from Little River, km 47.6.

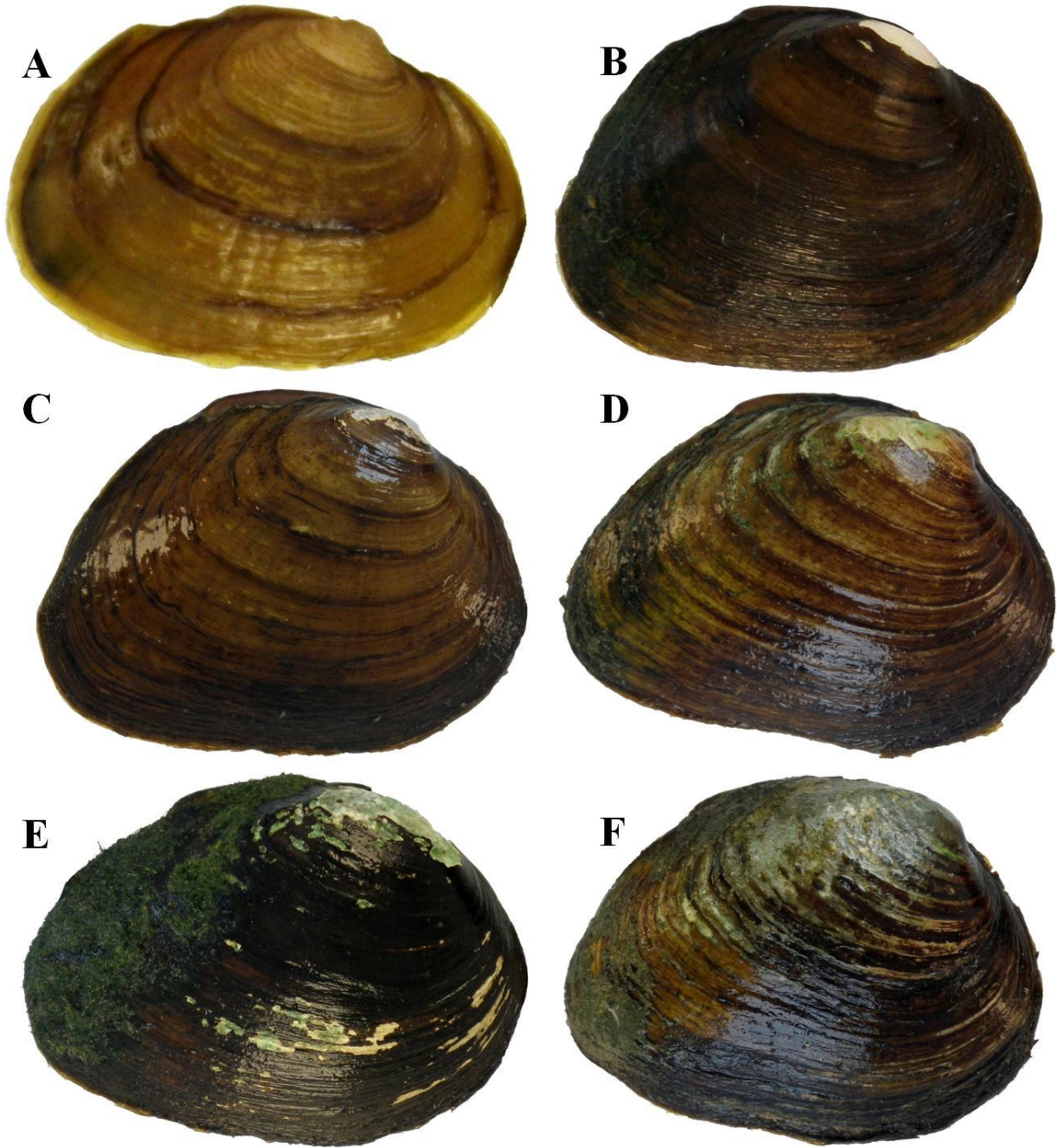


Figure 10. Individuals of *Pleuronaia barnesiana* depicting size classes and variation in periostracum color and ray patterns: (A) 29 mm from Copper Creek, km 4.2; (B) 45 mm from Beech Creek, km 10.8; (C) 60 mm from Possum Creek, km 12.2; (D) 63 mm from Copper Creek, km 21.7; (E) 72 mm from Powell River, km 210.5; (F) 80 mm Copper Creek, km 87.2.

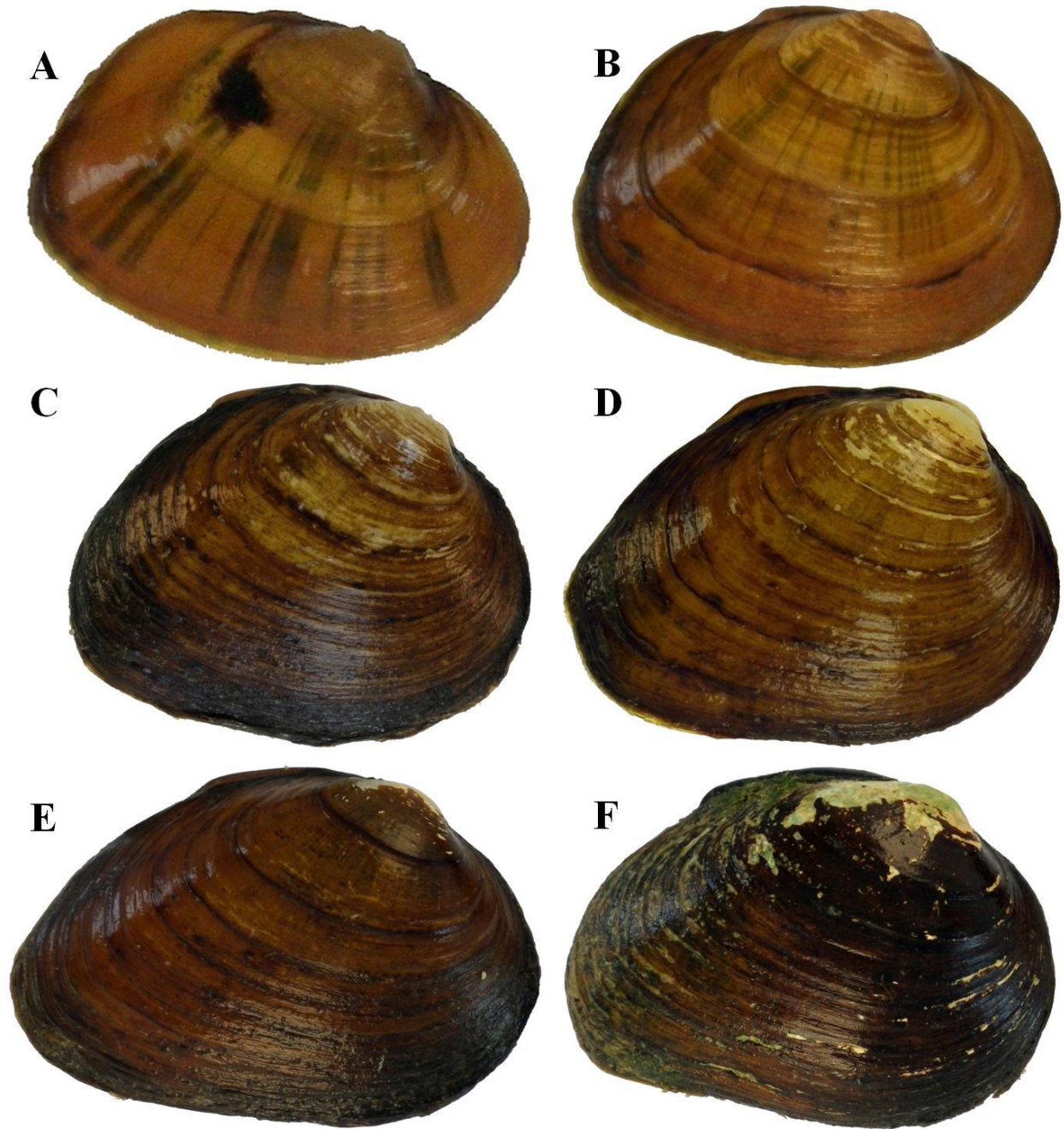


Figure 11. Individuals of *Pleuronaia* sp. cf. *barnesiana* depicting size classes and variation in periostracum color and ray patterns: (A) 28 mm from Clinch River, km 441.9; (B) 35 mm from Clinch River, km 435.8; (C) 47 mm from Copper Creek, km 24.1; (D) 55 mm from Indian Creek (Powell Drainage), km 0.3; (E) 60 mm from Clinch River, km 435.8; (F) 71 mm from Clinch River, km 435.8.

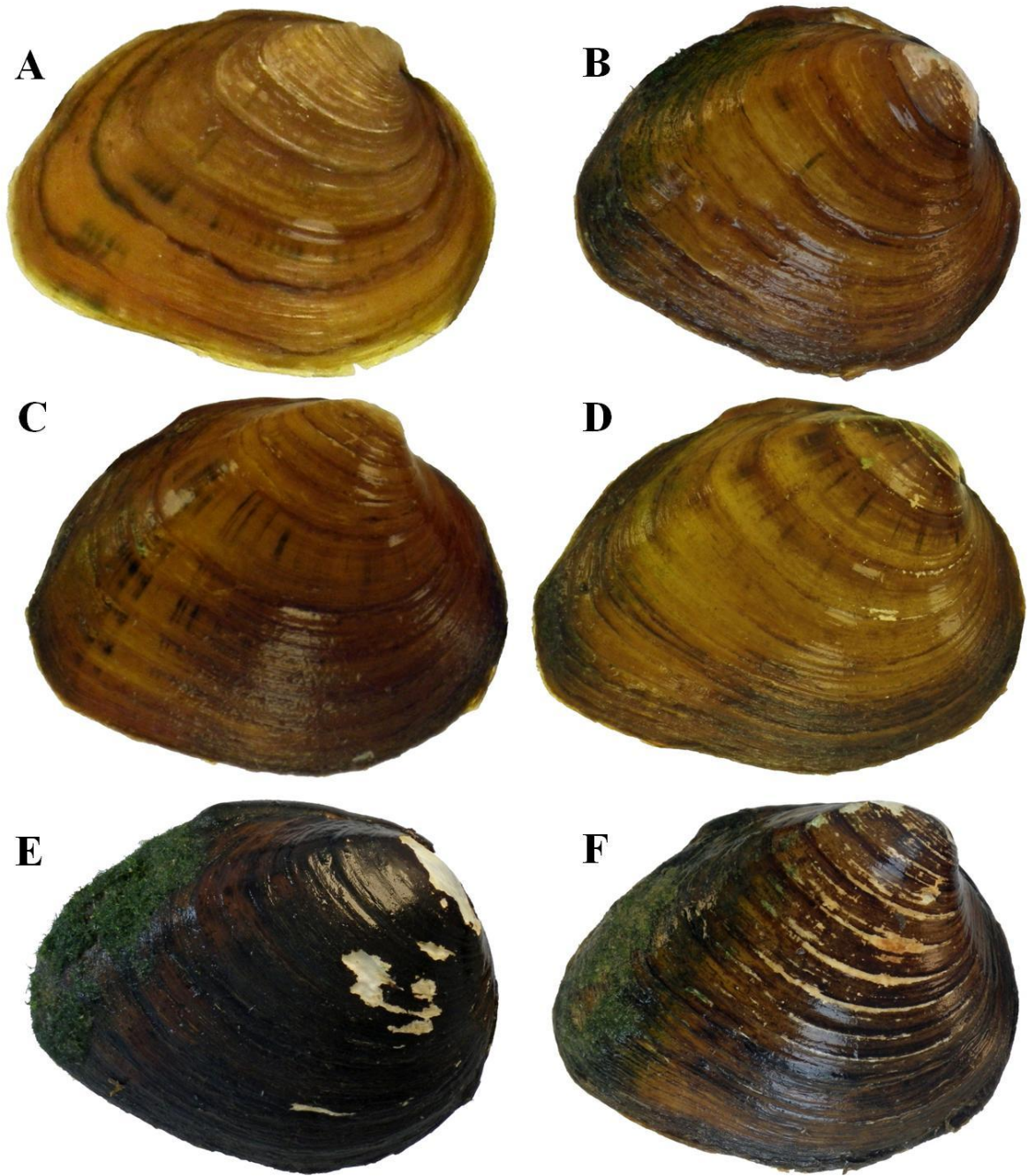


Figure 12. Individuals of *Pleuronaia dolabelloides* depicting size classes and variation in periostracum color and ray patterns: (A) 25 mm from Clinch River, km 435.8; (B) 43 mm from Clinch River, km 441.9; (C) 49 mm from Middle Fork Holston River, km 15.4; (D) 58 mm from Clinch River, km 441.9; (E) 69 mm from Powell River, km 210.5; (F) 83 mm from Middle Fork Holston River, km 16.3.

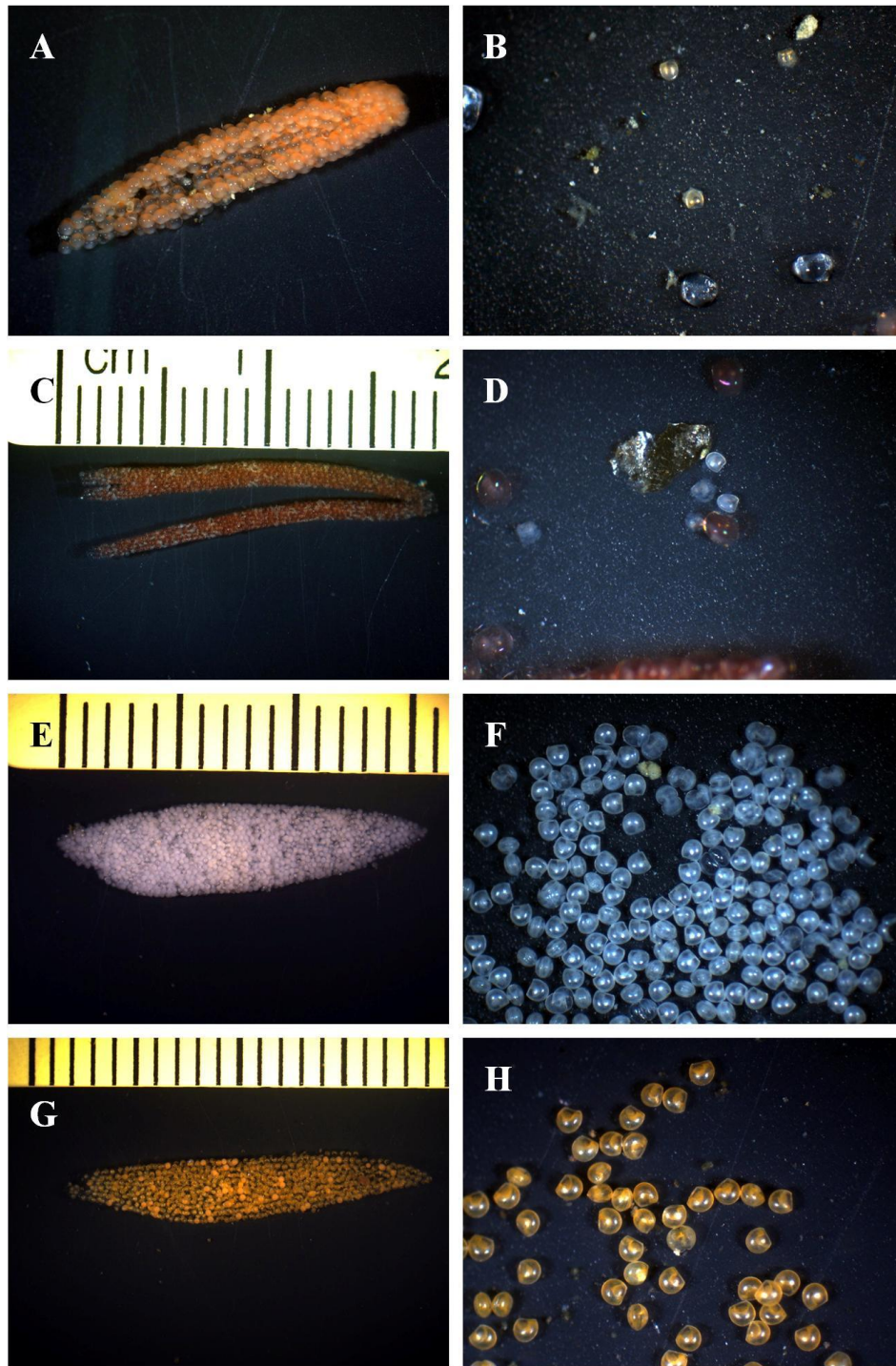


Figure 13. Conglutinates and glochidia of: *Fusconaia cor* (A, B) from Clinch River (rkm 435.8); *Fusconaia subrotunda* (C, D) from Clinch River (rkm 441.9); *Pleurobema oviforme* (E, F) from North Fork Holston River (rkm 175.2); and *Pleurobema* sp. cf. *oviforme* from Little River (rkm 47.6).

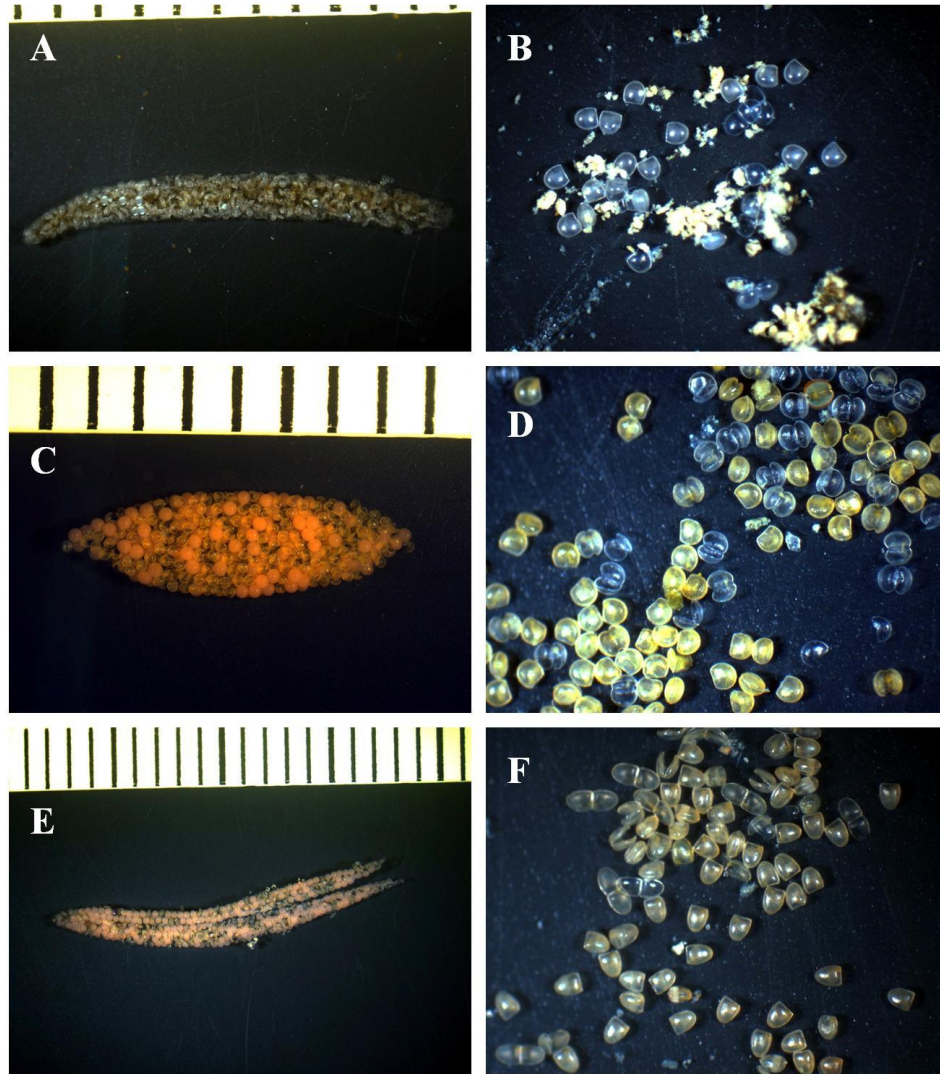


Figure 14. Conglutinates and glochidia of: *Pleuroaia barnesiana* (A, B) from Copper Creek (rkm 21.7) and Possum Creek (rkm 12.2), respectively; *Pleuroaia* sp. cf. *barnesiana* (C, D) from Clinch River (rkm 441.9) and Copper Creek (rkm 21.7), respectively; and *Pleuroaia dolabelloides* from Middle Fork Holston River (rkm 16.3).

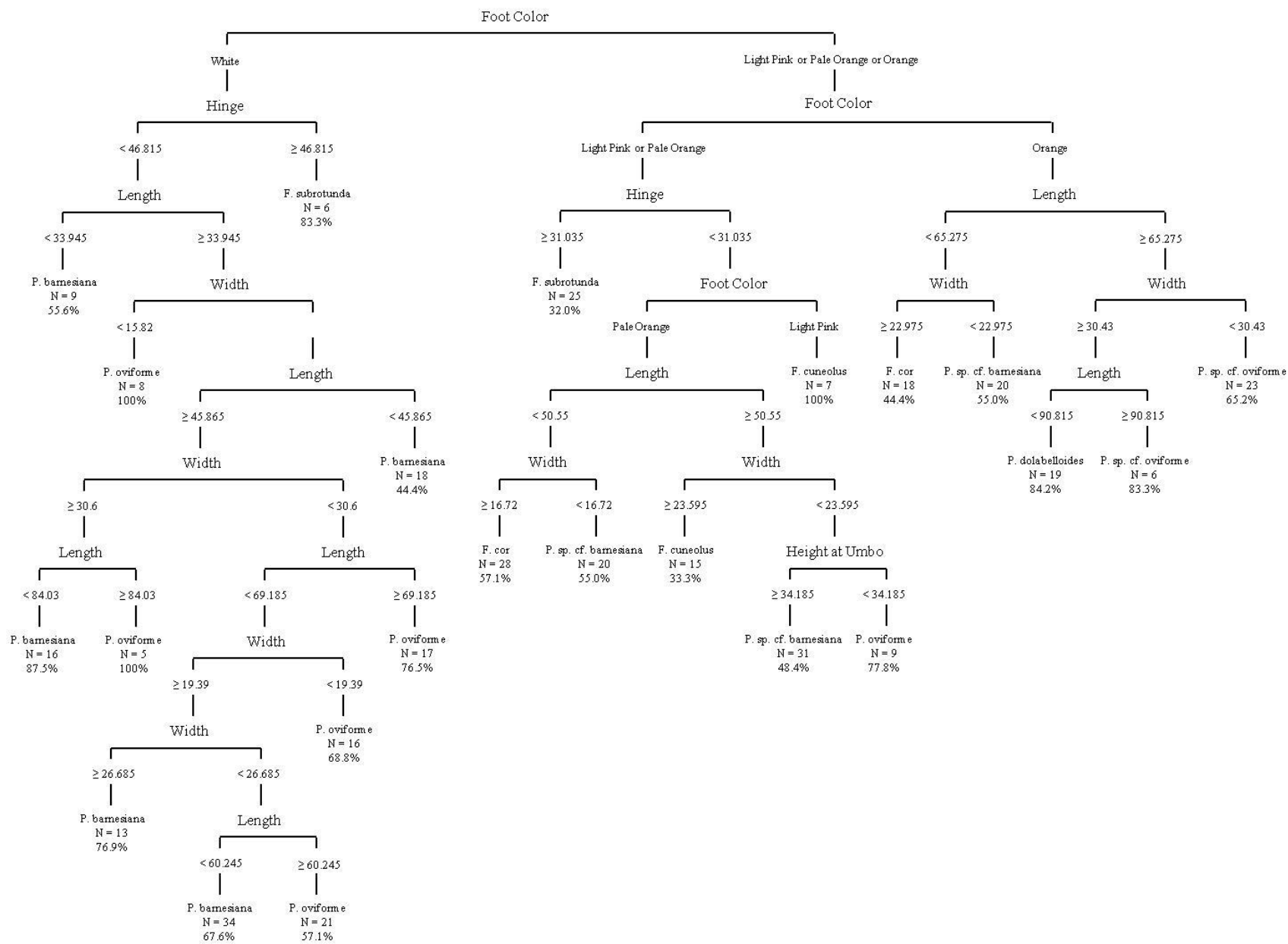


Figure 15. Decision tree from classification and regression tree analysis using traditional morphometric and foot color data. Overall accuracy on terminal nodes was 61.98%.

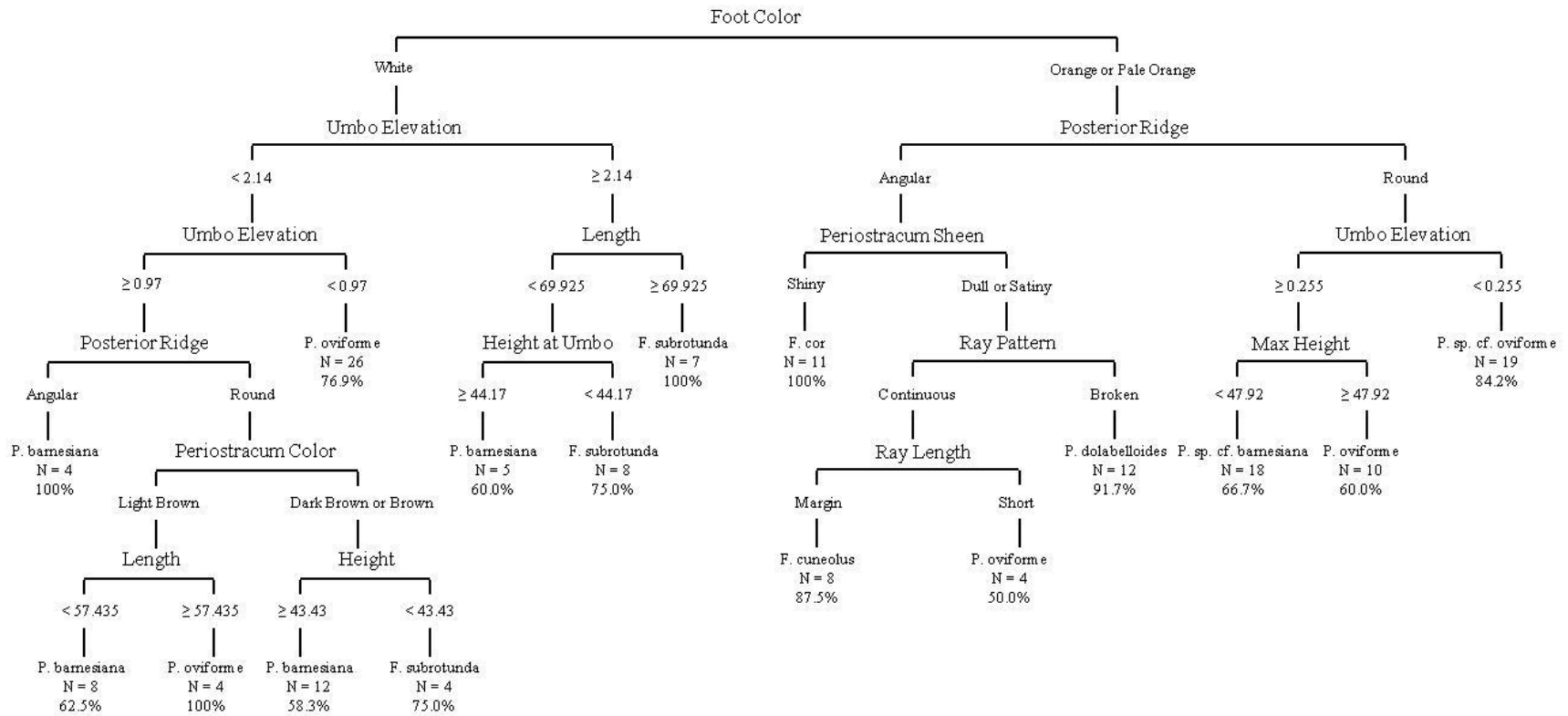


Figure 16. Decision tree from classification and regression tree analysis using quantitative, foot color, and categorical variables from individuals sacrificed to represent live individuals. These data include non-genetically identified individuals from the FMCC shell collection. Overall accuracy on terminal nodes was 77.50%.

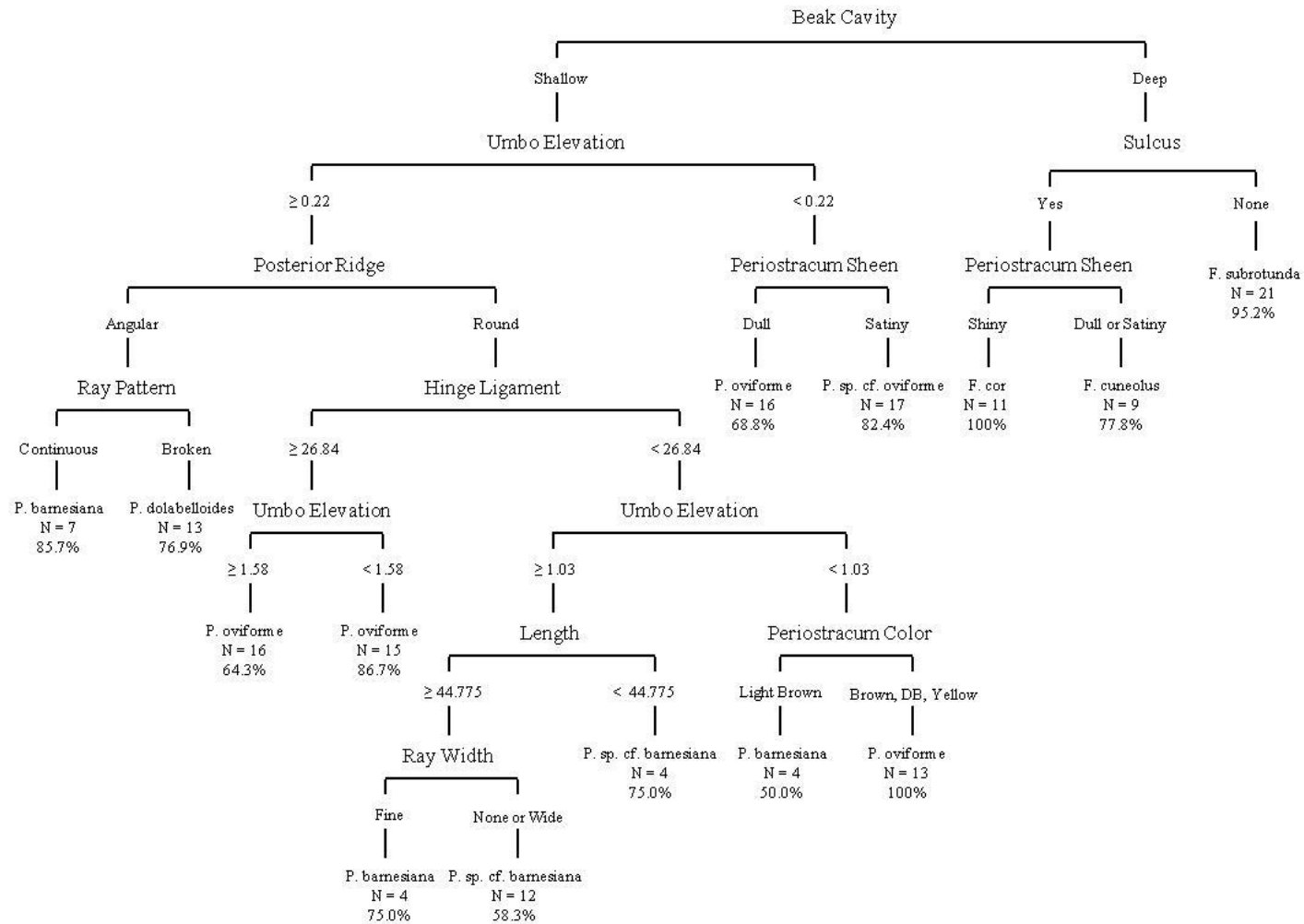


Figure 17. Decision tree from classification and regression tree analysis using quantitative and categorical variables from individuals sacrificed to represent shell-only individuals. These data include non-genetically identified individuals from the FMCC shell collection. Overall accuracy on terminal nodes was 80.63%.

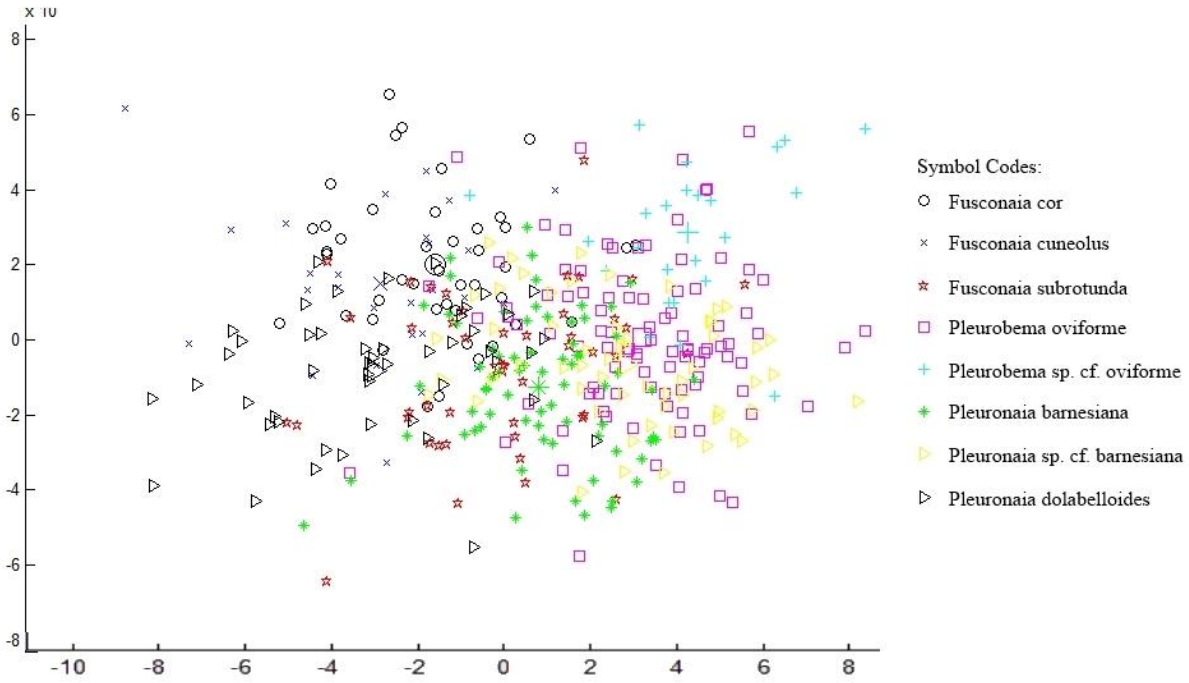


Figure 18. Canonical variates analysis (CVA) plot using geometric morphometric data depicting canonical variates one and two as X- and Y- axes, respectively. Larger symbols indicate species means.

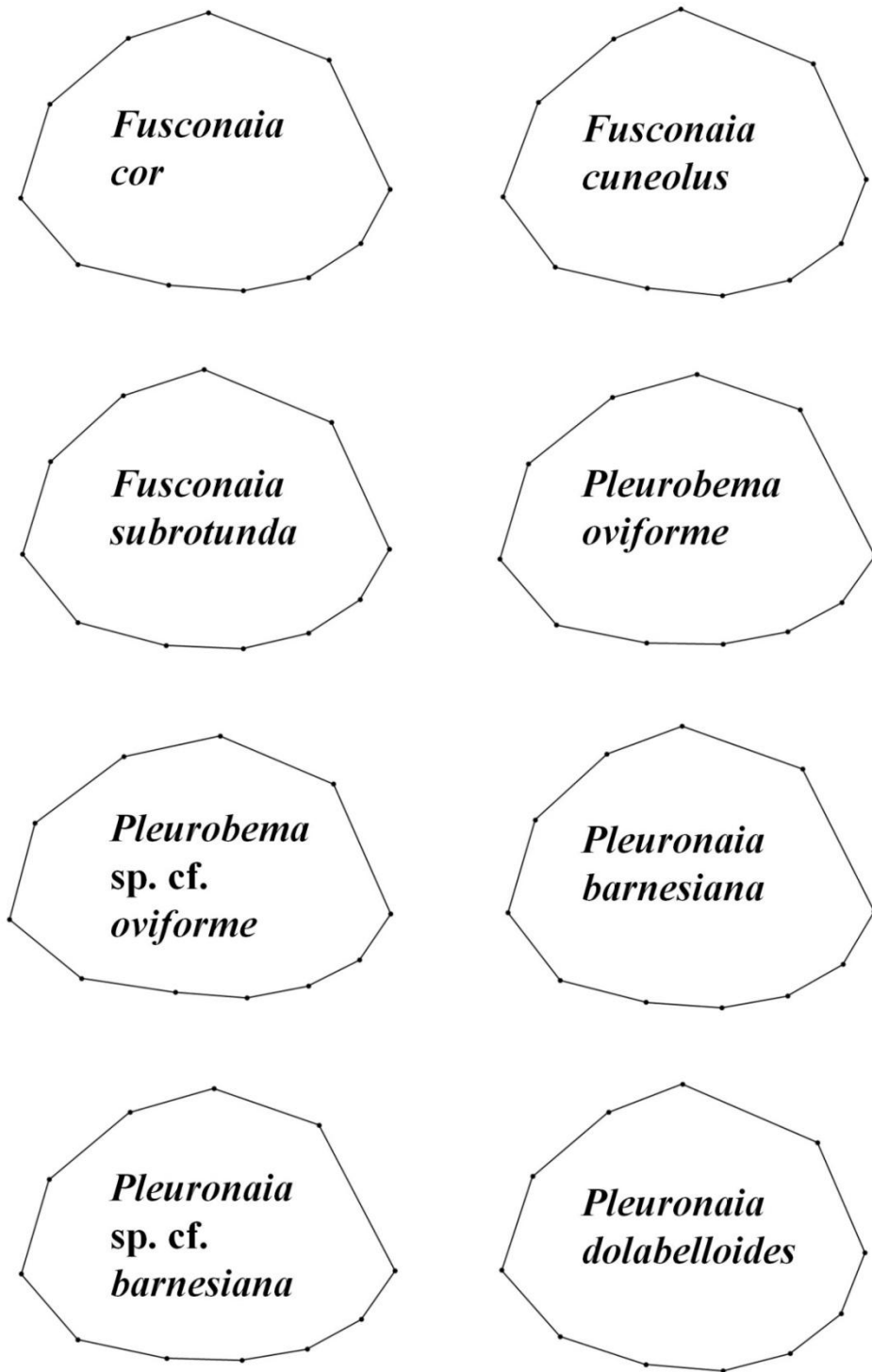


Figure 19. Mean outline of shells for each species using coordinates from geometric morphometrics data; outlines were created by displaying mean coordinates for each species, then lines were manually drawn.

CHAPTER 3

Development and testing of morphology-based dichotomous keys for selected freshwater mussels in the genera *Fusconaia*, *Pleurobema*, and *Pleuronaia* in the upper Tennessee River basin of Tennessee and Virginia

ABSTRACT

The purpose of this study was to develop and test a set of morphology-based identification keys for *Fusconaia cor*, *F. cuneolus*, *F. subrotunda*, *Pleurobema oviforme*, *Pleurobema barnesiana*, *P. dolabelloides*, and two unrecognized taxa, *Pleurobema* sp. cf. *oviforme* and *Pleurobema* sp. cf. *barnesiana* in the upper Tennessee River basin. Two dichotomous keys were created from classification and regression tree analyses to identify species based on their morphological characters. The first key was created to identify shell material from non-living individuals and the second key to identify live individuals. Both keys contained quantitative measurements and categorical variables to identify mussels, and were tested by biologists with mussel identification skill levels ranging from novice to expert. Overall, the expert group correctly identified mussels at higher rate than novices. Novices and experts correctly identified mussels using the shell key with an accuracy of 51% and 58%, and correctly identified mussels using the live key with an accuracy of 50% and 68%, respectively. While these keys assisted participants to identify shells and live mussels greater than random chance (1/8 or 12.5%), they were not accurate enough to use in the field. Morphological overlap of continuous and categorical variables among investigated species made unambiguous identifications of shells and live individuals difficult. Training on how to assess morphological characters used in the key is recommended, but due to the morphological overlap exhibited by my study species, I do not anticipate mean identification rates from the dichotomous keys to exceed the 80% rate obtained in the CART analysis. If the collection of a mussel is thought to be a new distribution or location record for the species, especially if it is endangered, I recommend that it be identified genetically.

KEYWORDS: Freshwater mussels, *Fusconaia*, *Pleurobema*, *Pleuronaia*, Dichotomous key

INTRODUCTION

Traditionally, taxonomists have classified freshwater mussels into their respective species, genera, and higher taxonomic categories based upon shell morphology (Kat 1983). Revisions of mussel taxonomy have occurred through time as naturalists have incorporated additional phenotypic traits such as soft anatomy, larval morphology and life history traits into their species descriptions (Williams et al. 2008). Molecular DNA markers have further allowed scientists to resolve polyphyletic lineages, especially for similar looking species (Campbell et al. 2005). Morphological similarities among species and individuals belonging to the genera *Fusconaia*, *Pleurobema*, and *Pleuronaia* are common and can make identification of species difficult, especially in the field (Baker et al. 2003; Christian et al. 2008).

Most freshwater mussel descriptions have utilized shell characters, including external shape, color, and ray pattern (Parmalee and Bogan 1998; Williams et al. 2008). For example, species with rayed and pustulated shells typically are easier to identify than species lacking distinct external shell characters (Shea et al. 2011). Terminology used to describe external shell shape include *sub-triangular*, *sub-quadrate* and *oval*; however, these descriptive terms are difficult to visualize and quantify and therefore are of marginal value to field biologists. Further, the characters used to identify mussels often are passed from an expert to a novice during an apprenticeship period, which can introduce bias and inconsistent application of characters to identify species. While the teaching of mussel identification skills in this manner has advantages, such as the trainee being able to see a greater range of phenotypic variation in the field, the approach is slow and not standardized. Further, quantitative data such as length-to-height ratios can be applied only after the specimen of interest is narrowed down to a particular group, which still requires basic mussel identification skills. Further, traditional descriptions of

mussel species often do not provide discriminating characters to separate species, but rather list general descriptions of the morphological characters.

The purpose of this study was to develop and test morphological trait-based identification keys to identify species in the genera *Fusconaia*, *Pleurobema*, and *Pleuonaia*, and have biologists with varying levels of mussel identification skills test the keys to determine their efficacy. The keys, one to identify shell and the second to identify live mussels, were arranged in a classical dichotomous format in order to facilitate mussel identifications. The efficacy of the keys was determined by users' ability to correctly identify a panel of mussel shells.

METHODS

Creating the Dichotomous Keys. – Freshwater mussels were collected from 2012 through 2014, primarily in streams of the upper Tennessee River basin in Tennessee and Virginia, where sample sizes for each species ranged from 8 to 49 individuals. Some of these individuals were obtained from the shell collection housed at the Freshwater Mollusk Conservation Center at Virginia Tech and were not genetically verified. See Chapter 2 for sample sizes of genetically and non-genetically identified individuals. Classification and regression tree (CART) analyses were conducted on two data sets containing morphological characters for freshwater mussels to represent shells and live individuals (see Chapter 2); this approach was chosen because CART provides accuracy on terminal nodes, as well as overall accuracy of the analysis. The output for each analysis was a graphical representation of a dichotomous key; from these results, a key was written in textual format to identify either shells or live individuals (Tables 1 and 2). The keys were then tested by participants to determine their ability to correctly identify mussels to their respective species. A third key was created to identify species using gravid mussels but was not

tested by participants; therefore, it has no statistical support (Table 3). In order to assist with training of morphological traits used in the shell and live mussel keys, supplementary material was created to include: an image of a shell illustrating key external and internal features (Figure 1), a list of terms and respective definitions used in the keys (Table 4), and accounts with photographs illustrating key traits for each species (Figures 2 to 9).

Testing the Dichotomous Keys. – Each key was tested to determine how effective it was in guiding users to identify mussels. In order to account for the users' prior knowledge, mussel identification success was tested across two levels, novice and expert. Novices were categorized as participants with no experience with mussel identification and experts were classified as participants with at least three years of experience identifying mussels. Testing was conducted in compliance with Virginia Tech's Institutional Review Board requirements that protects the rights and safety of study participants.

Training and testing of the keys took place in a classroom located in Cheatham Hall at Virginia Tech and for the second group of experts, at the U.S. Fish and Wildlife Services' Southwestern Virginia Field Office in Abingdon, Virginia. Testing the keys had three main sections: an introduction, a training session, and testing of the two keys. Due to the varying skill levels of the participants, a brief introduction lasting approximately ten minutes was given to illustrate the following: the mussel species that were used in the test, anatomical features of a mussel shell, how and where to take shell measurements, categorical variables used in the keys and examples. The training session was composed of two parts, each taking approximately 15 minutes. First, the participants were trained on how to read and use the key to assess morphological traits for each dichotomous couplet in the key. During this part of the training

session, participants were allowed to ask questions and receive clarification on couplets of each key they thought were confusing or ambiguous. I then guided the participants through the dichotomous key for three mussel species, *Fusconaia cor*, *Pleuonaia barnesiana*, and *Pleuonaia dolabelloides*, using illustrations on an overhead projector. They were provided with mussel shells of each species as examples and led through each couplet of the key. Examples of each shell trait in the keys were provided and each participant was shown how the character was being assessed. The second part of the training was designed to allow the participants to navigate the dichotomous key on their own and ask questions or seek clarification during any step. Once participants were familiarized with the key and how to assess the shell characters, I administered the mussel identification tests. I asked participants to use the key and any information in the packet to guide them to a species identification. In addition, expert participants were asked to follow the key rather than identify the mussel using their prior knowledge.

The dichotomous key for shell or non-live individuals was tested first by participants. Each participant was given a collection of eight mussel shells, each representing a different species in the key. To minimize elimination-based identification, participants were told that the eight mussel shells could represent any random grouping from eight different species to eight individuals of the same species. Eight dichotomous keys were given to participants so they could circle each couplet they used to arrive at each respective species identification. Further, participants were asked to write down any steps that were confusing or whether characters on the mussel seemed ambiguous.

The dichotomous key for live mussels was tested by participants who were willing to take additional time after testing the shell only key. The format was similar to the testing for the shell

key, except that mussel valves were closed with rubber bands to illustrate a "live" mussel. Each participant was given a new set of eight mussels; due to the impracticality of arranging eight different foot-color illustrations of each shell for all participants, the foot color for each mussel was provided to the participant as text. Mussels that had been identified with molecular genetics and foot color recorded were assigned the foot color observed. Non-genetically identified mussels were assigned the modal foot-color that was observed for genetically identified individuals of that same species. Again, participants were given eight keys, each for identifying an individual mussel.

Effectiveness of the Dichotomous Keys. – Correct identifications of individual mussels were counted and scored for each participant. The percentage correct for each participant was recorded as well as identification as either a novice or an expert. An overall or mean, percent correct identification was determined for each group for all individuals combined. A confusion matrix was created to relate correct identification for each combination of experience (i.e., novice or expert) and key type (i.e., shell or live). A confusion matrix illustrates the true identity of the species in the rows and the predicted classification (i.e., the identifications made by participants) in the columns. The matrix allows for a comparison of correct identifications, false negatives or type-two errors (the species in question labeled as different species), and false positives or type-one errors (other species labeled as the species in question). A Wilcoxon signed rank test was conducted on results from each key to determine if the median rank scores between novices and experts were significantly different from each other; this is a nonparametric test that does not make any assumptions about the normality of the data. Tests were considered significant at an alpha level of ≤ 0.05 .

RESULTS

Testing the Effectiveness of Dichotomous Keys. – A total of twenty participants tested the key to identify shell material, of which nine were novices and eleven were experts (Table 5). Seventeen of these participants tested the key for live individuals, of which six were novices and eleven were experts. The shell key had thirteen couplets and fourteen terminal nodes that identified species (Table 1), the live key fifteen couplets and sixteen terminal nodes that identified species (Table 2), and the key for gravid mussels had eight couplets and nine terminal nodes that identified species (Table 3). This latter key for gravid mussels was not tested by participants.

Novices correctly identified mussels with an overall accuracy of 51% using the shell key, with their accuracy ranging from 25% to 88% (Table 5). A confusion matrix for the identification results showed that the true or actual identifications (row data) for shells of each species ranged from a low of 11% for *P. sp. cf. barnesiana* to a high of 89% for *F. subrotunda* and *P. sp. cf. oviforme* (Table 6). The participant identifications (column data) for each species showed that the other seven species were likely to be confused with *F. cor* only 25% of the time, while other species were most likely to be confused as *P. oviforme* and *P. dolabelloides*, 75% of the time. Imperiled species were classified correctly 55% of the time, while other species were incorrectly identified as an imperiled species 44% of the time.

Experts correctly identified mussels with an overall accuracy of 58% using the shell key, with their accuracy ranging from 38% to 75% correct (Table 5). A confusion matrix for the identification results showed that the true or actual identifications (row data) for shells of each species ranged from a low of 27% for *P. sp. cf. barnesiana* to a high of 91% accuracy for *F. cor*

(Table 7). The participant identifications (column data) for each species showed that the other seven species were likely to be confused as *F. cuneolus* only 14% of the time, while other species were most likely to be confused as *P. barnesiana* 69% of the time. Imperiled species were identified correctly 64% of the time, while other species were incorrectly identified as an imperiled species 27% of the time.

Novices correctly identified mussels with an overall accuracy of 50% using the live dichotomous key, with their accuracy ranging from 38% to 63% (Table 5). A confusion matrix for the identification results showed that the true or actual identifications (row data) for live individuals of each species ranged from 0% for *P. barnesiana* to 83% for *P. sp. cf. oviforme* (Table 8). The participant identifications (column data) for each species showed that the other seven species were likely to be confused as *F. cor* only 20% of the time, while other species were most likely to be confused as *P. barnesiana* 100% of the time. Imperiled species were identified correctly 50% of the time, while other species were incorrectly identified as an imperiled species 32% of the time.

Experts correctly identified mussels with an overall accuracy of 68% using the live key, with their accuracy ranging from 50% to 88% (Table 5). A confusion matrix for the identification results showed that the true or actual identifications (row data) for live individuals of each species ranged from 27% for *P. barnesiana* to 100% for *P. sp. cf. oviforme* (Table 9). The participant identifications (column data) for each species showed that the other seven species were likely to be confused as *P. sp. cf. oviforme* none of the time, while other species were most likely to be confused as *P. barnesiana* 56% of the time. Imperiled species were identified correctly 73% of the time, while other species were incorrectly identified as an imperiled species 18% of the time.

Combining novices and experts identifications for the shell key resulted in an overall accuracy of 55% (Table 5). True species identifications ranged from 20% to 85% and individual species identifications accuracy were: *F. cor* (80%), *F. cuneolus* (60%), *F. subrotunda* (85%), *P. oviforme* (35%), *P. sp. cf. oviforme* (85%), *P. barnesiana* (35%), *P. sp. cf. barnesiana* (20%), and *P. dolabelloides* (40%). Combining novices and experts identifications for the live key resulted in an overall accuracy of 62% (Table 5). True species identifications ranged from 18% to 94% and individual species identifications accuracy were: *F. cor* (76%), *F. cuneolus* (47%), *F. subrotunda* (71%), *P. oviforme* (41%), *P. sp. cf. oviforme* (94%), *P. barnesiana* (18%), *P. sp. cf. barnesiana* (76%), and *P. dolabelloides* (71%).

No significant difference was measured between novices ($N=9$, mean=51.6, 95% confidence interval=38.5-64.8) and experts ($N=11$, mean=58.2, 95% confidence interval=48.8-67.5) using the shell key ($P=0.29$), but a significant difference was measured between novices ($N=6$, mean=50.3, 95% confidence interval=38.6-62.1) and experts ($N=11$, mean=68.3, 95% confidence interval=58.8-77.9) using the live key ($P=0.02$).

DISCUSSION

Creating the Dichotomous Keys. – These are the first freshwater mussel keys to be created based on the results of classification trees (Chapter 2) in contrast to an individual scientist or mussel biologist based on their knowledge of diagnostic characters. In addition, the mussel identification keys were tested by novices and experts to determine their accuracy. In this context, it is important to assess the user's ability to correctly identify species using dichotomous keys, as simply creating one does not determine the key's effectiveness.

A drawback of creating the dichotomous key from CART analyses is that the key does not provide percentages of correct classifications on terminal nodes (final species identification) or use all character inputs. A notable example was observed for *F. subrotunda* in the live key, which exhibited foot colors in all three categories (i.e., white, pale orange, and orange), but white foot color was the only category that allowed participants to reach a final couplet for this species. Additionally the live key did not use sulcus as a variable due to replacing beak cavity for foot color. Therefore, incorporating sulcus as a variable into the shell key did not result in a key with higher accuracy on terminal nodes than the final live key. Another problem encountered was in couplet nine of the shell key. Both solutions to this couplet ended at *P. oviforme*; the CART analysis indicated that couplet 9a (umbo elevation > 1.6 mm) contained 87% *P. oviforme*, while couplet 9b (umbo elevation < 1.6 mm) contained 64% *P. oviforme*. While the CART analyses provided a level of accuracy on terminal nodes, the terminal nodes often contained other species, which could lead users of a CART-derived dichotomous key to the incorrect species.

Testing the Dichotomous Keys. – Participants wrote the most comments concerning their ability to measure or visually determine characters in this order of number of times mentioned: beak cavity depth ($N=6$), posterior ridge ($N=6$), umbo elevation ($N=6$), rays faint ($N=6$), periostracum color ($N=1$), sulcus presence ($N=1$), and hinge length ($N=1$). Difficulties in assessing or measuring these traits may have resulted from insufficient training, poor retention of knowledge during the training session, or shells used during testing possessing ambiguous characters. While novices learned these traits for the first time, these comments were evenly distributed between novices and experts. Interestingly, during the testing of the shell key, novices reused a species name 2.7 times per test, while experts reused a species name 1.4 times

per test; during the testing of the live mussel key, novices reused a species name 2.8 times per test, while experts reused a species names 1.4 times per test. It was mentioned to both groups during the training session that shells could represent the same species, but experts did not reuse species names as often as novices.

Effectiveness of the Dichotomous Keys. – There were two sessions in which experts were tested; during both sessions, explicit instructions were given to follow the key rather than use expert knowledge. However, in the second session, one participant identified the species, but wrote that the key was not used to do so. Notably, for the shell key, the second group of experts averaged 63% correct identification, while the first averaged 53%; for the live key, the second group of experts averaged 73% correct identification, while the first averaged 63%. Future studies examining the effectiveness of dichotomous keys should not list the species at terminating couplets, but rather list a code; this will reduce the participants ability to identify the mussel using prior knowledge. There was no significant difference observed in test scores between the two groups of novices for either the shell or live keys.

No significant difference was observed between median rank scores between novices and experts using the shell key. A significant difference was observed between novices and experts using the live key; however, if the second group of experts was removed from the analysis, the difference was not significant ($P=0.18$). While a significant difference was observed between novices and experts using the live key, this study was not designed to determine why experts scored higher than novices. Experts could have better assessed characters in the key either by greater retention of knowledge from training or by using their prior knowledge. Additionally, at

least one expert identified a mussel without using the key; while only one written observation occurred, other experts could have identified mussels without using the key.

Due to low sample sizes observed for gravid mussels, the key developed to identify species using gravid condition as a diagnostic character was not tested. Because the gravid state of mussels is very useful for identifying these species, I recommend that biologists locate and systematically examine and record gravid condition of mussels belonging to *Fusconaia*, *Pleurobema*, and *Pleuronaia* in the UTRB to determine if the number of charged gills and their color can further aid in identification of the species tested in the live key. To be of most value, collected individuals should be identified genetically.

Management Implications – Experts were able to correctly identify mussels using either key more frequently than novices; however, a statistical difference was observed only between the two groups for the live key. Experts correctly identified 7% more mussels using the shell key and 16% more mussels using the live key than novices. Combining novices' and experts' scores, participants were able to correctly identify mussels with an accuracy of 55% using the shell key and 62% with the live key. Considering the best testing scenario, live individuals identified by experts, only a 68% correct identification rate was achieved for the entire suite of eight species. However, when experts identified live individuals of certain species – such as *F. cor* (82%), *F. subrotunda* (82%), *P. sp. cf. oviforme* (100%), *P. sp. cf. barnesiana* (82%), and *P. dolabelloides* (82%) – higher identification rates were achieved (Table 9). Similarly, when experts used the shell key to identify *F. cor* (91%), *F. subrotunda* (82%), and *P. sp. cf. oviforme* (82%), higher identification rates were achieved (Table 7). These species have lower morphological overlap in their shell traits and are easier to identify in the field. When utilizing gravid individuals, more

definitive identification of the study species in *Fusconaia*, *Pleurobema*, and *Pleuonaia* may be possible for field collected mussels, and thus for establishing accurate species ranges and locations.

Knowledge of the distribution and local occurrence of species is important to effectively manage imperiled freshwater mussels. Therefore, the participant identification rates observed in this study would lead to a high incidence of incorrect species identifications or misidentifications. Such misidentifications of species could affect the results of field surveys and certain types of studies. For example, Tyre et al. (2003) stated that a false negative rate of 20% – recording that a species is absent when it is truly present – could greatly bias results of species distribution models. Typically, false negatives in the context of species distribution and occupancy modeling studies stem from non-detection of the target organism at a site when in fact, it was present but simply went undetected by surveyors or the sampling methodology. However, for mussel studies specifically, while false negatives could occur from the target species simply not being detected at a site, false negatives could also occur from species misidentifications. Independent of false negatives, false positives – indicating a species is present when it is truly not present – as high as 5% can bias species occupancy models (Royle and Link 2006). Further, Miller et al. (2011) found that increasing the number of sites that contained true positives was not sufficient to reduce the bias effects from false positives. Hence, controlling for the effects of false negatives and false positives stemming from misidentifications, would require stringent accuracy levels for species identifications to reduce bias in field surveys and certain types of studies with mussels. In my study, *P. sp. cf. oviforme* identified by experts using the live key was the only species identified at a false negative rate of <20% and a false positive rate of <5%. Another example is the work by Shea et al. (2011), who

illustrated that misidentification rates of *Villosa vibex* during pre- and post-drought surveys may have biased results to conclude a greater effect of a drought when in fact misidentification could have led to lower post-drought occurrences of *V. vibex*.

The 78-80% accuracy levels observed in the two CART analyses for live mussels and shells, and the subsequent lower accuracy levels obtained by participants using each key was primarily the result of morphological overlap among species in the genera *Fusconaia*, *Pleurobema*, and *Pleuronaia*. Due to the morphological overlap exhibited by these species, significant improvements in identification rates using these dichotomous keys to identify mussels in these genera may be difficult to achieve. For example, because the CART analysis for shells conducted in Chapter 2 had a mean accuracy of 80.6%, a biologist that correctly scored each character on a suite of mussels would only be able to achieve a mean identification accuracy to this level using this key. However, as stated above, higher identification rates likely could be achieved for some species, especially if adequate training is combined with diagnostic traits such as gravid condition of each species. Thus, I recommend that mussel identification workshops be held to facilitate teaching of shell and soft-anatomy characters of each species to improve identification rates as much as possible. Regulatory agencies should also explore certification programs that require training and testing of a biologist's knowledge of how to identify freshwater mussels. Additionally, I recommend that species occurrences outside known ranges be confirmed using mitochondrial DNA markers. The DNA sequences can be compared to those on GenBank or other databases to identify species.

LITERATURE CITED

- Baker A.M., C. Bartlett, S.E. Bunn, K. Goudkamp, F. Sheldon, J.M. Hughes. 2003. Cryptic species and morphological plasticity in long-lived bivalves (Unionoida: Hyriidae) from inland Australia. *Molecular Ecology*, 12 (10):2707-2717.
- Campbell D.C., J.M. Serb, J.E. Buhay, K.J. Roe, R.L. Minton, C. Lydeard. 2005. Phylogeny of North American amblemines (Bivalvia, Unionoida): Prodigious polyphyly proves pervasive across genera. *Invertebrate Biology*, 124 (2):131-164.
- Christian A.D., J.L. Harris, J.M. Serb. 2008. Preliminary analysis for identification, distribution, and conservation status of species of *Fusconaia* and *Pleurobema* in Arkansas. Report, Arkansas Game and Fish Commission, Perrytown, Arkansas. 40 pp.
- Kat P.W. 1983. Genetic and morphological divergence among nominal species of North American anodonta (Bivalvia: Unionidae). *Malacologia*, 23 (2):361-374.
- Miller D.A., J.D. Nichols, B.T. McClintock, E.H.C. Grant, L.L. Bailey, L.A. Weir. 2011. Improving occupancy estimation when two types of observational error occur: Non-detection and species misidentification. *Ecology*, 92 (7):1422-1428.
- Parmalee P.W., A.E. Bogan. 1998. *The Freshwater Mussels of Tennessee*. The University of Tennessee Press, Knoxville, Tennessee, USA.
- Royle J.A., W.A. Link. 2006. Generalized site occupancy models allowing for false positive and false negative errors. *Ecology*, 87 (4):835-841.
- Shea C.P., J.T. Peterson, J.M. Wisniewski, N.A. Johnson. 2011. Misidentification of freshwater mussel species (Bivalvia: Unionidae): Contributing factors, management implications, and potential solutions. *Journal of the North American Benthological Society*, 30 (2):446-458.

Tyre A.J., B. Tenhumberg, S.A. Field, D. Niejalke, K. Parris, H.P. Possingham. 2003. Improving precision and reducing bias in biological surveys: Estimating false-negative error rates.

Ecological Applications, 13 (6):1790-1801.

Williams J.D., A.E. Bogan, J.T. Garner. 2008. *Freshwater Mussels of Alabama and the Mobile Basin in Georgia, Mississippi and Tennessee*. The University of Alabama Press, Tuscaloosa, Alabama.

Table 1. Key to the shells of non-live individuals of select freshwater mussel species in the genera *Fusconaia*, *Pleurobema*, and *Pleuronaia* in the upper Tennessee River basin of Tennessee and Virginia using categorical and continuous variables. See Figure 1 for explanations of shell characters and the species accounts for illustrations of morphological traits (Figures 2-9).

1.	a. Beak Cavity: Deep (see <i>F. cor</i> or <i>F. subrotunda</i>).....	2
	b. Beak Cavity: Shallow (see <i>P. oviforme</i> or <i>P. barnesiana</i>).....	4
2.	a. Sulcus: Absent (see <i>F. subrotunda</i> or <i>P. barnesiana</i>).....	<i>F. subrotunda</i>
	b. Sulcus: Present (see <i>F. cor</i> or <i>F. cuneolus</i>).....	3
3.	a. Periostracum Sheen: Shiny	<i>F. cor</i>
	b. Periostracum Sheen: Dull or Satiny	<i>F. cuneolus</i>
4.	a. Umbo Elevation: Less than 0.22 mm	5
	b. Umbo Elevation: Greater than 0.22 mm	6
5.	a. Periostracum Sheen: Dull	<i>P. oviforme</i>
	b. Periostracum Sheen: Satiny	<i>P. sp. cf. oviforme</i>
6.	a. Posterior Ridge: Angular (see <i>F. cor</i> or <i>P. dolabelloides</i>).....	7
	b. Posterior Ridge: Round (see <i>P. oviforme</i> or <i>P. sp. cf. barnesiana</i>).....	8
7.	a. Ray Pattern: Continuous	<i>P. barnesiana</i>
	b. Ray Pattern: Broken	<i>P. dolabelloides</i>
8.	a. Hinge Ligament: Greater than 27 mm	9
	b. Hinge Ligament: Less than 27 mm	10
9.	a. Umbo Elevation: Greater than 1.6 mm	<i>P. oviforme</i>
	b. Umbo Elevation: Less than 1.6 mm	<i>P. oviforme</i>
10.	a. Umbo Elevation: Greater than 1 mm	11
	b. Umbo Elevation: Less than 1 mm	12
11.	a. Periostracum Color: Light Brown	<i>P. barnesiana</i>
	b. Periostracum Color: Dark Brown, Brown, or Yellow	<i>P. oviforme</i>
12.	a. Length: Less than 45 mm	<i>P. sp. cf. barnesiana</i>
	b. Length: Greater than 45 mm	13

- 13 a. Ray Width: Fine *P. barnesiana*
b. Ray Width: Wide or None *P. sp. cf. barnesiana*
-

Table 2. Key to the live individuals of select freshwater mussel species in the genera *Fusconaia*, *Pleurobema*, and *Pleuronaia* in the upper Tennessee River basin of Tennessee and Virginia using categorical and continuous variables. See shell diagram page for explanations of shell characters and species accounts for illustrations of morphological traits (Figures 2-9).

1.	a. Foot Color: Orange or Pale Orange (see <i>P. sp. cf. barnesiana</i> or <i>P. dolabelloides</i>)2
	b. Foot Color: White (see <i>P. oviforme</i> or <i>P. barnesiana</i>)8
2.	a. Posterior Ridge: Round (see <i>P. oviforme</i> or <i>P. sp. cf. barnesiana</i>)3
	b. Posterior Ridge: Angular (see <i>F. cor</i> or <i>P. dolabelloides</i>)5
3.	a. Umbo Elevation: Less than 0.25 mm <i>P. sp. cf. oviforme</i>
	b. Umbo Elevation: Greater than 0.25 mm4
4.	a. Maximum Height: Less than 48 mm <i>P. sp. cf. barnesiana</i>
	b. Maximum Height: Greater than 48 mm <i>P. oviforme</i>
5.	a. Periostracum Sheen: Shiny <i>F. cor</i>
	b. Periostracum Sheen: Dull or Satiny6
6.	a. Ray Pattern: Broken <i>P. dolabelloides</i>
	b. Ray Pattern: Continuous7
7.	a. Ray Length: Extending to Margin <i>F. cuneolus</i>
	b. Ray Length: Ceasing Short of Margin <i>P. oviforme</i>
8.	a. Umbo Elevation: Greater than 2 mm9
	b. Umbo Elevation: Less than 2 mm11
9.	a. Length: Greater than 70 mm <i>F. subrotunda</i>
	b. Length: Less than 70 mm10
10.	a. Height at Umbo: Greater than 44 mm <i>P. barnesiana</i>
	b. Height at Umbo: Less than 44 mm <i>F. subrotunda</i>
11.	a. Umbo Elevation: Less than 1 mm <i>P. oviforme</i>
	b. Umbo Elevation: Greater than 1 mm12
12.	a. Posterior Ridge: Angular (see <i>F. cor</i> or <i>P. dolabelloides</i>) <i>P. barnesiana</i>
	b. Posterior Ridge: Round (see <i>P. oviforme</i> or <i>P. sp. cf. barnesiana</i>)13

13.	a. Periostracum Color: Light Brown	14
	b. Periostracum Color: Brown or Dark Brown	15
14.	a. Length: Less than 57 mm	<i>P. barnesiana</i>
	b. Length: Greater than 57 mm	<i>P. oviforme</i>
15.	a. Maximum Height: Less than 43 mm	<i>F. subrotunda</i>
	b. Maximum Height: Greater than 43 mm	<i>P. barnesiana</i>

Table 3. Key to gravid individuals of select freshwater mussel species in the genera *Fusconaia*, *Pleurobema*, and *Pleuronaia* in the upper Tennessee River basin of Tennessee and Virginia using categorical variables. See Figure 1 for explanations of shell characters and species accounts for illustrations of morphological traits (Figures 2-9).

1.	a. Gills Charged: Outer Two	2
	b. Gills Charged: All Four	5
2.	a. Gill Color: White or Pink	3
	b. Gill Color: Orange	4
3.	a. Gill Color: White	<i>P. oviforme</i>
	b. Gill Color: Pink	<i>P. dolabelloides</i>
4.	a. Periostracum Sheen: Satiny	<i>P. sp. cf. oviforme</i>
	b. Periostracum Sheen: Dull	<i>P. oviforme</i>
5.	a. Gill Color: Tan	<i>P. barnesiana</i>
	b. Gill Color: Orange, Red, or Pink	6
6.	a. Gill Color: Orange	<i>P. sp. cf. barnesiana</i>
	b. Gill Color: Red or Pink	7
7.	a. Gill Color: Red	<i>F. subrotunda</i>
	b. Gill Color: Pink	8
8.	a. Periostracum Sheen: Shiny	<i>F. cor</i>
	b. Periostracum Sheen: Dull or Satiny	<i>F. cuneolus</i>

Table 4. List of terms used in the keys to identify shells and soft-anatomy of study species in the genera *Fusconaia*, *Pleurobema*, and *Pleuironaia* in the upper Tennessee River basin of Tennessee and Virginia; terms modified from Parmalee and Bogan (1998) and Williams et al. (2008).

Beak Cavity: depression in each valve located interiorly below the umbo

Foot: large muscular organ used primarily for locomotion and anchoring, as well as feeding during juvenile stages

Height (Maximum): maximum height measured perpendicular to maximum length

Height at Umbo: height posterior to umbo measured perpendicular to maximum length

Hinge Ligament: elongate, elastic structure uniting the valves dorsally that forces valves to open when adductor muscles are relaxed

Length: maximum distance across shell measured from external margins oriented from anterior to posterior

Periostracum: thin outer layer that protects shell

Posterior Ridge: raised ridge on the exterior of the shell extending from the umbo to the posterior-ventral margin

Ray: line of pigment on the periostracum, oriented radially from the umbo to the ventral margin

Sulcus: radial depression on exterior of shell, located anterior to the posterior ridge, oriented from umbo to the posterior-ventral margin

Umbo: dorsally raised, inflated area on the exterior of the shell located anterior to the hinge ligament

Width: maximum distance across both valves parallel to valves closed against one another

Table 5. Participant accuracy in correctly identifying select mussel species in the genera *Fusconaia*, *Pleurobema*, and *Pleuonaia* using the dichotomous keys based on quantitative and categorical variables.

<u>Shell Key</u>		<u>Live Key</u>	
Group	Score	Group	Score
Novice	0.50	Novice	0.63
	0.38		0.38
	0.88		0.50
	0.63		0.63
	0.50		0.50
	0.50		0.38
	0.25		–
	0.50		–
	0.50		–
Novice Mean	0.51	Novice Mean	0.50
Expert	0.38	Expert	0.63
	0.63		0.50
	0.50		0.50
	0.75		0.63
	0.38		0.88
	0.75		0.75
	0.75		0.75
	0.63		0.88
	0.50		0.50
	0.63		0.75
	0.50		0.75
Expert Mean	0.58	Expert Mean	0.68
Grand Mean	0.55	Grand Mean	0.62

Table 6. Species identifications ($N=72$) assigned by novices ($N=9$) using dichotomous key of shell-only quantitative and categorical variables. These data include non-genetically identified individuals from the FMCC shell collection. Actual species identifications are in the rows and participant's identifications are in the columns.

Species Assigned by Novices Using Dichotomous Key for Shell Only										
<u>Species</u>	<i>Fusconaia</i>	<i>Fusconaia</i>	<i>Fusconaia</i>	<i>Pleurobema</i>	<i>Pleurobema</i>	<i>Pleurobema</i>	<i>Pleurobema</i>	<i>Pleurobema</i>	<i>Pleurobema</i>	<u>% Correct Identification</u>
	<u>cor</u>	<u>cuneolus</u>	<u>subrotunda</u>	<u>oviforme</u>	sp. cf. <u>oviforme</u>	<u>barnesiana</u>	sp. cf. <u>barnesiana</u>	<u>dolabelloides</u>		
<i>Fusconaia cor</i>	6	1	2	0	0	0	0	0	0	0.6667
<i>Fusconaia cuneolus</i>	1	6	0	0	0	1	0	1	1	0.6667
<i>Fusconaia subrotunda</i>	1	0	8	0	0	0	0	0	0	0.8889
<i>Pleurobema oviforme</i>	0	0	1	2	1	2	1	2	2	0.2222
<i>Pleurobema</i> sp. cf. <i>oviforme</i>	0	0	0	1	8	0	0	0	0	0.8889
<i>Pleurobema barnesiana</i>	0	0	0	1	1	3	0	4	4	0.3333
<i>Pleurobema</i> sp. cf. <i>barnesiana</i>	0	1	1	2	0	2	1	2	2	0.1111
<i>Pleurobema dolabelloides</i>	0	1	1	2	1	1	0	3	3	0.3333
% Correct Identification	0.7500	0.6667	0.6154	0.2500	0.7273	0.3333	0.5000	0.2500		

Table 7. Species identifications ($N=88$) assigned by experts ($N=11$) using dichotomous key of shell-only quantitative and categorical variables. These data include non-genetically identified individuals from the FMCC shell collection. Actual species identifications are in the rows and participant's identifications are in the columns.

<u>Species</u>	Species Assigned by Experts Using Dichotomous Key for Shell Only								<u>% Correct Identification</u>
	<i>Fusconaia</i> <u>cor</u>	<i>Fusconaia</i> <u>cuneolus</u>	<i>Fusconaia</i> <u>subrotunda</u>	<i>Pleurobema</i> <u>oviforme</u>	<i>Pleurobema</i> sp. cf. <u>oviforme</u>	<i>Pleurobema</i> <u>barnesiana</u>	<i>Pleurobema</i> sp. cf. <u>barnesiana</u>	<i>Pleurobema</i> <u>dolabelloides</u>	
<i>Fusconaia cor</i>	10	0	0	0	0	1	0	0	0.9091
<i>Fusconaia cuneolus</i>	4	6	0	0	0	0	0	1	0.5455
<i>Fusconaia subrotunda</i>	0	1	9	1	0	0	0	0	0.8182
<i>Pleurobema oviforme</i>	0	0	0	5	0	5	1	0	0.4545
<i>Pleurobema</i> sp. cf. <i>oviforme</i>	0	0	1	1	9	0	0	0	0.8182
<i>Pleurobema barnesiana</i>	0	0	1	3	0	4	1	2	0.3636
<i>Pleurobema</i> sp. cf. <i>barnesiana</i>	0	0	0	5	0	3	3	0	0.2727
<i>Pleurobema dolabelloides</i>	0	0	3	0	3	0	0	5	0.4545
% Correct Identification	0.7143	0.8571	0.6429	0.3333	0.7500	0.3077	0.6000	0.6250	

Table 8. Species identifications ($N=48$) assigned by novices ($N=6$) using dichotomous key quantitative and categorical variables representing live mussels. These data include non-genetically identified individuals from the FMCC shell collection. Actual species identifications are in the rows and participant's identifications are in the columns.

Species Assigned by Novices Using Dichotomous Key for Live Individuals										
<u>Species</u>	<i>Fusconaia</i>	<i>Fusconaia</i>	<i>Fusconaia</i>	<i>Pleurobema</i>	<i>Pleurobema</i>	<i>Pleurobema</i>	<i>Pleurobema</i>	<i>Pleurobema</i>	<i>Pleurobema</i>	% Correct <u>Identification</u>
	<u>cor</u>	<u>cuneolus</u>	<u>subrotunda</u>	<u>oviforme</u>	sp. cf. <u>oviforme</u>	<u>barnesiana</u>	sp. cf. <u>barnesiana</u>	<u>dolabelloides</u>		
<i>Fusconaia cor</i>	4	1	0	0	1	0	0	0	0	0.6667
<i>Fusconaia cuneolus</i>	0	2	0	3	0	0	0	1	0	0.3333
<i>Fusconaia subrotunda</i>	0	0	3	0	0	1	2	0	0	0.5000
<i>Pleurobema oviforme</i>	0	0	0	3	0	1	2	0	0	0.5000
<i>Pleurobema</i> sp. cf. <i>oviforme</i>	0	0	0	1	5	0	0	0	0	0.8333
<i>Pleurobema barnesiana</i>	0	0	3	2	0	0	1	0	0	0.0000
<i>Pleurobema</i> sp. cf. <i>barnesiana</i>	1	0	0	0	1	0	4	0	0	0.6667
<i>Pleurobema dolabelloides</i>	0	1	0	0	1	0	1	3	0	0.5000
% Correct Identification	0.8000	0.5000	0.5000	0.3333	0.6250	0.0000	0.4000	0.7500		

Table 9. Species identification ($N=88$) assigned by experts ($N=11$) using dichotomous key of quantitative and categorical variables representing live mussels. These data include non-genetically identified individuals from the FMCC shell collection. Actual species identifications are in the rows and participant's identifications are in the columns.

Species Assigned By Experts Using Dichotomous Key for Live Individuals										
<u>Species</u>	<i>Fusconaia</i>	<i>Fusconaia</i>	<i>Fusconaia</i>	<i>Pleurobema</i>	<i>Pleurobema</i>	<i>Pleurobema</i>	<i>Pleurobema</i>	<i>Pleurobema</i>	<i>Pleurobema</i>	% Correct <u>Identification</u>
	<u>cor</u>	<u>cuneolus</u>	<u>subrotunda</u>	<u>oviforme</u>	sp. cf. <u>oviforme</u>	<u>barnesiana</u>	sp. cf. <u>barnesiana</u>	<u>dolabelloides</u>		
<i>Fusconaia cor</i>	9	2	0	0	0	0	0	0	0	0.8182
<i>Fusconaia cuneolus</i>	2	6	0	3	0	0	0	0	0	0.5455
<i>Fusconaia subrotunda</i>	0	0	9	0	0	0	2	0	0	0.8182
<i>Pleurobema oviforme</i>	0	0	2	4	0	4	1	0	0	0.3636
<i>Pleurobema</i> sp. cf. <i>oviforme</i>	0	0	0	0	11	0	0	0	0	1.0000
<i>Pleurobema barnesiana</i>	0	0	5	1	0	3	1	1	1	0.2727
<i>Pleurobema</i> sp. cf. <i>barnesiana</i>	0	0	0	2	0	0	9	0	0	0.8182
<i>Pleurobema dolabelloides</i>	0	0	0	0	0	0	2	9	9	0.8182
% Correct Identification	0.8182	0.7500	0.5625	0.4000	1.0000	0.4286	0.6000	0.9000		

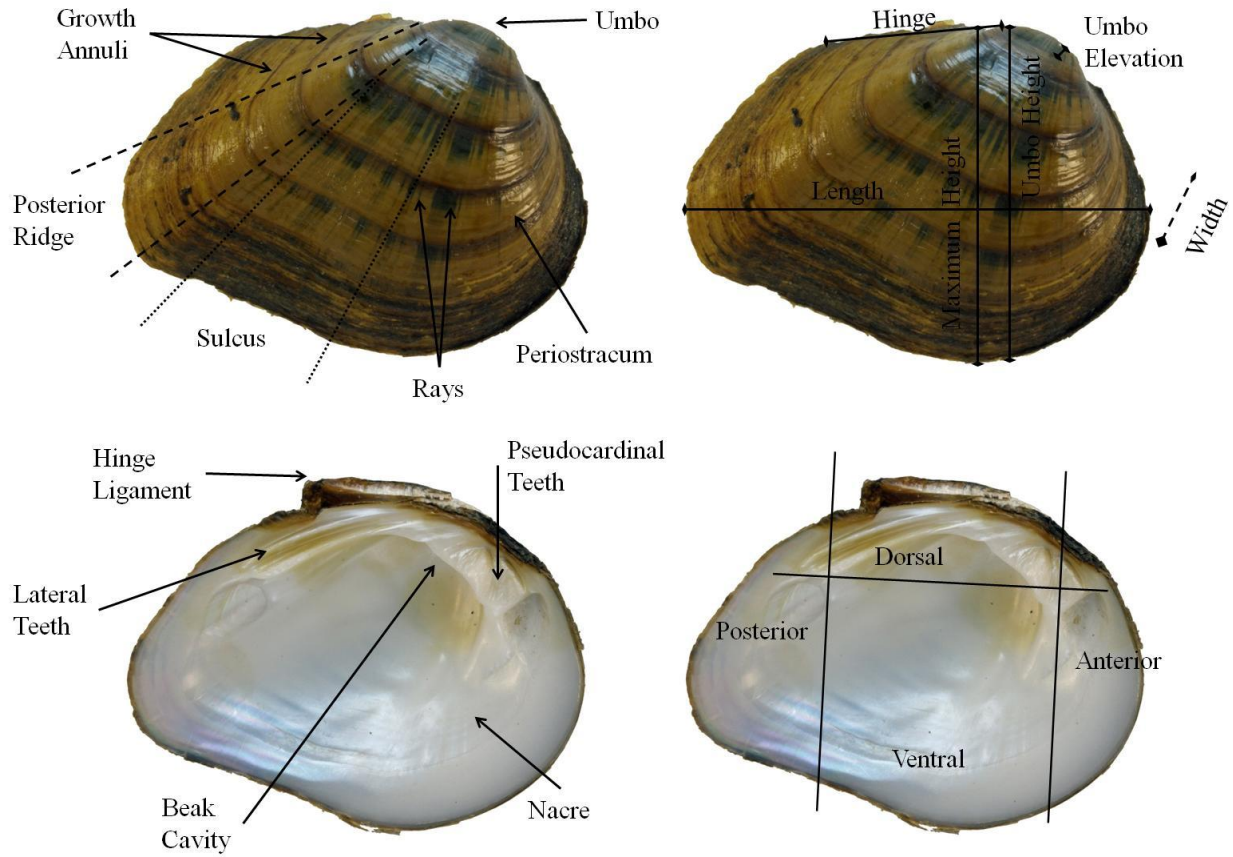
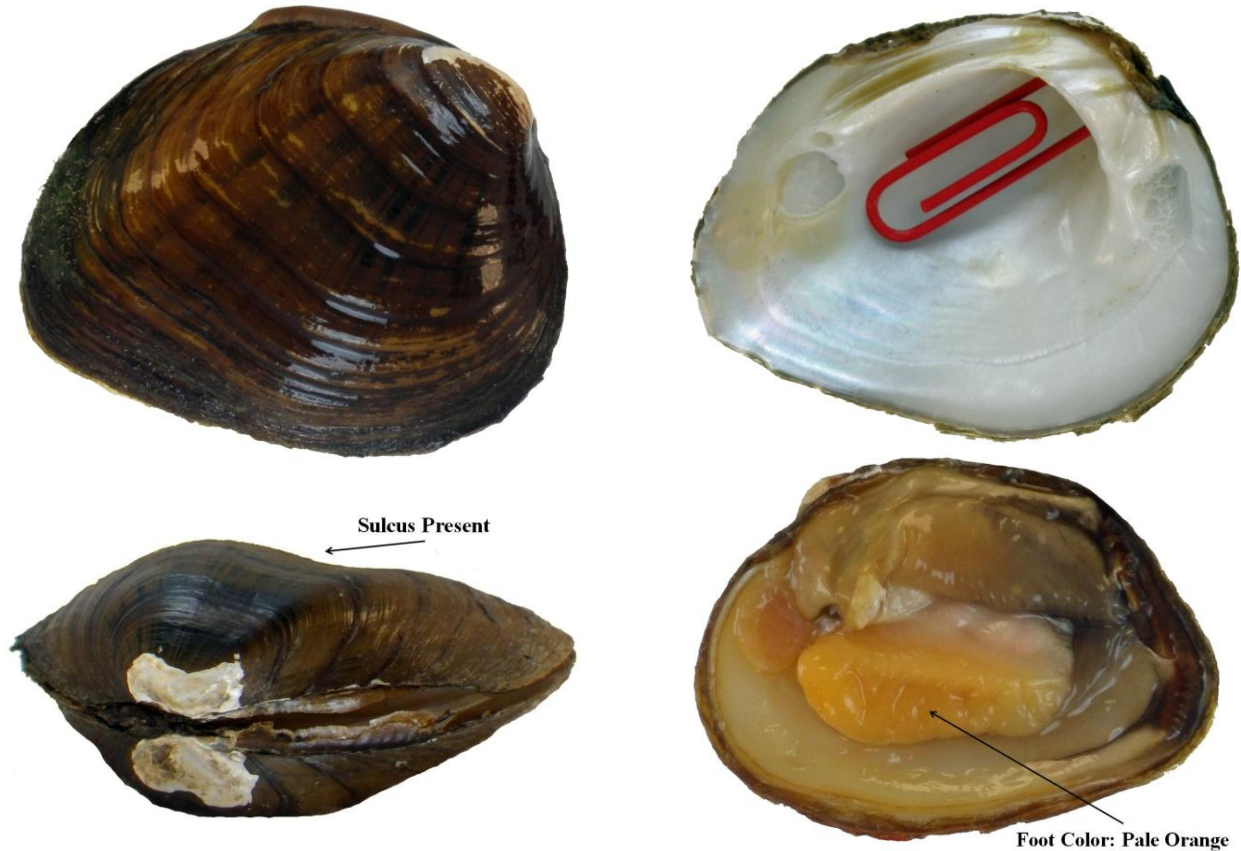


Figure 1. External (top) and internal (bottom left) shell characters investigated in this study, including anatomical regions (bottom right) of the shell.



Typical External Traits:

Periostracum Color: brown, but varies from yellow to dark brown

Periostracum Sheen: shiny, occasionally satiny or dull

Ray Length: extending to shell margin, but occasionally interrupted or broken

Ray Width: conspicuously wide, 1-2 mm or wider

Posterior Ridge: angular

Sulcus: present, often extending from ventral margin to 3/4 the length of the shell toward the umbo

Umbo Elevation: moderate to high, approximately 2-4 mm

Typical Internal Traits:

Beak Cavity: deep ≥ 3 mm

Foot Color: pale orange, but varies from white to orange

Number of Charged Gills: all four gills charged

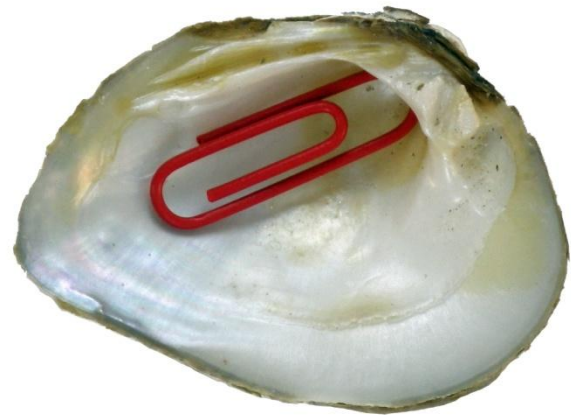
Color of Charged Gills: pink

Color of Conglutinate: pink, appear like a "+" from the side

Key Traits:

Shell with shiny periostracum and prominent sulcus; deep beak cavity

Figure 2. Typical external and internal traits of *Fusconaia cor*.



Typical External Traits:

Periostracum Color: brown, but varies from yellow to dark brown

Periostracum Sheen: satiny or dull

Ray Length: extending to shell margin, but occasionally interrupted or broken

Ray Width: narrow, 1 mm or less

Posterior Ridge: angular

Sulcus: present, often extending from ventral margin to 2/3 the length of the shell, but not onto the umbo

Umbo Elevation: moderate to high, approximately 2-4 mm

Typical Internal Traits:

Beak Cavity: deep ≥ 3 mm

Foot Color: pale orange, but varies from white to orange, occasionally light pink

Number of Charged Gills: all four gills charged

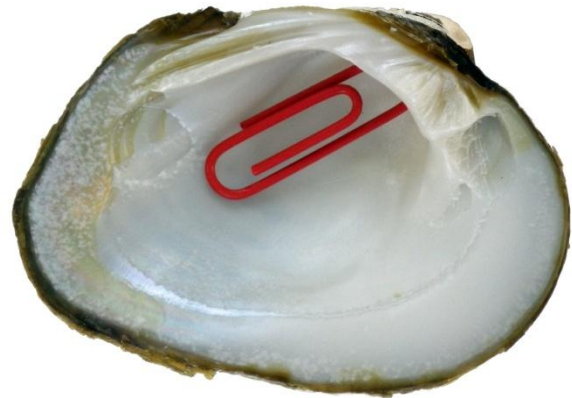
Color of Charged Gills: listed as pink in literature

Color of Conglutinate: listed as pink in literature

Key Traits:

Shell with satiny periostracum and sulcus not extending onto umbo; deep beak cavity

Figure 3. Typical external and internal traits of *Fusconaia cuneolus*.



Typical External Traits:

Periostracum Color: dark brown, but varies from light to dark brown

Periostracum Sheen: satiny or dull

Ray Length: extending to shell margin, but occasionally interrupted or broken

Ray Width: narrow, 1 mm or less

Posterior Ridge: typically rounded to flat

Sulcus: absent, occasionally a slight sulcus is present

Umbo Elevation: moderate, approximately 2 mm

Typical Internal Traits:

Beak Cavity: deep ≥ 3 mm

Foot Color: varies from white to orange

Number of Charged Gills: all four gills charged

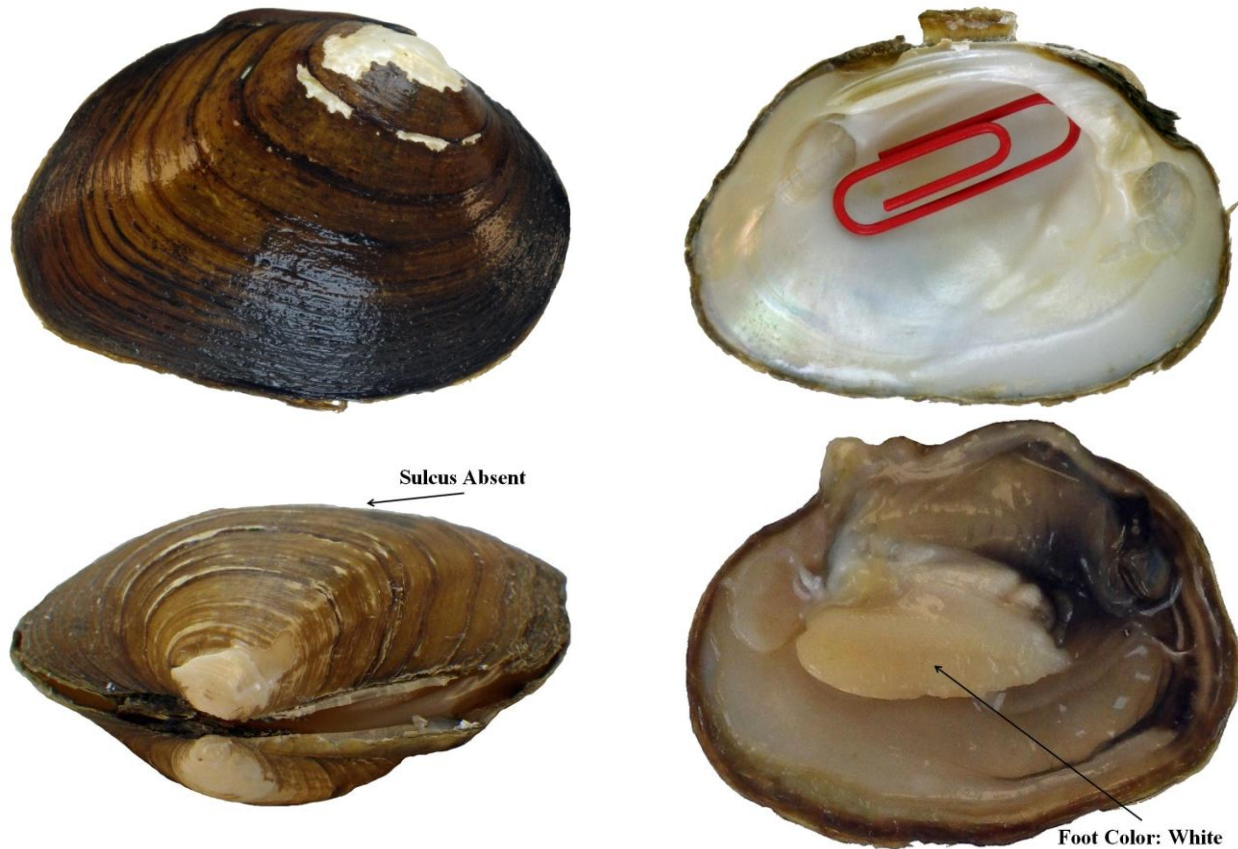
Color of Charged Gills: red

Color of Conglutinate: red, elongate, slender and conical, sometimes being bifurcate

Key Traits:

Shell with satiny or dull periostracum and typically no sulcus; deep beak cavity; adults have heavy large shell >70 mm

Figure 4. Typical external and internal traits of *Fusconaia subrotunda*.



Typical External Traits:

Periostracum Color: light brown, but varies from light to dark brown

Periostracum Sheen: satiny or dull

Ray Length: extending to shell margin, but occasionally interrupted or broken

Ray Width: wide, 1-2 mm or wider

Posterior Ridge: rounded

Sulcus: absent, occasionally slight sulcus present

Umbo Elevation: low to moderate, 1 mm or less

Typical Internal Traits:

Beak Cavity: shallow

Foot Color: white, occasionally pale-orange to orange

Number of Charged Gills: outer two gills charged

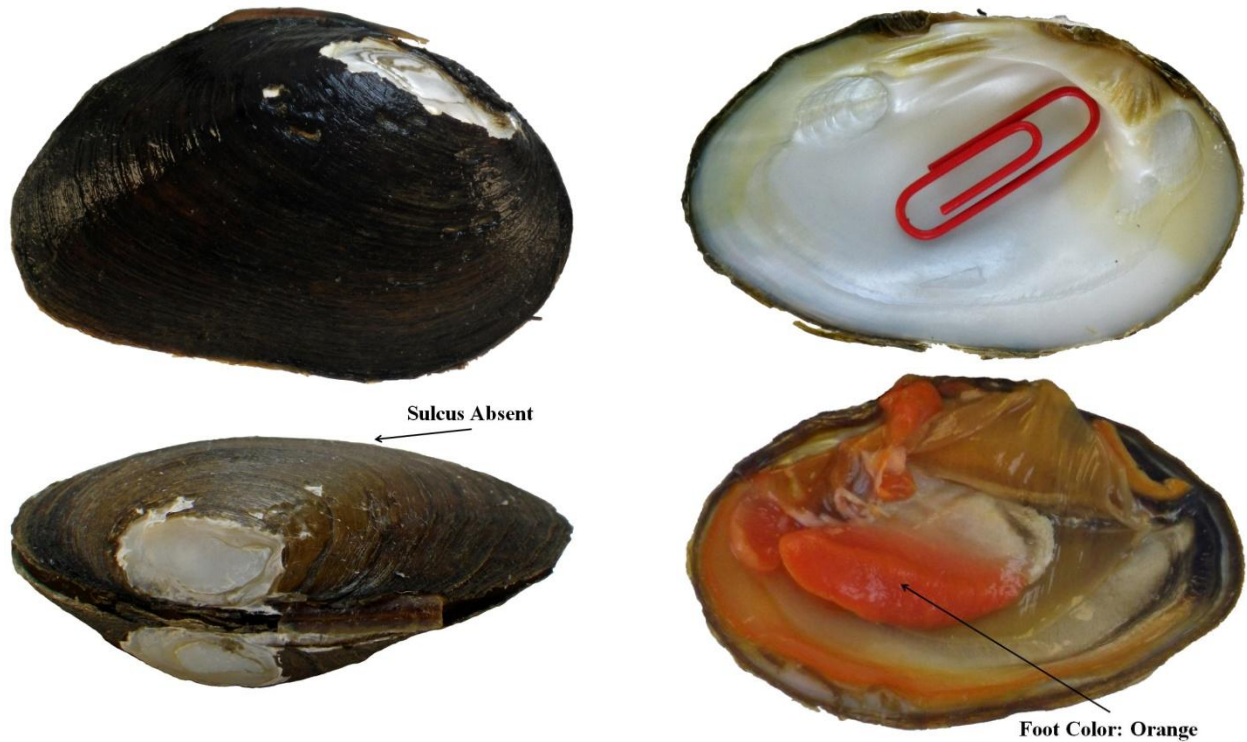
Color of Charged Gills: white, occasionally pale-orange

Conglutinate: white, occasionally pale-orange, sometimes bifurcate, football shaped in outline

Key Traits:

Shell with satiny or dull periostracum and no sulcus; shallow beak cavity; only outer two gills charged

Figure 5. Typical external and internal traits of *Pleurobema oviforme*.



Typical External Traits:

Periostracum Color: brown, but varies from light to dark brown

Periostracum Sheen: very satiny, occasionally dull

Ray Length: extending to shell margin, occasionally very faint to absent

Ray Width: narrow, 1 mm or less

Posterior Ridge: rounded

Sulcus: absent

Umbo Elevation: very low, 1 mm or less, often flush with dorsal margin

Typical Internal Traits:

Beak Cavity: shallow

Foot Color: orange

Number of Charged Gills: outer two gills charged

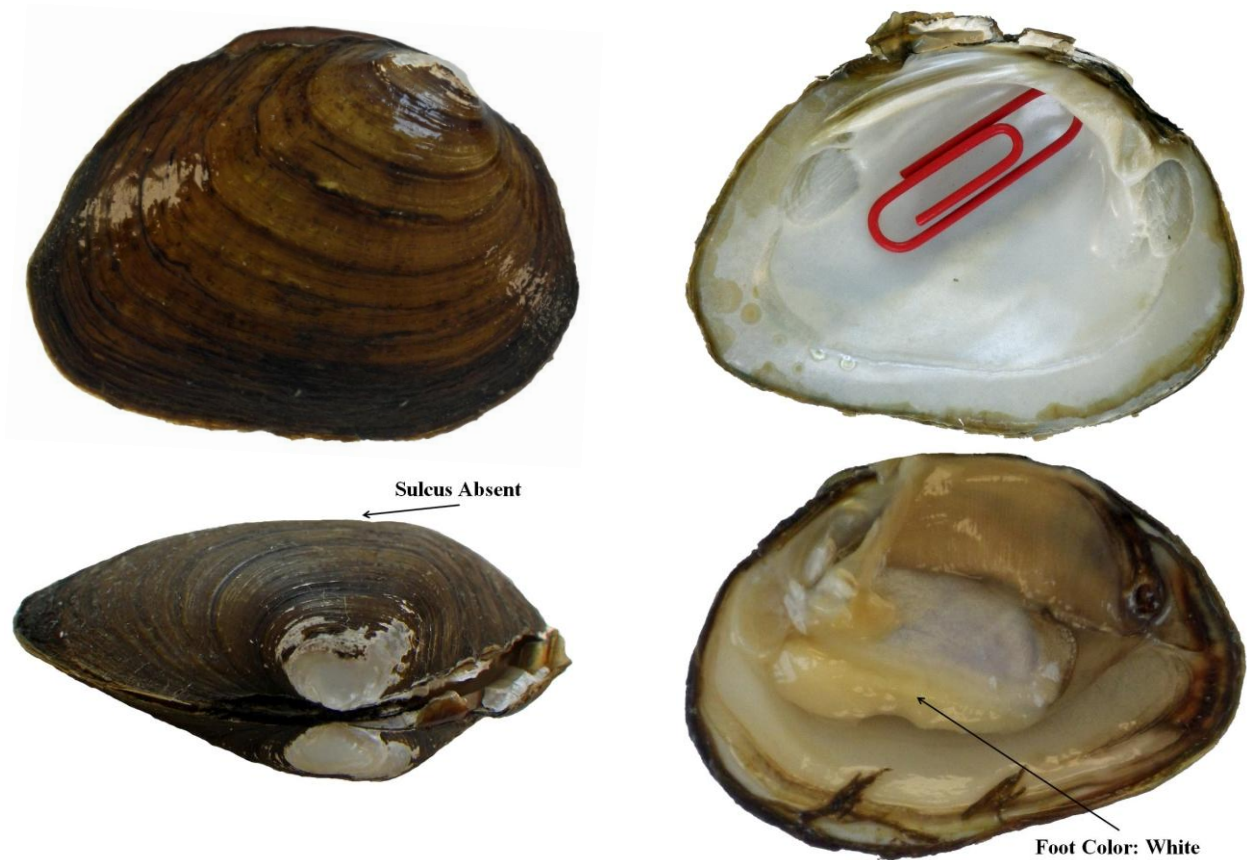
Color of Charged Gills: orange

Color of Conglutinate: orange, sometimes bifurcate, football shaped in outline

Key Traits:

Shell elongate with very satiny periostracum, low umbo and shallow beak cavity

Figure 6. Typical external and internal traits of *Pleurobema* sp. cf. *oviforme*.



Traditional External Traits:

Periostracum Color: varies from light to dark brown, occasionally yellow

Periostracum Sheen: satiny or dull

Ray Length: extending to shell margin, occasionally broken or none present

Ray Width: narrow, 1-2 mm, occasionally wider

Posterior Ridge: rounded

Sulcus: absent

Umbo Elevation: low to moderate, 1 mm or less

Traditional Internal Traits:

Beak Cavity: shallow

Foot Color: white, occasionally pale-orange

Number of Charged Gills: all four gills charged

Color of Charged Gills: light-tan

Color of Conglutate: light-tan, slender and conical

Key Traits:

Shell with satiny or dull periostracum and no sulcus; shallow beak cavity; white foot; tan colored conglutinates

Figure 7. Typical external and internal traits of *Pleuroaia barnesiana*.



Typical External Traits:

Periostracum Color: varies from light to dark brown, occasionally yellow

Periostracum Sheen: satiny or dull

Ray Length: extending to shell margin, occasionally none present

Ray Width: narrow, 1-2 mm, occasionally wider

Posterior Ridge: rounded

Sulcus: absent

Umbo Elevation: low to moderate, 1 mm or less

Typical Internal Traits:

Beak Cavity: shallow

Foot Color: pale-orange, occasionally orange

Number of Charged Gills: all four gills charged

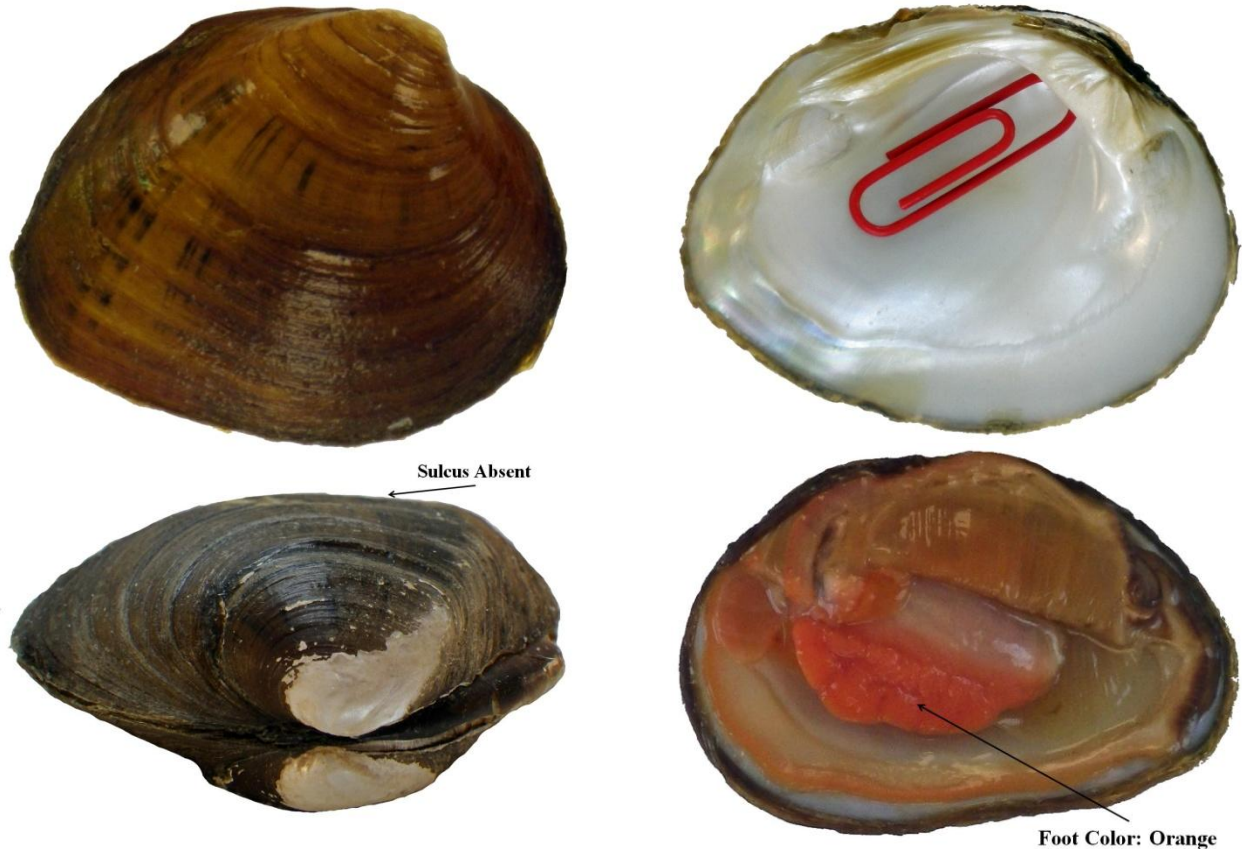
Color of Charged Gills: pale-orange

Color of Conglutinate: pale-orange, sometimes bifurcate, football shaped in outline

Key Traits:

Shell with satiny or dull periostracum and shallow beak cavity

Figure 8. Typical external and internal traits of *Pleuronaia* sp. cf. *barnesiana*.



Typical External Traits:

Periostracum Color: yellow, but varies from light to dark brown

Periostracum Sheen: satiny or dull

Ray Length: interrupted or broken, but occasionally extending to shell margin

Ray Width: wide, 1-2 mm or wider

Posterior Ridge: angular, occasionally rounded

Sulcus: absent

Umbo Elevation: low to moderate, 1 mm or less

Typical Internal Traits:

Beak Cavity: shallow

Foot Color: orange, occasionally pale-orange, rarely white

Number of Charged Gills: outer two gills charged

Color of Charged Gills: pink

Color of Conglutinate: pink, elongate, slender and conical, sometimes being bifurcate, trifurcate, or multifurcate

Key Traits:

Shell with wide interrupted or broken rays; shallow beak cavity; only outer two gills charged

Figure 9. Typical external and internal traits of *Pleuronaia dolabelloides*.